A FINITE ELEMENT ANALYSIS OF HIGH KAPPA, HIGH FIELD GINZBURG-LANDAU TYPE MODEL OF SUPERCONDUCTIVITY

by

Rossitza A. Karamikhova

Dissertation submitted to the faculty of the

Virginia Polytechnic Institute and State University

in partial fulfillment of the requirements for the degree of

DOCTOR OF PHILOSOPHY

in

Mathematics

APPROVED:

Janet S. Peterson

Janet S. Peterson, Chairman

John A. Burns

John A. Burns

Max D. Gunzburger

Terry L. Herdman

Terry L. Herdman

Tao Lin

August, 1995

Blacksburg, Virginia

A FINITE ELEMENT ANALYSIS OF A HIGH KAPPA, HIGH FIELD GINZBURG-LANDAU TYPE MODEL OF SUPERCONDUCTIVITY

by

Rossitza A. Karamikhova

Committee Chairman: Janet S. Peterson

Department of Mathematics

(ABSTRACT)

This work is concerned with the formulation and analysis of a simplified Ginzburg-Landau type model of superconductivity which is valid for large κ and large magnetic field strengths. This model, referred to as the High kappa model, is derived via formal asymptotic expansion of the full, time-dependent Ginzburg-Landau equations. The model accounts for the effects of both applied magnetic fields and currents of constant magnitude. A notable feature of our model is that the systems for the leading order terms for the magnetic potential and the order parameter are decoupled.

Finite element approximations of the High kappa model are introduced using standard Galerkin discretization in space and Backward-Euler and Crank-Nicolson discretization schemes in time. We establish existence and uniqueness results for the fully-discrete equations as well as optimal L^2 and H^1 error estimates for the Backward-Euler-Galerkin and the Crank-Nicolson-Galerkin problems.

Computational experiments are performed with several combinations of spatial and time discretizations of the High kappa model equations. Among other things our numerical approximations show good agreement for rates of convergence in space and time with the corresponding theoretical values. Finally, some well known steady-state and dynamic phenomena valid for type II superconductors are illustrated numerically.

ACKNOWLEDGEMENTS

My first contact with superconductivity came through the seminar presented by Max Gunzburger here at Virginia Tech. Without this excellent seminar I probably wouldn't have started this work. I also wish to thank Max Gunzburger for the many discussions in which he introduced me to the fundamental ideas of superconductivity and finite elements.

I express my warm gratitude to Janet Peterson, my advisor, for her constant support and encouragement throughout the time I have spent in graduate school. Many thanks are due to her for the patient and careful reading of all drafts of my work, making numerous corrections and valuable suggestions. Without her help many of the results in this work would not be possible.

I offer special thanks to my committee members, John Burns, Tao Lin, and Terry Herdman, who have been always very supportive and ready to help. In particular, I wish to thank Tao Lin for the numerous discussions which helped me to understand a lot about time dependent problems. I am also grateful to Vassilios Dougalis and Vidar Thomée who shared with me their experience and knowledge of nonlinear Galerkin methods. I wish to thank my colleagues John Burkardt and Jeff Borggaard for their help and in particular for guiding me through UNIX and Macintosh.

Through all this years I had the complete support of my family and in particular, Pavel Bochev. His constant encouragement, understanding and help were instrumental for finishing this work. I have special thanks to Simeon who patiently endured these four years of hard work. Finally, I wish to thank my parents for being with me when I needed it most.

I am grateful for the support of the Department of Energy through contract DE-FG05-93ER25175.

TABLE OF CONTENTS

LIST OF FIGURES

LIST OF TABLES

Chapter 1

Introduction

In the first section of Chapter 1, we present a brief historical introduction to superconductivity. Our goal is to highlight the main results from the discovery of the superconductivity to the recently found high-temperature superconducting materials. We proceed with a discussion of some basic properties of conventional superconductors. We present, in historical order, some of the well known macroscopic models emphasizing the Ginzburg-Landau (G-L) model on which this work is based. In order to show that this model is reliable, we briefly explain its connection with the microscopic BCS model. We end this section with a discussion of some properties of the high-T_c superconductors which are important for practical applications.

In the second section of Chapter 1 we present the well-known G-L equations and their generalization to the time-dependent G-L system (TDG-L). Since the material in this section is well known and there are many references available, our presentation is rather short, but it provides us with the fundamentals necessary for our further developments.

The next two sections of Chapter 1 are presented in order to make this work more self-contained. They provide standard results needed in the proofs found in the following chapters. In Section 1.3, we present a summary of well-known results and definitions from functional analysis. All Sobolev spaces, norms and seminorms relevant to this work are introduced in Section 1.4.

We conclude this introductory chapter with a summary of the main results presented in this work.

1.1 Short History of Superconductivity

1.1.1 The Discovery of Superconductivity

There are many good books written on superconductivity, see e.g. [24], [25], [49], [60], [70] and [78]. Here, we present a short historical introduction in which we try to highlight the most important events from its original discovery to the recent developments in this dynamic field.

Superconductivity was not observed until the early part of twentieth century. The reason is that materials become superconducting only at extremely low temperatures. As a result, the discovery of superconductivity had to be postponed until the proper technology was developed.

By 1870, despite the great number of experiments, hydrogen, nitrogen and oxygen still remained unliquified. Liquid oxygen was first obtained in 1877 at a temperature of 90.2 K (recall that $0\ K = -273^0\ C$). Six years later, in 1883, nitrogen was liquified at 77.4 K, and the liquification of hydrogen at 20 K was achieved in 1898 by Deward. At that time, the only elemental gas remaining unliquified was helium, which had been discovered in 1869. The search for "new liquids" was concluded by the dutch physicist Heike Kamerlingh-Onnes. On July 10, 1908, as a result of an exhausting 16-hour experiment, the first amount of liquid helium was produced. The boiling point of liquid helium is just 4.2 K which is significantly lower than that of liquid hydrogen.

After liquifying the last natural gas and attaining record low temperatures, Kamerlingh-Onnes changed the direction of his research. He started a systematic study of the electric resistivity of metals at liquid helium temperature. Kamerlingh-Onnes originally began working with platinum and gold samples, but then he turned his attention to mercury because it could be obtained in sufficiently pure form.

The surprise came in 1911 when Kamerlingh-Onnes (more precisely, his assistant Gilles Holst) discovered that at a temperature close to 4 K, the electric resistivity of mercury vanishes. This unexpected feature of the experiment, in his own words, was that "*The disappearance did not take place gradually, but abruptly*". He reported that "*... the mercury at 4.2 K has entered a new state, which owing to its particular electrical properties, can be called the state of superconductivity*". The highest temperature, below which superconductivity occurs is called the **critical temperature** and is denoted by T_c. It would later be determined that the critical temperature depends not only on the chemical composition, but also on the crystal structure of the material.

In 1913, Kamerlingh-Onnes won the Nobel prize in physics for "research on the properties of matter at low temperatures". His discovery was followed by a large number of experiments which resulted in finding new superconducting materials.

In 1913, Kamerlingh-Onnes found that there was a certain intensity of the current that can be carried by a superconducting sample before it reverts to its **normal** or nonsuperconducting state. This intensity is known as the **critical current density** and is denoted by J_c. A year later, Kamerlingh-Onnes discovered that a sufficiently strong applied magnetic field can also destroy the perfect conductivity of the sample. This magnitude of the field is known as the **critical magnetic field**, and is denoted by H_c. Kamerlingh-Onnes also found that both J_c and H_c are functions of the temperature and increase when the temperature is lowered below T_c. The absence of any resistance below T_c is a fundamental characteristic of superconductors. However, superconductors are more that just **perfect conductors**, they

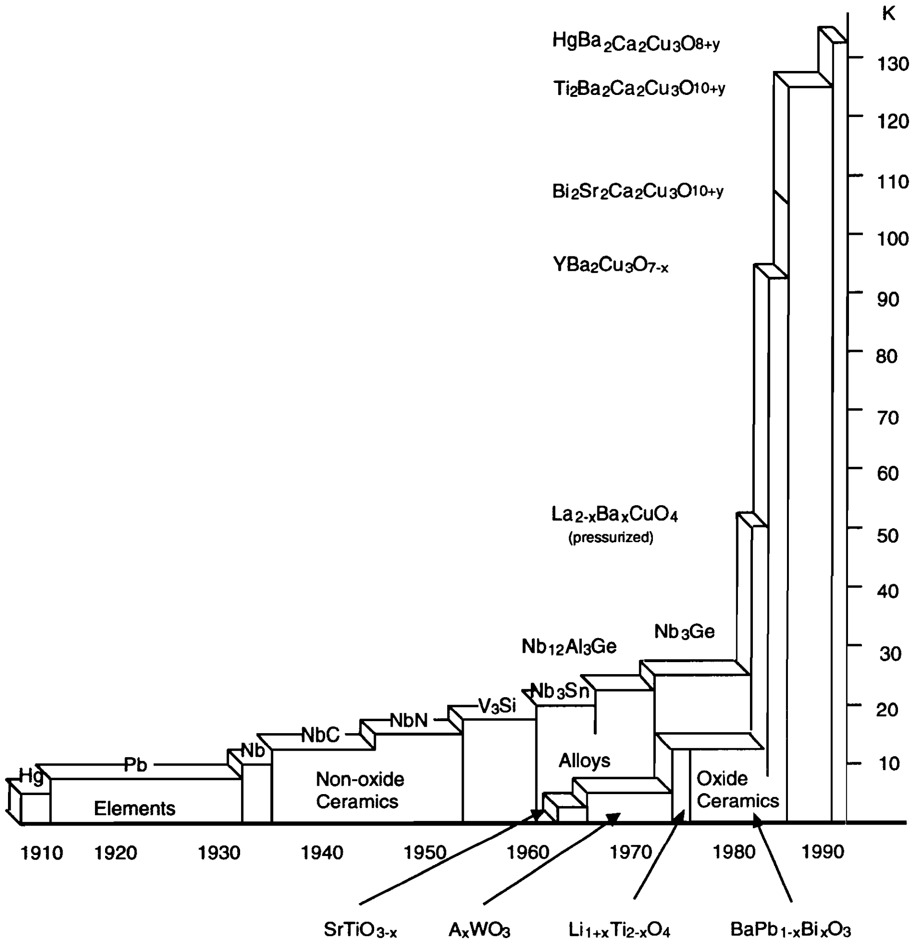

Figure 1.1: History of superconducting critical temperatures in metals, non-oxide ceramics, allows and oxide ceramics.

are also **perfect diamagnets**.

In 1933, Walter Meissner and Robert Ochsenfeld found that at temperatures below T_c and for sufficiently weak external magnetic fields, the magnetic flux is expelled from the interior of the superconductor. This effect is called the **Meissner effect** after its discoverers. Over the years there have been many attempts to find superconducting materials with higher critical temperatures, see Figure 2.1. Early researchers first investigated the metallic elements. It was found that elemental metals did not produce high enough critical temperatures. Today, the pure element with the highest transition temperature is niobium with T_c =9.26 K. Next, attention of the researchers turned to finding superconducting alloys and compounds. For several years the maximum transition temperature was gradually increased from the 4 K in 1911 to the 23 K in 1972. As a result of this slow progress many scientists abandoned their research in superconductivity since they believed that achieving a substantial advance was unlikely and even impossible. In the early 1980's the prospect of discovering a new class of superconducting materials of practical importance seemed very remote.

On January 27, 1986, a new era began in the area of superconductivity. The discovery was made by Karl Alex Müller and Johan Georg Bendorz while working at the IBM's Zürich Research Laboratory. It reflected two and a half years of exhausting experiments on oxides and resulted in carefully reported indications of superconductivity at temperatures exceeding 30 K. For their discovery, which finally changed the long standing temperature record of 23 K; they won the Nobel prize in 1988.

At first, few physicists believed their result. However, Paul Chu was one of the believers. A team in Houston started working on the new compound. By the end of 1986 they not only confirmed, but even improved Müller and Bendorz's result by discovering a new class of superconductors with transition temperatures in the range of 30-40 K. In February 1987, the group of Maw-Kuen Wu working at the University of Alabama, in collaboration with Paul Chu, announced a critical temperature of 92 K. They also have reported indications of superconductivity at much higher temperatures. This was the first superconducting material which could be cooled using inexpensive liquid nitrogen which brought about the belief that the superconductivity had entered the era of practical applications. A year later,

Table 1.1: The critical temperature T_c and critical magnetic field H_c for selected superconducting materials.

Conventional superconductors	T_c/K	H_c/T
Metallic elements:		
Al	1	0.01
Pb	7	0.08
Nb	9	0.2
Binary alloys:		
$Nb-Ti$	9	14
Binary compounds:		
Nb_3Ge	18	24
Nb_3Ge	23	38
Organic phases:		
$\kappa-(BEDT-TTF)_2Cu(NCS)_2$	12	20
Chevrel phases:		
$PbMo_6S_8$	15	60
High-T_c cuprate oxides:	T_c/K	H_c/T
$La_{2-x}Sr_xCuO_4$	38	40
$YBa_2Cu_3O_7$	92	≥ 100
$Bi_2Ca_2Sr_2Cu_3O_{10}$	110	≥ 120
$Tl_2Ca_2Ba_2Cu_3O_{10}$	125	≥ 130

in 1988, the record transition temperature of 125 K (that is $0\ K = -148^0\ C$) was announced. This is the last confirmed result so far, see Table 2.1. The majority of superconductors are not pure elements, but alloys and compounds. Today over 6000 superconducting materials are known, and this number is constantly growing.

Superconductivity has a very wide spectrum of potential applications. However, the practical applications of superconductivity have been limited because of the difficulties and the cost of cooling to the very low temperatures and due to unexpected mechanical problems. Some of the most important existing applications of superconductivity include very sensitive magnetometers, powerful supermagnets and fast electronic devices. For example, superconducting magnets are used in magnetic resonance imaging, particle colliders and magnetic bearings.

High T_c superconductivity is a young and developing discipline. Recent developments during 1988-1989 appear to have thrown new light on the question of the critical current that is essential from the point of view of applications. However, experiments suggest that the behavior of the oxide superconductors in a magnetic field may very well be fundamentally different from that of conventional T_c superconductors. Some properties of the newly discovered T_c materials suggest delay for many of the potential applications.

1.1.2 Models of Superconductivity

Ever since its discovery in 1911, scientists are trying to better understand and explain the nature of the superconducting phenomena. Over the years, a series of models were proposed, which revealed the superconducting mechanism in various degrees. Any theory trying to describe the superconducting nature must include its electric as well as its magnetic properties.

In 1934, the year following the discovery of the Meissner effect, Fritz and Heinz London proposed a simple two-fluid model, see [65]. It is often referred to as the **classical model** of superconductivity. The London model incorporated the basic superconducting properties, namely zero resistivity and perfect diamagnetism. The London model explained the Meissner effect and also predicted the existence of the so called **penetration depth**, usually denoted by λ. This parameter is a characteristic length which determines how far the static magnetic flux penetrates into the surface of the superconducting sample. Despite its empirical character, the London model was very useful since it helped to reveal the nature of several important superconducting applications such as superconducting memories and magnetically levitated trains. However, this model was unable to explain certain phenomena that were exhibited by superconductors with high critical temperatures.

In 1948 Fritz London proposed the **macroscopic quantum model**. He showed that the electromagnetic constitutive relations proposed in the London model were, in fact, a result of the quantum mechanical nature of superconductivity. In this way he showed that the electromagnetic and the quantum mechanical properties of the superconductivity were related. Today, this model is used to study **Josephson effects**, postulated in 1962 by Brian Josephson.

In 1950, Vitaly Ginzburg and Lev Landau proposed an intuitive, phenomenological theory. In this **macroscopic** theory, they incorporated not only the electromagnetic, but also the thermodynamic, properties of superconductivity, see [44]. The **Ginzburg – Landau** (G-L) theory was itself based on a more general theory for phase transitions in fluids, introduced by Landau in 1937. It provided a phenomenological description of superconductivity as a new type of phase transition. Ginzburg and Landau postulated that the global minimizer of the Helmholtz energy, calculated from a scalar **order parameter** ψ and a vector **magnetic potential A**, determines the electromagnetic state of the material. This remarkably powerful theory provides a significant contribution to the general understanding of superconducting phenomena.

In 1957 Alexei Abrikosov, a former student of Landau, studied the behavior of superconductors in the presence of an external magnetic field, see [2]. He discovered that one can distinguish two types of superconducting materials: **type I** and **type II**, having surprisingly different behavior. For type I materials, the phase transition from the normal to the superconducting state at H_c, the critical magnetic field, is of first order and is irreversible. In contrast, the type II materials exhibit a reversible second order phase transition at $\mathbf{H}_c$, see Figure 2.2.

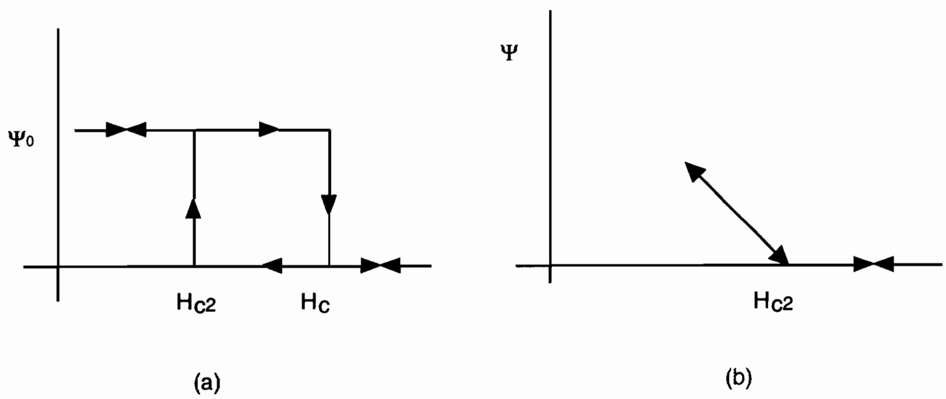

Figure 1.2: The transition from the normal to the superconducting state. (a) Hysteresis loop for type I superconductors. (b) Reversible, second order transition for type II superconductors.

A remarkable feature of the G-L theory was that it allowed for prediction of the type II superconductors before they were observed experimentally. In his work Abrikosov also showed that for type II superconductors there exists one more phase, in addition to the normal and superconducting states. It is known as the **mixed state** because of the coexisting of the normal and superconducting phases. In the mixed state, the magnetic field penetrates the superconducting sample in tiny tubes of normal states. These tiny tubes are called **vortices** since each vortex consist of currents circulating around a normal (non-superconducting) core. As the field increases, more vortices appear and they become packed closer together. The practical implication of these vortices is one of the most active topic of investigation in the study of superconductivity.

It is known that when a transport current is applied to a type II material, the vortices will move because of various forces acting on them, see Figure 2.3. It is established that the motion of vortices causes resistance and thus loss of superconductivity. Therefore, there is a major theoretical as well as practical interest in studying the dynamics of vortices.

Two length scales play important roles in the understanding of the superconductivity.

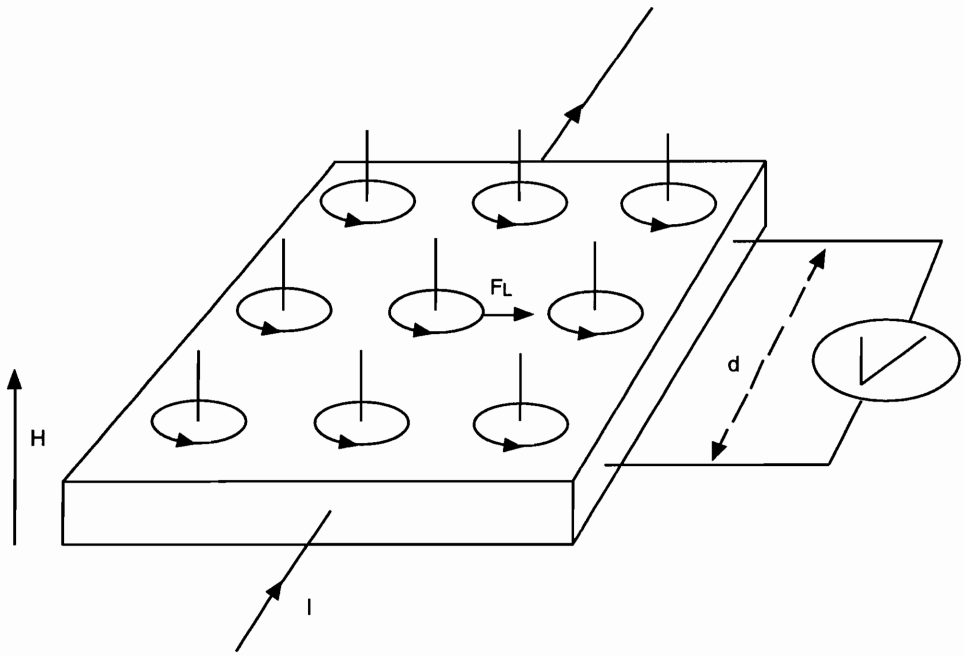

Figure 1.3: Fluxoid motion due to Lorentz force F_L, from a passing current.

The (London) penetration length λ was already introduced. The other length scale, which gives the variations of the order parameter ψ, is introduced in the Ginzburg Landau theory. It is called the (G-L) **coherence length** and is usually denoted by ξ. These two length scales are typically temperature dependent and diverge as the temperature approaches the critical temperature T_c. The ratio of the penetration length to the coherence length is known as the **Ginzburg Landau parameter** and is denoted by κ. It is a roughly temperature independent quantity and characterizes the property of the material. The importance of κ lies in the fact that the G-L equations can be expressed in terms of this single parameter.

Abrikosov found that if $\kappa < 1/\sqrt{2}$, the surface energy of a normal-superconducting interface is positive, and the material is a type I superconductor. These materials tend to have low critical temperatures. They also loose superconductivity at relatively low critical magnetic fields which makes them unattractive from a technological point of view.

On the other hand, if $\kappa > 1/\sqrt{2}$ the surface energy is negative and the material is of type II. A type II superconductor typically has longer penetration depth λ than coherence length ξ. This makes type II materials the technologically interesting superconductors since they remain superconducting at higher applied magnetic fields and currents.

As we have mentioned, superconductors are characterized by the value of κ. It is known that the recently experimentally discovered high temperature superconductors have rather large values of κ which fall in the range of 100-200. This justifies the interest in exploring the behavior of superconductors in the limit of high κ. There are many studies of models in the high κ limit. In most of them is assumed that the applied magnetic field is of fixed strength and is independent of κ, see [1], [10], [40], [54], [61], [78]. The present work is in close relation with the model derived in [19] and [37]. High magnetic fields are also of technological interest and have been considered in ; e.g., [1], [56].

Despite its power, the G-L theory did not explain how superconductivity occurs. Since superconductivity is a microscopic quantum phenomena, it was not possible to explain its nature before sufficient advance were made in the field of quantum mechanics. In 1957, John Bardeen, Leon Cooper, and Robert Schrieffer at the University of Illinois proposed a complete **microscopic** theory of superconductivity, see [8]. It is referred to as the **BCS theory**. This theory not only explained what was known about superconductivity, but also predicted new phenomena, which was later confirmed by experiment. The BCS theory is based on the notion that the conduction electrons travel without meeting resistance because they move in pairs, known as **Cooper pairs**. According to the BCS theory, at temperatures above T_c thermal fluctuations destroy the Cooper pairs and consequently the material loses superconductivity. For their innovative work Bardeen, Cooper, and Schrieffer won the Nobel prize.

Despite its power and elegance, the BCS theory is usually not necessary for the description of most superconducting applications. Moreover, the BCS theory may not be adequate in explaining the phenomena of high T_c superconductivity. However, the BCS theory still provides the basis for our understanding of superconductivity in "conventional" materials and plays a role of the "reference" theory in the search for the description of superconductivity in the high T_c oxides.

Initially, the G-L theory was not widely accepted mainly due to its phenomenological character. In 1959 L. Gorkov, see [46], showed that the microscopic BCS theory reduces to the macroscopic G-L theory near the critical temperature T_c. This showed that the important conclusions in the more tractable phenomenological G-L model are consistent with the microscopic BCS theory. As a result, the G-L phenomenological theory was widely accepted as valid and Ginzburg and Landau won the Nobel prize.

In conclusion of this short survey, we want to list some of the many excellent references that may be consulted for detailed descriptions of both the microscopic and macroscopic theories of superconductivity. Among these are [12], [43], [61], [54], [78]. In particular, for more information on the G-L model one may consult [10], [15], [20], [21], [38], [57], [69], [74], [75], [81], [82].

1.2 The Time-Independent and Time-Dependent G-L Models

We start with a brief introduction of the steady-state G-L equations. According to Ginzburg and Landau the Helmholtz free energy per unit volume of a superconducting material is given by

$$f = f_n + \alpha|\psi|^2 + \frac{\beta}{2}|\psi|^4 + \frac{|\mathbf{h}|^2}{8\pi} + \frac{1}{2m_s}\left|\left(-i\hbar\nabla - \frac{e_s\mathbf{A}}{c}\right)\psi\right|^2,$$

where f_n is the free energy of the normal state in the absence of an applied magnetic field $\mathbf{H}$, α and β are constants depending on the temperature T, ψ is the complex-valued order parameter, $\mathbf{A}$ is the vector-valued magnetic potential, $\mathbf{h}$ is the magnetic field in the sample, e_s and m_s are the charge and mass of the superconducting carriers, c is the speed of light and $2\pi\hbar$ is Planck's constant.

We are interested in the behavior of the superconducting sample in the presence of an applied magnetic field $\mathbf{H}$. In this case the appropriate thermodynamical potential is the Gibbs free energy g. It essentially differs from f by the work done by the electromagnetic force induced by the applied field and is given explicitly by

$$g = f - \frac{\mathbf{h}\cdot\mathbf{H}}{4\pi}.$$

If Ω denotes the region occupied by the superconducting sample, then in the presence of a magnetic field $\mathbf{H}$ the Gibbs free energy of the sample is given by

$$\mathcal{G}(\psi, \mathbf{A}) = \int_\Omega g \, d\Omega.$$

The **basic thermodynamic postulate** of the G-L theory says that the superconducting sample is in a state such that the Gibbs free energy $\mathcal{G}$ is minimized. A detailed discussion concerning existence of various minimizers of $\mathcal{G}$ and their properties is given in [35].

In order to derive nondimensionalized equations we introduce a length scale l and make the following change of variables

$$\tilde{\mathbf{x}} = \frac{\mathbf{x}}{l},$$

$$\tilde{\mathbf{A}} = \frac{\mathbf{A}}{\sqrt{2} l H_c}, \qquad \tilde{\psi} = \frac{\psi}{\psi_s}, \tag{1.2.1}$$

where

$$\psi_s = \left(-\frac{\alpha}{\beta}\right)^{1/2} \quad \text{(the value corresponding to perfect conductivity)},$$

$$H_c = \left(\frac{4\pi\alpha^2}{\beta}\right)^{1/2} \quad \text{(the thermodynamic magnetic field)},$$

$$\lambda = \left(-\frac{\beta m_s c^2}{4\pi\alpha e_s^2}\right)^{1/2} \quad \text{(the penetration depth)}, \tag{1.2.2}$$

$$\xi = \left(-\frac{\hbar^2}{2m_s\alpha}\right)^{1/2} \quad \text{(the coherence length)}. \tag{1.2.3}$$

Both constants α and β are temperature dependent. For $\mathcal{G}$ to have a minimum, β must be positive. On the other hand, α may be positive or negative. If we neglect the boundary effects then positive α corresponds to a minimizer $(\psi = 0, \mathbf{h} = \mathbf{H})$, i.e. the material is in a normal (nonsuperconducting) state. If α is negative then the minimizer of $\mathcal{G}$ is $(\psi = \psi_s, \mathbf{h} = 0)$ and the sample is a perfect superconductor.

Using (1.2.1) and keeping the same notation, one can write the Gibbs free energy in the following non-dimensional form

$$\begin{aligned} \mathcal{G}(\psi, \mathbf{A}) &= \int_\Omega \left(f_n - |\psi|^2 + \tfrac{1}{2}|\psi|^4 + \left| \left(-i\left(\tfrac{\xi}{l}\right)\nabla - \left(\tfrac{l}{\lambda}\right)\mathbf{A}\right)\psi \right|^2 \right) d\Omega \\ &\quad + \int_\Omega \left(|\mathbf{h}|^2 - 2\mathbf{h}\cdot\mathbf{H} \right) d\Omega. \end{aligned} \tag{1.2.4}$$

A very important property of the energy functional (1.2.4) is its invariance under **gauge transformations**. This means that if ϕ denotes any sufficiently smooth real-valued function on Ω then the transformed pair $(\bar{\psi}, \bar{\mathbf{A}})$

$$\bar{\psi} = \psi\, e^{i\kappa\phi}, \quad \bar{\mathbf{A}} = \mathbf{A} + \nabla\phi$$

yields the same energy as that of $(\psi, \mathbf{A})$. Indeed, $(\psi, \mathbf{A})$ and $(\bar{\psi}, \bar{\mathbf{A}})$ are considered as equivalent representatives of the same magnetic state of the material.

This **gauge invariance** has several consequences. First, there is not only one single minimizer to the free energy, but an entire class of gauge equivalent solutions. Second, we can search for solutions that have special properties. The extraction of a unique solution has traditionally been called "fixing the gauge". For more detailed discussion of the possible gauge choices and their implications in the numerical simulations one may refer to [33] and [35].

Following [19] we note that if the superconductor occupies an infinite cylinder having bounded cross-section Ω and if the applied field $\mathbf{H}_e$ is perpendicular to this cross-section, then the field in the region exterior to the cylinder is constant and equal to the applied field. In this case we need only to consider a bounded region $\Omega \subset \mathbb{R}^2$ when forming the Gibbs free energy, see [19]. We denote the boundary of Ω by Γ. Let $\mathbf{n}$ be the unit outer normal vector to Γ. The nondimensional time independent G-L equations may be derived by minimizing the Gibbs free energy $\mathcal{G}$ with respect to the order parameter ψ and the magnetic potential $\mathbf{A}$ over a suitable function space. Using standard techniques from Calculus of Variations the nondimensional time-independent G-L equations are given by

$$-\psi + \psi|\psi|^2 + \left(-i\left(\frac{\xi}{l}\right)\nabla - \left(\frac{l}{\lambda}\right)\mathbf{A}\right)^2 \psi = 0 \quad \text{in} \quad \Omega, \tag{1.2.5}$$

$$\mathbf{curl}\ \mathrm{curl}\ \mathbf{A} = -\frac{i}{2}\left(\frac{\xi}{\lambda}\right)(\psi^*\nabla\psi - \psi\nabla\psi^*) - \left(\frac{l}{\lambda}\right)^2 |\psi|^2\mathbf{A} + \mathrm{curl}\ \mathbf{H} \quad \text{in} \quad \Omega, \tag{1.2.6}$$

where ψ^* denotes the complex conjugate of ψ along with the nondimensional natural boundary conditions

$$\left(i\left(\frac{\xi}{l}\right)\nabla\psi + \left(\frac{\lambda}{l}\right)\mathbf{A}\psi\right)\cdot\mathbf{n} = 0 \quad \text{on} \quad \Gamma, \tag{1.2.7}$$

$$\text{curl}\,\mathbf{A} \quad = \quad \mathbf{H} \quad \text{on} \quad \Gamma. \tag{1.2.8}$$

For more details on the derivation of the steady state G-L models, one may consult some of the many good references available, e.g. [1], [16], [20], [35], [42], [54], [61], [62], [78] and [82].

The objective of this work is to derive and analyze a time-dependent G-L type model valid for large values of κ which accounts for effects of both applied magnetic field and current. Our model is based on the time-dependent G-L system (TDG-L) presented in 1968 by Gor'kov and Kopnin in [47], see also [1], [16], [47] and [78]. Their derivation consists of averaging the BCS theory under the assumption that the temperature is close to T_c. The relations between TDG-L and the basic hypotheses in the G-L theory were discussed in [33]. Similar TDG-L models were studied in [82]. Other time dependent models are presented in [16], [20], [41], [52], [64] and [71].

The TDG-L system derived in [47] is given by

$$\gamma\left(\hbar\frac{\partial\psi}{\partial t} + ie_s\Phi\psi\right) + \alpha\psi + \beta|\psi|^2\psi + \frac{1}{2m_s}\left(i\hbar\nabla + \frac{e_s\mathbf{A}}{c}\right)^2\psi = 0 \text{ in } \Omega\times[0,\infty), \tag{1.2.9}$$

$$\begin{aligned} &\frac{\sigma_n}{c}\left(\frac{1}{c}\frac{\partial\mathbf{A}}{\partial t} + \nabla\Phi\right) + \frac{1}{4\pi}\mathbf{curl}\,\text{curl}\,\mathbf{A} \\ &+\frac{e_s^2}{m_sc^2}|\psi|^2\mathbf{A} + \frac{ie_s\hbar}{2m_sc}\left(\psi^*\nabla\psi - \psi\nabla\psi^*\right) \quad = \quad 0 \quad \text{in} \quad \Omega\times[0,\infty), \end{aligned} \tag{1.2.10}$$

$$\left(i\hbar\nabla\psi + \frac{e_s}{c}\mathbf{A}\psi\right)\cdot n = 0 \text{ on } \Gamma\times[0,\infty), \tag{1.2.11}$$

$$\text{curl}\,\mathbf{A} = \mathbf{H} \text{ on } \Gamma\times[0,\infty), \tag{1.2.12}$$

$$\psi|_{t=0} = \psi^0 \text{ in } \Omega, \tag{1.2.13}$$

$$\mathbf{A}|_{t=0} = \mathbf{a} \text{ in } \Omega\,, \tag{1.2.14}$$

where Φ is the scalar electric potential, σ_n and γ are microscopic parameters, c and $\hbar$ are as defined in the time-independent G-L model. We note that in two dimensions applying the *curl* operator to a vector results in a scalar and applying it to a scalar results in a vector. The above equations are also used in [37].

Using (1.2.1) and nondimensionalizing the new variables as follows

$$\begin{aligned} \tilde{t} &= \tau_0 t, \\ \tilde{\Phi} &= \varphi_0 \Phi, \end{aligned}$$

we can write (1.2.9)-(1.2.10) in the following form

$$\begin{aligned} \gamma\hbar\tau_0\psi_0\frac{\partial\tilde{\psi}}{\partial\tilde{t}} + \frac{i\gamma e_s\psi_0}{\varphi_0}\tilde{\Phi}\tilde{\psi} + \alpha\psi_0\tilde{\psi} + \beta\psi_0^3|\tilde{\psi}|^2\tilde{\psi} & \\ +\frac{1}{2m_s}\left(\frac{i\hbar}{l}\tilde{\nabla} + \frac{e_s\sqrt{2}lH_c}{c}\tilde{\mathbf{A}}\right)^2\psi_0\tilde{\psi} &= 0, \end{aligned} \tag{1.2.15}$$

and

$$\begin{aligned} \frac{\sigma_n\sqrt{2}lH_c\tau_0}{c^2}\frac{\partial\tilde{\mathbf{A}}}{\partial t} + \frac{\sigma_n}{c\varphi_0 l}\tilde{\nabla}\tilde{\Phi} + \frac{\sqrt{2}H_c}{4\pi l}\tilde{\mathbf{curl}}\,\tilde{\mathrm{curl}}\;\tilde{\mathbf{A}} & \\ +\frac{e_s^2\psi_0^2\sqrt{2}lH_c}{m_s c^2}|\tilde{\psi}|^2\tilde{\mathbf{A}} + \frac{ie_s\hbar|\psi_0|^2}{2m_s cl}\left(\tilde{\psi}^*\tilde{\nabla}\tilde{\psi} - \tilde{\psi}\tilde{\nabla}\tilde{\psi}^*\right) &= 0. \end{aligned} \tag{1.2.16}$$

In order to simplify the coefficients of $|\tilde{\psi}|^2\tilde{\psi}$ and $|\tilde{\psi}|^2\tilde{\mathbf{A}}$, we multiply (1.2.15) by $(\beta\psi_0^3)^{-1}$ and (1.2.16) by $m_s c^2 l^2/(e_s^2\psi_0^2\sqrt{2}lH_c\lambda^2)$, where λ and ξ are given in (1.2.2) and (1.2.3). One gets

$$\gamma\hbar\tau_0\frac{\partial\tilde{\psi}}{\partial\tilde{t}} + \frac{i\gamma e_s}{\varphi_0|\alpha|}\tilde{\Phi}\tilde{\psi} - \tilde{\psi} + |\tilde{\psi}|^2\tilde{\psi} - \left(i\left(\frac{\xi}{l}\right)\tilde{\nabla} + \left(\frac{l}{\lambda}\right)\tilde{\mathbf{A}}\right)^2\tilde{\psi} = 0 \tag{1.2.17}$$

and

$$\begin{aligned} \frac{\sigma_n\sqrt{2}lH_c\tau_0}{c^2}\frac{\partial\tilde{\mathbf{A}}}{\partial\tilde{t}} + \frac{\sigma_n}{c\varphi_0 l}\tilde{\nabla}\tilde{\Phi} + \frac{\sqrt{2}H_c}{4\pi l}\tilde{\mathbf{curl}}\,\tilde{\mathrm{curl}}\;\tilde{\mathbf{A}} & \\ +\frac{e_s^2\psi_0^2\sqrt{2}lH_c}{m_s c^2}|\tilde{\psi}|^2\tilde{\mathbf{A}} + \frac{ie_s\hbar\psi_0^2}{2m_s cl}\left(\tilde{\psi}^*\tilde{\nabla}\tilde{\psi} - \tilde{\psi}\tilde{\nabla}\tilde{\psi}^*\right) &= 0. \end{aligned} \tag{1.2.18}$$

We multiply (1.2.18) by $4\pi l/(\sqrt{2}H_c)$ and denote

$$\sigma = \sigma_n \frac{4\pi|\alpha|l^2}{\gamma\hbar c^2}. \tag{1.2.19}$$

Choosing $\varphi_0 = \gamma e_s/(|\alpha|)$ and and $\tau_0 = |\alpha|/(\gamma\hbar)$ we get

$$\left(\frac{\partial\tilde{\psi}}{\partial\tilde{t}} + i\tilde{\Phi}\tilde{\psi}\right) - \tilde{\psi} + |\tilde{\psi}|^2\tilde{\psi} + \left(i\left(\frac{\xi}{l}\right)\tilde{\nabla} + \left(\frac{l}{\lambda}\right)\tilde{\mathbf{A}}\right)^2\tilde{\psi} = 0, \tag{1.2.20}$$

and

$$\begin{aligned} \sigma\left(\frac{\partial\tilde{\mathbf{A}}}{\partial\tilde{t}} + \left(\frac{\lambda}{l}\right)\left(\frac{\xi}{l}\right)\tilde{\nabla}\tilde{\Phi}\right) + \tilde{\mathbf{curl}}\ \tilde{\mathrm{curl}}\ \tilde{\mathbf{A}} & \\ + \left(\frac{l}{\lambda}\right)^2|\tilde{\psi}|^2\tilde{\mathbf{A}} + \frac{i}{2}\left(\frac{\xi}{\lambda}\right)\left(\tilde{\psi}^*\tilde{\nabla}\tilde{\psi} - \tilde{\psi}\tilde{\nabla}\tilde{\psi}^*\right) &= 0. \end{aligned} \tag{1.2.21}$$

Keeping the same notation as for the dimensional variables, we arrive at the following nondimensional initial boundary-value system for the complex valued order parameter ψ, the vector valued magnetic potential $\mathbf{A}$ and the scalar electric potential Φ

$$\left(\frac{\partial\psi}{\partial t} + i\Phi\psi\right) - \psi + |\psi|^2\psi + \left(i\left(\frac{\xi}{l}\right)\nabla + \left(\frac{l}{\lambda}\right)\mathbf{A}\right)^2\psi = 0 \ \text{ in } \ \Omega \times [0,\infty), \tag{1.2.22}$$

$$\begin{aligned} &\sigma\left(\frac{\partial\mathbf{A}}{\partial t} + \left(\frac{\lambda}{l}\right)\left(\frac{\xi}{l}\right)\nabla\Phi\right) + \mathbf{curl}\ \mathrm{curl}\ \mathbf{A} + \left(\frac{l}{\lambda}\right)^2|\psi|^2\mathbf{A} \\ &\quad + \frac{i}{2}\left(\frac{\xi}{\lambda}\right)(\psi^*\nabla\psi - \psi\nabla\psi^*) = 0 \quad \text{in} \quad \Omega \times [0,\infty), \end{aligned} \tag{1.2.23}$$

$$\left(i\left(\frac{\xi}{l}\right)\nabla\psi + \left(\frac{l}{\lambda}\right)\mathbf{A}\psi\right)\cdot\mathbf{n} = 0 \ \text{ on } \ \Gamma \times [0,\infty), \tag{1.2.24}$$

$$\mathrm{curl}\ \mathbf{A} = \mathbf{H} \ \text{ on } \ \Gamma \times [0,\infty), \tag{1.2.25}$$

$$\psi|_{t=0} = \psi^0 \ \text{ in } \Omega, \tag{1.2.26}$$

$$\mathbf{A}|_{t=0} = \mathbf{a} \ \text{ in } \ \Omega. \tag{1.2.27}$$

The nondimensionalized physical variables of interest are

$$
\begin{aligned}
\mathbf{h} &= \text{curl } \mathbf{A} \ \ \text{(the magnetic field)},\\
\mathbf{j} &= \text{curl } \mathbf{h} \ \ \text{(the current)},\\
N_s &= |\psi|^2 \ \ \text{(the density of superconducting charge carriers)}
\end{aligned}
$$

and

$$
\mathbf{E} = -\left(\frac{\partial \mathbf{A}}{\partial t} + \left(\frac{\lambda}{l}\right)\left(\frac{\xi}{l}\right)\nabla\Phi\right) \ \ \text{(the electric field)}.
$$

The TDG-L system (1.2.22)-(1.2.27) has the gauge invariant property, see [33], [78]. Since the equations lack uniqueness of solutions, it follows that they are not well-posed. In order to obtain a mathematically well-posed system, one may fix the gauge by imposing extra conditions on the solutions. This is usually done by requiring the solutions to satisfy appropriate essential boundary conditions. For different possible gauge choices in the TDG-L equations one may consult [33]. The particular gauge choice in the High kappa model will be given in Chapter 2.

There are many TDG-L type models proposed in the literature to approximate the behavior of high-T_c materials see, e.g., [17], [18], [19], [32], [33], [34], [35] and [37]. They are based on different modifications of the G-L equations. Among them is the High kappa time independent G-L type model presented in [19] valid for high values of the applied magnetic field $\mathbf{H}$ and the G-L parameter κ. In this work we present a TDG-L type model, referred as the High kappa model, for approximating the behavior of high-T_c superconductors under applied electric current and magnetic field. The High kappa model may be viewed as a generalization of the time independent high kappa model presented in [19] and was originally presented in [37]. The two aspects of the generalization are the fact that the High kappa model is time dependent and in addition to the applied magnetic field it also incorporates effects of applied constant current.

1.3 Summary of Standard Results from Functional Analysis

In order to make this work more self contained, in this section we have collected some standard definitions and theoretical results used throughout this work.

We assume that the reader is familiar with the concepts of a vector (linear) and normed vector spaces. In what follows we assume that $\Omega \subset \mathbb{R}^n$ is a bounded set with a Lipschitz continuous boundary Γ. We recall the following standard definition, see [72].

Definition 1.1 *A normed vector space is called a* **Banach** *space if it is complete, i.e. if every Cauchy sequence converges.*

For $\Omega \subset \mathbb{R}^n$ and $1 \leq p < \infty$ we define the standard normed vector spaces $\tilde{L}^p(\Omega)$ as follows

Definition 1.2 *Let $\tilde{L}^p(\Omega)$ be the set of all continuous functions $u : \bar{\Omega} \longrightarrow \mathbb{R}$ for which*

$$||u||_p = \left(\int_\Omega |u(x)|^p \, dx \right)^{1/p} < \infty.$$

We recall the following well known result.

Lemma 1.1 *(Hölder's inequality) Let $f \in \tilde{L}^p(\Omega)$, $g \in \tilde{L}^q(\Omega)$, where p, $q \in (1, \infty)$ with $p^{-1} + q^{-1} = 1$. Then $fg \in \tilde{L}^1(\Omega)$ and*

$$||fg||_1 \leq ||f||_p \, ||g||_q \quad \Box. \tag{1.3.1}$$

Following [55], we continue with a few simple concepts from linear algebra. Let B be a linear space.

Definition 1.3 *We say that* $L(\cdot)$ *is a* **linear form** *on* B *if* $L: \; B \longrightarrow \mathbb{R}$ *and for all* $v, w \in B$ *and for* $\alpha, \beta \in \mathbb{R}$ *we have*

$$L(\alpha v + \beta w) = \alpha L(v) + \beta L(w). \tag{1.3.2}$$

Definition 1.4 *We say that* $a(\cdot,\cdot)$ *is a* **bilinear form** *on* $B \times B$ *if* $a: B \times B \longrightarrow \mathbb{R}$ *and for all* $u, v, w \in B$ *and* $\alpha, \beta \in \mathbb{R}$, *we have*

$$a(u, \alpha v + \beta w) = \alpha a(u, v) + \beta a(u, w) \tag{1.3.3}$$

and

$$a(\alpha u + \beta v, w) = \alpha a(u, w) + \beta a(v, w). \tag{1.3.4}$$

Definition 1.5 *We say that* $b(\cdot,\cdot,\cdot)$ *is a* **trilinear form** *on* $B \times B \times B$ *if* $b: B \times B \times B \longrightarrow \mathbb{R}$ *is linear in each argument.*

Definition 1.6 *The bilinear for* $a(\cdot,\cdot)$ *on* $B \times B$ *is* **symmetric** *if*

$$a(v, w) = a(w, v) \quad \forall\, v, w \in B. \tag{1.3.5}$$

Definition 1.7 *A symmetric bilinear form* $a(\cdot,\cdot)$ *on* $B \times B$ *is a* **scalar product** *on* B *if*

$$a(v, v) > 0 \quad \forall\, v \in B\,, \quad v \neq 0. \tag{1.3.6}$$

Definition 1.8 *The* **norm** $\|\cdot\|_a$, *associated with a scalar product* $a(\cdot,\cdot)$, *is defined by*

$$\|v\|_a = (a(v, v))^{1/2}. \tag{1.3.7}$$

Definition 1.9 *If $(\cdot,\cdot)$ is a scalar product, with corresponding norm $||\cdot||$, then we have the* **Cauchy-Schwarz inequality**

$$|(v, w)| \leq ||v|| \, ||w||. \tag{1.3.8}$$

We will make use of the following definitions.

Definition 1.10 *If B is a linear space, with a scalar product and corresponding norm $||\cdot||$, then B is said to be a* **Hilbert space**, *if B is complete.*

Now, let B be a Hilbert space with scalar product $(\cdot,\cdot)$ and corresponding norm $||\cdot||_B$. Let $a(\cdot,\cdot)$ be a bilinear form on $B \times B$ and $L(\cdot)$ a linear form on B. Then we have the following definition.

Definition 1.11 *$a(\cdot,\cdot)$ is* **continuous** *if there exists a constant $C_c > 0$ such that*

$$|a(v, w)| \leq C_c ||v||_B \, ||w||_B \quad \forall \, v, w \in B. \tag{1.3.9}$$

Definition 1.12 *$a(\cdot,\cdot)$ is* **coercive** *if there exists a constant $C_a > 0$ such that*

$$|a(v, v)| \geq C_a ||v||_B^2 \quad \forall \, v \in B. \tag{1.3.10}$$

Definition 1.13 *$L(\cdot)$ is* **continuous** *if there exists a constant $C_F > 0$ such that*

$$|L(v)| \leq C_F ||v||_B \quad \forall \, v \in B. \tag{1.3.11}$$

We continue with a list of some well known results which will be used in the sequel. Our presentation closely follows [22].

Lemma 1.2 *(Lax-Milgram Lemma) Let V be a real Hilbert space, let $a(\cdot,\cdot)$ be a continuous, coercive bilinear form on $V \times V$, and let $f : V \longrightarrow \mathbb{R}$ be a continuous linear form. Then the abstract weak problem:*

Seek $u \in V$ such that

$$a(u,v) = f(v) \quad \forall\, v \in V, \tag{1.3.12}$$

has one and only one solution.

Lemma 1.3 *(Cea's Lemma) Let the assumptions in the Lax-Milgram Lemma hold. In addition, let $\{V_h\}$ denote a family of finite dimensional subspaces of the space V. Let $u_h \in V_h$ be the solution of the associated discrete problem*

$$a(u_h, v_h) = f(v_h) \quad \forall\, v_h \in V_h. \tag{1.3.13}$$

Then there exists a constant C independent of the subspace V_h, such that the following abstract error estimate holds

$$\|u - u_h\| \le C \inf_{v_h \in V_h} \|u - v_h\|, \tag{1.3.14}$$

where $\|\cdot\|$ denotes the norm on the space.

Cea's Lemma provides us with a convergence result in the norm on V which is the space where the abstract weak problem (1.3.12) has been defined. In order to derive convergence results in weaker norms one can use a duality argument known as the Aubin-Nitsche Lemma. Before we state this lemma some notation must be established.

We consider the **dual problem** of problem (1.3.12) given by

Seek $\varphi \in V$ such that

$$a(v,\varphi) = g(v) \quad \forall\, v \in V \tag{1.3.15}$$

where g is continuous linear form on V.

Let X, Y be normed spaces and let f be an operator from X into Y.

We say that the normed space X is **imbedded** in the normed space Y, if X is a vector subspace of Y, and the identity operator I defined on X into Y by $Ix = x \quad \forall x \in X$ is continuous.

Definition 1.14 *We say that X is* **compactly imbedded** *in Y if the imbedding operator I is compact.*

In what follows, the notation $X \hookrightarrow Y$ indicates that the normed linear space X is contained in the normed linear space Y with a continuous injection. Also, the notation $X \overset{c}{\subset} Y$ indicates in addition the compactness of the injection.

Lemma 1.4 *(Aubin-Nitsche Lemma) Let the hypotheses in Cea's Lemma hold. In addition, let H be a Hilbert space with norm $|\cdot|$ and an inner product $(\cdot,\cdot)$ such that*

$$\bar{V} = H \quad \textit{and} \quad V \hookrightarrow H.$$

For any $g \in H$ let $\varphi_g \in V$ be the unique solution of the variational problem

$$a(v, \varphi_g) = (g, v) \quad \forall\, v \in V. \tag{1.3.16}$$

Then, one has the estimate

$$|u - u_h| \leq M\|u - u_h\| \left(\sup_{g \in H} \left\{ \frac{1}{|g|} \inf_{\varphi_h \in V_h} \|\varphi_g - \varphi_h\| \right\} \right). \tag{1.3.17}$$

Let J be an interval of real numbers with nonempty interior. Then we define $C(J)$ as

$$C(J) = \{f : f \textit{ maps } J \textit{ into } \mathbb{R} \textit{ and } f \textit{ is continuous}\}. \tag{1.3.18}$$

Similarly, for any subset $D \in \mathbb{R}^d$ one can define $C(D)$. We have the following definition.

Definition 1.15 *A function* $f \in C(D)$ *is said to be* **Lipschitz continuous** *in* **x** *with a Lipschitz constant L if*

$$|f(t,x) - f(t,y)| \le L|x - y|. \tag{1.3.19}$$

For the last definition one may consult [67].

1.4 Notation

In this section we introduce the notation for the spaces that will be used throughout this work and state several imbedding theorems. For further details, the reader may refer to a standard text on Sobolev spaces, such as [3].

Let $\mathcal{D}$ be a domain in $\mathbb{R}^d, d = 2,3$ and let Γ denote its boundary. By $\mathbf{n}$ we shall denote the outward normal to Γ.

With α and $|\alpha|$ we denote a multiindex and its norm, that is $\alpha = (\alpha_1, ..., \alpha_d)$ and $|\alpha| = \sum_{i=1}^{d} \alpha_i$, respectively. Finally $\partial^\alpha v$ will denote the generalized derivative of order $|\alpha|$ for the function v.

Let $L^p(\mathcal{D})$ denote the completion of the space $\tilde{L}^p(\mathcal{D})$ with respect to the norm $\|\cdot\|_p$. Following [45], for each integer $m \ge 0$ and real p with $1 \le p \le \infty$, we define the Sobolev spaces:

$$W^{m,p}(\mathcal{D}) = \{v \in L^p(\mathcal{D}); \partial^\alpha v \in L^p(\mathcal{D}) \ \forall\, |\alpha| \le m\} \tag{1.4.1}$$

Definition 1.16 *We will equip the spaces* $W^{m,p}$ *with the following norms*

$$\|v\|_{m,p} = \left(\sum_{|\alpha| \le m} \int_{\mathcal{D}} |\partial^\alpha v(x)|^p dx \right)^{1/p} \quad \text{for} \quad p < \infty$$

and

$$\|v\|_{m,\infty} = \max_{|\alpha| \le m} \left(ess \ \sup_{x \in \mathcal{D}} |\partial^\alpha v(x)| \right) \quad \text{for} \ \ p = \infty. \tag{1.4.2}$$

We note that with the norms (1.4.2) the space $W^{m,p}$ is Banach space. In addition to the above norms we also consider the following seminorms on $W^{m,p}(\mathcal{D})$.

$$|v|_{m,p} = \left(\sum_{|\alpha|=m} \int_{\mathcal{D}} |\partial^\alpha v(x)|^p dx \right)^{1/p} \quad \text{for} \quad p < \infty, \tag{1.4.3}$$

and

$$|v|_{m,\infty} = \max_{|\alpha|=m} \left(ess \ \sup_{x \in \mathcal{D}} |\partial^\alpha v(x)| \right) \quad \text{for} \quad p = \infty.$$

When $p = 2$, $W^{m,2}(\mathcal{D})$ is usually denoted by $H^m(\mathcal{D})$, and if there is no ambiguity, we shall drop the subscript $p = 2$, when referring to its norm and seminorm. $H^m(\mathcal{D})$ is a Hilbert space with the scalar product

$$(u, v)_m = \sum_{|\alpha| \le m} \int_{\mathcal{D}} \partial^\alpha u(x) \partial^\alpha v(x) \, dx. \tag{1.4.4}$$

We will write the scalar product of $L^2(\mathcal{D}) = W^{0,2}(\mathcal{D}) = H^0(\mathcal{D})$ with no subscripts and the L^2 norm with a subscript zero; i.e., we will write $(\cdot, \cdot)$ and $\|\cdot\|_0$, respectively.

Let $\mathcal{H}^m(\mathcal{D})$ be the Sobolev space of all complex-valued functions having square integrable spatial generalized derivatives of order up to m in $\mathcal{D}$. $\mathcal{H}^m(\mathcal{D})$ is a Hilbert space with the scalar product

$$(u, v)_m = \sum_{|\alpha| \le m} \int_{\mathcal{D}} \partial^\alpha u(x) (\partial^\alpha v(x))^* dx, \tag{1.4.5}$$

where $(\cdot)^*$ denotes the complex conjugate.

Let $\mathbf{H^m}(\mathcal{D})$ be the Sobolev space of all vector-valued functions each of whose components belongs to $H^m(\mathcal{D})$; i.e., $\mathbf{H^m}(\mathcal{D}) = [H^m(\mathcal{D})]^d$. Norms of functions, belonging to $H^m(\mathcal{D})$, $\mathcal{H}^m(\mathcal{D})$ and $\mathbf{H^m}(\mathcal{D})$ will be defined componentwise and will be denoted by $\|\cdot\|_m$, the type of the norm being determined by the type of the argument.

Throughout this work, we will also make use of the following two subspaces of $\mathbf{H^1}(\mathcal{D})$

$$\mathbf{H^1_n}(\mathcal{D}) = \{ \mathbf{Q} \in \mathbf{H^1}(\mathcal{D}) \mid \mathbf{Q} \cdot \mathbf{n} = 0 \ \text{ on } \ \Gamma \} \tag{1.4.6}$$

and

$$\mathbf{H}_n^1(\text{div};\mathcal{D}) = \{\mathbf{Q} \in \mathbf{H}^1(\mathcal{D}) \mid \text{ div } \mathbf{Q} = 0 \text{ in } \mathcal{D} \text{ and } \mathbf{Q} \cdot \mathbf{n} = 0 \text{ on } \Gamma\}. \tag{1.4.7}$$

We recall that if $\mathcal{D}$ is bounded, then

$$\|\mathbf{Q}\|_{\mathbf{H}_\mathbf{n}^1(\mathcal{D})} = \left(\|\text{curl } \mathbf{Q}\|_0^2 + \|\text{div } \mathbf{Q}\|_0^2\right)^{1/2}, \tag{1.4.8}$$

and

$$\|\mathbf{Q}\|_{\mathbf{H}_n^1(\text{ div};\Omega)} = \|\text{curl } \mathbf{Q}\|_0 \tag{1.4.9}$$

define norms on $\mathbf{H}_\mathbf{n}^1(\mathcal{D})$ and $\mathbf{H}_n^1(\text{ div};\mathcal{D})$ which are equivalent to the standard $\mathbf{H}^1(\mathcal{D})$-norm $\|\mathbf{Q}\|_1$; see [45] for details.

We now state two standard imbedding theorems which will be used throughout this work.

Theorem 1.1 *(Sobolev's Imbedding Theorem) Let Ω be an open subset of $\mathbb{R}^N$ with Lipschitz continuous boundary. Let $p \in \mathbb{R}$ with $1 \leq p < \infty$ and m and $n \in N$. The following imbeddings hold algebraically and topologically:*

$$W^{m,p}(\Omega) \subset W^{n,q}(\Omega) \quad \textit{if} \quad 1/q = 1/p - (m-n)/N > 0 \tag{1.4.10}$$

$$W^{m,p} \hookrightarrow C^n(\Omega) \quad \textit{provided} \quad 1/p < (m-n)/N. \tag{1.4.11}$$

The special case $p = q$ is presented below.

Theorem 1.2 *(Rellich Theorem) The following compact imbedding holds*

$$H^1(\Omega) \subset L^2(\Omega). \tag{1.4.12}$$

In this work we will be dealing with functions of the form $v(\mathbf{x}, t)$ where $\mathbf{x}$ denotes a spatial variable and t denotes a time variable. We extend the usual spaces $W^{m,p}$ for such functions as follows. Let $\mathbf{B}$ be a Banach space with norm $\|\cdot\|_{\mathbf{B}}$. Then for $1 \leq p < \infty$ we introduce the space

$$L^p(0,T;\mathbf{B}) = \left\{ f : [0,T] \longrightarrow \mathbf{B} \mid \left(\int_0^T \|f(t)\|_{\mathbf{B}}^p \; dt \right)^{1/p} < \infty \right\}, \tag{1.4.13}$$

and for $p = \infty$ the space

$$L^\infty(0,T;\mathbf{B}) = \left\{ f : [0,T] \longrightarrow \mathbf{B} \mid \text{ess} \sup_{0 \leq t \leq T} \|f(t)\|_{\mathbf{B}} < \infty \right\}. \tag{1.4.14}$$

We also define

$$\mathcal{H}^m(0,T;)) = \left\{ f : [0,T] \longrightarrow \mathbf{B} \mid \left(\int_0^T \left\| \frac{\partial^s}{\partial t^s} f(t) \right\|_{\mathbf{B}}^2 \; dt \right)^{1/2} < \infty \,; s = 0, ..., m \right\}. \tag{1.4.15}$$

Finally, we introduce the following two notations

$$\mathcal{V} = L^\infty \left(0, T; \mathcal{H}^1(\mathcal{D})\right) \cap \mathcal{H}^1 \left(0, T; L^2(\mathcal{D})\right), \tag{1.4.16}$$

$$V = \mathcal{H}^1(\Omega). \tag{1.4.17}$$

1.5 Overview of Results

The main objectives of this work are to present a model of high temperature superconductivity, discretize the problem using the finite element method and derive optimal error estimates. In addition, we present numerical results which illustrate both our theoretical and well-known experimental results.

In view of the time-independent macroscopic model proposed by Ginzburg and Landau in 1950 a superconductor may be characterized by a single parameter κ, known as the Ginzburg-Landau parameter. This almost temperature independent quantity is defined as the ratio $\frac{\lambda}{\xi}$, where λ and ξ are two temperature dependent microscopic characteristic lengths called the penetration depth and the coherence length, respectively. The value of κ is determined by the property of the material. From a practical point of view, we are interested in materials which retain superconductivity at moderate temperatures and applied magnetic fields. Such materials are usually called type II superconductors. Typically they have short coherence lengths ξ and long penetration depths λ and are characterized by the high value of the Ginzburg-Landau parameter κ. This motivates our interest in developing and analyzing models valid for large values of κ.

The unknown functions in the Ginzburg-Landau model are the complex-valued order parameter ψ and the vector-valued magnetic potential $\mathbf{A}$. Equations for these two functions are coupled and must be solved simultaneously. In this work we present a simple model of high temperature superconductivity valid for large κ and strong applied magnetic fields. This model also accounts for applied currents of constant magnitude. A similar model was presented for the time-independent case in [19] and the time-dependent case in [37]. Our model, referred to as the High kappa model, is presented in Chapter 2. To define the model we begin with the time-dependent generalization of the original Ginzburg-Landau system presented in Chapter 1. We perform a formal asymptotic expansion in the limit of high κ. In particular, we fix the coherence length ξ and expand in terms of the penetration depth λ. After collecting all first order terms the resulting systems for the leading orders magnetic potential $\mathbf{A}_0$ and order parameter ψ_0 decouple. Moreover, under appropriate assumptions on the initial conditions for $\mathbf{A}_0$ one can choose the magnetic potential to be time independent. Thus, by neglecting the higher order terms in the expansions, the original full Ginzburg-Landau time-dependent system of nonlinear coupled equations reduces to two decoupled problems: a linear boundary-value problem for $\mathbf{A}_0$ and a nonlinear initial-boundary-value problem for ψ_0. As a result, one may first solve for $\mathbf{A}_0$ and then substitute into the system for ψ_0. Once the model has been defined we derive appropriate weak formulations for both systems. We conclude Chapter 2 with existence and uniqueness results for weak solutions. The existence and uniqueness of the magnetic potential follows directly from standard elliptic theory. The existence and uniqueness for the order parameter was demonstrated in [37].

In general, the two systems for the leading order magnetic potential $\mathbf{A}_0$ and order parameter ψ_0 cannot be solved explicitly. Thus our next goal is to obtain numerical approximations for the solutions of these problems. For this purpose in Chapter 3 we consider discretizations by the finite element method. We first define the appropriate finite element spaces, denoted by $\mathbf{W}^h$ and V^h, respectively, and discuss their properties. Then we introduce the approximate problems by discretizing the spatial variable in the magnetic potential system and the spatial and temporal variables in the order parameter system. We use a standard Galerkin discretization for the spatial variables and two different time discretization schemes having first and second order of accuracy, respectively. The corresponding approximate solutions are denoted by $\mathbf{A}_h$ and Ψ^n, respectively.

The bulk of this work consists in deriving optimal error estimates and proving existence and uniqueness results for the finite element approximations of the magnetic potential $\mathbf{A}_h$ and the order parameter Ψ^n. In Chapter 4 we present approximation results for the magnetic potential which are established using standard elliptic finite element theory. In addition, under suitable regularity assumptions we derive $\mathbf{L}^\infty$ estimates valid for the weak solution $\mathbf{A}$

and for its approximation $\mathbf{A}_h$. These uniform estimates, along with a uniform boundedness result for ψ, are used repeatedly in the derivation of the optimal error estimates for Ψ^n.

A major part of this work is devoted to the derivation of optimal $\mathcal{L}^2$ and $\mathcal{H}^1$ estimates for Ψ^n. We present detailed proofs for both the Backward-Euler-Galerkin and Crank-Nicolson-Galerkin problems. These results are collected in Chapters 5-8. In contrast to the straightforward proofs for the magnetic potential, here one does not have a standard theory in hand. In general our proofs follow some of the well established techniques for time dependent problems; see e.g., [77]. However, our variational problem involves several terms which pose serious difficulties for a straightforward application of the ideas of [77]. In particular, our weak problem involves a trilinear form similar to one appearing in the Navier-Stokes equations along with a cubic nonlinearity. As a result we have to deal with right-hand sides which fail to be globally Lipschitz. In order to derive the necessary bounds for the trilinear form we use the optimal error estimates and the uniform bounds established in Chapter 2. To handle the cubic nonlinearity we follow the approach of [5] and introduce an auxiliary problem, parameterized by δ, in which this term is replaced by a suitably defined globally Lipschitz function. In order to derive optimal error estimates for the original fully-discrete problems for Ψ^n one first derives such results for the solutions Ψ^n_δ of the auxiliary problems. These results are presented in Chapters 5-7. In Chapter 8 we use the optimal results for Ψ^n_δ, together with a property of the finite element space V^h, to obtain the desired estimates for Ψ^n. The proof of the existence and uniqueness for Ψ^n follows the same idea.

To illustrate our theoretical results numerically we perform computational experiments with the Backward-Euler-Galerkin and Crank-Nicolson-Galerkin formulations presented in Chapter 3. In our computations we use both bilinear and biquadratic finite elements. According to the theoretical error estimates proved in Chapter 8 the finite element approximations converge optimally to all sufficiently regular solutions of the High kappa model in both $\mathcal{L}^2$ and $\mathcal{H}^1$ norms. In Chapter 9 we investigate the numerical convergence rates exhibited by the finite element method for the High kappa model. Our numerical results illustrate the theoretical rates of $O\left(h^2\right)$ in $\mathcal{H}^1$ and $O\left(h^3\right)$ in $\mathcal{L}^2$ using bilinear finite elements. Using bilinear elements we observe numerically the expected lower rates of $O\left(h\right)$ in $\mathcal{H}^1$ and $O\left(h^2\right)$ in $\mathcal{L}^2$. Moreover, the optimal rates of convergence for both the Backward-Euler-Galerkin and the Crank-Nicolson-Galerkin method are illustrated by our numerical experiments. Finally, our numerical results illustrate several well-known experimentally observed phenomena valid for type II materials.

Chapter 2

The High kappa Model

This chapter is organized in four sections. In the first section we derive the High kappa model by starting with the TDG-L system given in Section 1.2, performing a formal asymptotic expansion and fixing the gauge appropriately. As a result we obtain an initial boundary-value problem for the leading order vector-valued magnetic potential $\mathbf{A}$ and the complex-valued order parameter ψ. Similar techniques have been used in [19] and [37]. An important feature of the High kappa model, which has significant practical implications, is the fact that the leading order system for $\mathbf{A}$ decouples from the leading order nonlinear time-dependent system for ψ. In addition, under appropriate assumptions $\mathbf{A}$ may be chosen to be time independent.

After deriving the model we proceed as follows. In the second section we define weak formulations for the leading order systems. Then we discuss which form of the weak problem for the order parameter is the most beneficial from the point of view of proving optimal error estimates for the fully discrete solutions. In the third section we prove an existence and uniqueness result for the weak solution $\mathbf{A}$ of the leading order equation for the magnetic potential which follows standard elliptic finite element theory. In the last section, following the presentation of [37], we state an existence and uniqueness result for the weak solution ψ of the leading order problem for the order parameter.

2.1 Derivation of the Model

In this section we introduce the High-*kappa* model which is a modification of the high kappa Ginzburg-Landau model, given in [19]. The modifications include time dependence and incorporating an applied current of constant magnitude. A similar model is also presented in [37]. To derive the model we formally expand the vector-valued magnetic potential $\mathbf{A}$, the complex-valued order parameter ψ, the scalar electric potential $\mathbf{\Phi}$, the applied current $\mathbf{J}$, and the applied magnetic field $\mathbf{H}$ in powers of $(\frac{\lambda}{l})$, where λ is the penetration length and l is the unit length scale. We fix the gauge and choose the initial data appropriately to arrive at two decoupled systems for the leading order terms $\mathbf{A}_0$ and ψ_0. Moreover, under appropriate hypotheses, the system for $\mathbf{A}_0$ is time independent and has a divergence free solution.

Let us consider the nonlinear time-dependent coupled system of equations for the magnetic potential $\mathbf{A}$ and the order parameter ψ given in (1.2.22)-(1.2.27),

$$\begin{aligned} \sigma\left(\frac{\partial \mathbf{A}}{\partial t} + \left(\frac{\lambda}{l}\right)\left(\frac{\xi}{l}\right)\nabla\Phi\right) + \mathbf{curl}\ \mathrm{curl}\ \mathbf{A} + \left(\frac{l}{\lambda}\right)^2 |\psi|^2\mathbf{A} & \\ + \frac{i}{2}\left(\frac{\xi}{\lambda}\right)(\psi^*\nabla\psi - \psi\nabla\psi^*) = 0 \quad \text{in} \quad \Omega\times[0,\infty), & \qquad (2.1.1) \\ \mathrm{curl}\ \mathbf{A} = \mathbf{H} \quad \text{on} \quad \Gamma\times[0,\infty), & \qquad (2.1.2) \\ \mathbf{A}(\mathbf{0}) = \mathbf{a} \quad \text{in} \quad \Omega & \qquad (2.1.3) \end{aligned}$$

and

$$\begin{aligned} \frac{\partial\psi}{\partial t} + i\mathbf{\Phi}\psi -, \psi + |\psi|^2\psi + \left(i\left(\frac{\xi}{l}\right)\nabla + \left(\frac{l}{\lambda}\right)\mathbf{A}\right)^2\psi = 0 \quad \text{in} \quad \Omega\times[0,\infty) & \qquad (2.1.4) \\ \left(i\left(\frac{\xi}{l}\right)\nabla\psi + \left(\frac{l}{\lambda}\right)\mathbf{A}\psi\right)\cdot\mathbf{n} = 0 \quad \text{on} \quad \Gamma\times[0,\infty), & \qquad (2.1.5) \\ \psi(0) = \psi^0 \quad \text{in}\ \Omega, & \qquad (2.1.6) \end{aligned}$$

where σ is a microscopic parameter defined in (1.2.19). We note that equation (2.1.1) may be viewed as a combination of the following equations

$$\begin{aligned} \mathbf{h} &= \text{curl } \mathbf{A} \ \text{(definition of } \mathbf{A}), \\ \text{curl } \mathbf{h} &= \mathbf{j} = \mathbf{j}_s + \mathbf{j}_n \ \text{(Ampére's law)}, \end{aligned}$$

where the superconducting current is given by

$$\mathbf{j}_s = -\left(\frac{l}{\lambda}\right)^2 |\psi|^2 \mathbf{A} - \frac{i}{2}\left(\frac{\xi}{\lambda}\right)(\psi^* \nabla \psi - \psi \nabla \psi^*),$$

and the normal current is related with the electric field $\mathbf{E}$ via Ohm's law as follows

$$\mathbf{j}_n = \sigma \mathbf{E} = -\sigma\left(\frac{\partial \mathbf{A}}{\partial t} + \left(\frac{\lambda}{l}\right)\left(\frac{\xi}{l}\right)\nabla \Phi\right).$$

Let us consider the following formal expansion of the variables in (2.1.1) in powers of $\left(\frac{\lambda}{l}\right)^2$

$$\mathbf{a} = \sum_{j=0}^{\infty} \left(\frac{\lambda}{l}\right)^{-2j+1} \mathbf{a}_j, \tag{2.1.7}$$

$$\mathbf{A} = \sum_{j=0}^{\infty} \left(\frac{\lambda}{l}\right)^{-2j+1} \mathbf{A}_j, \tag{2.1.8}$$

$$\mathbf{H} = \sum_{j=0}^{\infty} \left(\frac{\lambda}{l}\right)^{-2j+1} \mathbf{H}_j, \tag{2.1.9}$$

$$\Phi = \sum_{j=0}^{\infty} \left(\frac{\lambda}{l}\right)^{-2j} \Phi_j, \tag{2.1.10}$$

$$\psi^0 = \sum_{j=0}^{\infty} \left(\frac{\lambda}{l}\right)^{-2j} \psi_j^0, \tag{2.1.11}$$

$$\psi = \sum_{j=0}^{\infty} \left(\frac{\lambda}{l}\right)^{-2j} \psi_j. \tag{2.1.12}$$

Let us assume that a_0, $\mathbf{A}_0$, $\mathbf{H}_0$, ψ_0, and Φ_0 are independent of λ/l, i.e. $\mathbf{a}_0 = O(1)$, $\mathbf{A}_0 = O(1)$, $\mathbf{H}_0 = O(1)$, $\psi_0 = O(1)$ and $\Phi_0 = O(1)$. Throughout this work the parameter

σ is fixed so that $\sigma = O(1)$. For other possible choices of this parameter one may consult [37].

We obtain the equation for the leading order term $\mathbf{A}_0$ by substituting the expansions (2.1.7)-(2.1.10) into (2.1.1)-(2.1.3) to get

$$\begin{aligned}
&\sigma\left[\left(\frac{\lambda}{l}\right)\frac{\partial \mathbf{A}_0}{\partial t} + \left(\frac{l}{\lambda}l\right)\frac{\partial \mathbf{A}_1}{\partial t} + \left(\frac{\lambda}{l}\right)\left(\frac{\xi}{l}\right)\nabla\Phi_0 + \left(\frac{l}{\lambda}l\right)\left(\frac{\xi}{l}\right)\nabla\Phi_1\right] \\
+ \quad & \left(\frac{\lambda}{l}\right)\mathbf{curl}\ \mathrm{curl}\ \mathbf{A}_0 + \left(\frac{l}{\lambda}\right)\mathbf{curl}\ \mathrm{curl}\ \mathbf{A}_1 \\
+ \quad & \left(\frac{l}{\lambda}\right)^2\left[|\psi_0|^2 + \left(\frac{l}{\lambda}\right)^2(\psi_0\psi_1^* + \psi_0^*\psi_1)\right]\left[\left(\frac{\lambda}{l}\right)\mathbf{A}_0 + \left(\frac{l}{\lambda}\right)\mathbf{A}_1\right] \\
+ \quad & \frac{i}{2}\left(\frac{\xi}{\lambda}\right)\left[\psi_0^*\nabla\psi_0 - \psi_0\nabla\psi_0^* + \left(\frac{l}{\lambda}\right)^2(\psi_0^*\nabla\psi_1 + \psi_0\nabla\psi_1^* + \nabla\psi_0\psi_1^* + \psi_1\nabla\psi_0^*)\right] \\
+ \quad & O\left(\left(\frac{l}{\lambda}\right)^3\right) = 0 \quad \text{in} \quad \Omega\times[0,\infty),
\end{aligned}$$

$$\begin{aligned}
\left(\frac{\lambda}{l}\right)\mathrm{curl}\ \mathbf{A}_0 + \left(\frac{l}{\lambda}\right)\mathrm{curl}\ \mathbf{A}_1 = \left(\frac{\lambda}{l}\right)\mathbf{H}_0 + \left(\frac{l}{\lambda}\right)\mathbf{H}_1 \\
O\left(\left(\frac{l}{\lambda}\right)^3\right) \quad \text{on} \quad \Gamma\times[0,\infty),
\end{aligned}$$

$$\left(\frac{\lambda}{l}\right)\mathbf{A}_0(\mathbf{0}) + \left(\frac{l}{\lambda}\right)\mathbf{A}_1(\mathbf{0}) + O\left(\left(\frac{l}{\lambda}\right)^3\right) = \left(\frac{\lambda}{l}\right)\mathbf{a}_0 + \left(\frac{l}{\lambda}\right)\mathbf{a}_1 \quad \text{in} \quad \Omega.$$

Collecting all terms in front of $\left(\frac{\lambda}{l}\right)$, we arrive at the following leading order time-dependent system for $\mathbf{A}_0$

$$\sigma\left(\frac{\partial \mathbf{A}_0}{\partial t} + \left(\frac{\xi}{l}\right)\nabla\Phi_0\right) + \mathbf{curl}\ \mathrm{curl}\ \mathbf{A}_0 = 0 \text{ in } \Omega\times[0,\infty), \tag{2.1.13}$$

$$\mathrm{curl}\ \mathbf{A}_0 = \mathbf{H}_0 \text{ on } \Gamma\times[0,\infty), \tag{2.1.14}$$

$$\mathbf{A}_0|_{t=0} = \mathbf{a}_0 \text{ in } \Omega. \tag{2.1.15}$$

Note that the leading order system for $\mathbf{A}_0$ is independent of ψ_0. Hence, we can first solve the linear system for $\mathbf{A}_0$, and then substitute its solution into the equation for ψ_0. For comparison, the original nonlinear equation for $\mathbf{A}$ depends on ψ, and hence both equations must be solved simultaneously. This obvious advantage of the leading order problem for $\mathbf{A}_0$ will simplify both the theoretical analysis and the computational implementation.

Let us consider an applied constant current of magnitude J directed in the y-direction of the sample plane Ω. Let us consider the following expansion in terms of $\left(\frac{\lambda}{l}\right)^2$.

$$\mathbf{J} = \sum_{j=0}^{\infty} \left(\frac{\lambda}{l}\right)^{-2j+1} \mathbf{J}_j. \tag{2.1.16}$$

According to (2.1.16) we have

$$\mathbf{J} = (0, J, 0)^T, \tag{2.1.17}$$

where $J = \left(\frac{\lambda}{l}\right) J_0$ and $J_0 = O(1)$.

Let the applied magnetic field $\mathbf{H}$ be directed in the z-direction, i.e., $\mathbf{H} = (0, 0, H)^T$. If there is no applied current, then the external field $\mathbf{H}_e$ is equal to the applied field $\mathbf{H}$. In this case using (2.1.9) we have $H_e = \left(\frac{\lambda}{l}\right) H_{0_e}$ with $H_{0_e} = O(1)$. In order to satisfy Ampére's law, the applied field $\mathbf{H}$ should satisfy $\mathbf{H} = (0, 0, H)^T = (0, 0, H_e - Jx)^T$.

As a result of the above discussion, we assume that the applied current $\mathbf{J}$ and the applied magnetic field $\mathbf{H}$ are given by

$$\mathbf{J} = (0, J, 0)^T = \left(\frac{\lambda}{l}\right) (0, J_0, 0)^T, \tag{2.1.18}$$

$$\mathbf{H} = (0, 0, H)^T = (0, 0, H_e - Jx)^T = \left(\frac{\lambda}{l}\right) (0, 0, H_{0_e} - J_0 x)^T, \tag{2.1.19}$$

where $J_0 = O(1)$ and $H_{0_e} = O(1)$.

Let us fix the gauge in the time-dependent leading order system for $\mathbf{A}_0$ given in (2.1.13)-(2.1.15) by requiring that

$$\Phi = -\left(\frac{l}{\lambda}\right)\left(\frac{l}{\xi}\right)\frac{1}{\sigma} J y \quad \text{in} \quad \Omega \tag{2.1.20}$$

and

$$\mathbf{A} \cdot \mathbf{n} = 0 \quad \text{on} \quad \Gamma \times [0, \infty). \tag{2.1.21}$$

Then (2.1.10) and (2.1.16) imply

$$\Phi_0 \;=\; -\left(\frac{1}{\lambda}\right)\left(\frac{1}{\xi}\right)\frac{1}{\sigma} J_0 y. \tag{2.1.22}$$

Thus one has

$$-\sigma\left(\frac{\xi}{l}\right)\nabla\Phi_0 = (0, J_0)^T. \tag{2.1.23}$$

Substituting (2.1.23) into the leading order equation (2.1.13), we get the following time-dependent leading order equation for $\mathbf{A}_0$

$$\sigma\frac{\partial \mathbf{A}_0}{\partial t} + \mathbf{curl}\ \text{curl}\ \mathbf{A}_0 = (0, J_0)^T \quad \text{in} \quad \Omega \times [0, \infty). \tag{2.1.24}$$

To summarize, we have carried on a formal asymptotic expansion of the equations for the magnetic potential given in (2.1.1)-(2.1.3). This resulted in a leading order time-dependent system for $\mathbf{A}_0$ given in (2.1.13)-(2.1.15). Then we have defined the applied magnetic field $\mathbf{H}$ and current $\mathbf{J}$, see (2.1.19) and (2.1.18), respectively. Finally, fixing the gauge according to (2.1.20) and (2.1.21), we arrive at the following time-dependent leading order system for $\mathbf{A}_0$

$$\begin{aligned}
\sigma\frac{\partial \mathbf{A}_0}{\partial t} + \mathbf{curl}\ \text{curl}\ \mathbf{A}_0 &= (0, J_0)^T \quad \text{in} \quad \Omega \times [0, \infty),\\
\text{curl}\ \mathbf{A}_0 &= \mathbf{H}_0 \ \text{ on } \ \Gamma \times [0, \infty),\\
\mathbf{A}_0 \cdot \mathbf{n} &= 0 \ \text{ on } \ \Gamma \times [0, \infty),\\
\mathbf{A}_0|_{t=0} &= \mathbf{a}_0 \ \text{ in } \ \Omega.
\end{aligned} \tag{2.1.25}$$

Let us now assume that the initial data $\mathbf{a}_0$ satisfies

$$\text{div}\ \mathbf{a}_0 = 0 \quad \text{in} \quad \Omega. \tag{2.1.26}$$

Taking the divergence of the leading order equation in (2.1.25) and using the fact that divergence of a curl is zero, we get

$$\frac{\partial}{\partial t}(\text{div } \mathbf{A}_0) = 0 \quad \text{in} \quad \Omega \times [0, \infty).$$

Thus, if the initial condition $\mathbf{a}_0$ in the system (2.1.25) is divergence free, then the solution $\mathbf{A}_0$ itself will have the property

$$\text{div } \mathbf{A}_0 = 0 \quad \text{in} \quad \Omega \times [0, \infty); \tag{2.1.27}$$

i.e., $\mathbf{A}_0$ will be divergence free for all $t \geq 0$.

It remains to show that if one chooses the initial data $\mathbf{a}_0$ appropriately then the solution $\mathbf{A}_0$ will be time-independent. Indeed, let us consider the following linear system for $\mathbf{a}_0$

$$\begin{aligned} \mathbf{curl}\,\text{curl } \mathbf{a}_0 &= (0, J_0)^T \quad \text{in} \quad \Omega, && (2.1.28)\\ \text{div } \mathbf{a}_0 &= 0 \quad \text{in} \quad \Omega, && (2.1.29)\\ \mathbf{a}_0 \cdot \mathbf{n} &= 0 \quad \text{on} \quad \Gamma, && (2.1.30)\\ \text{curl } \mathbf{a}_0 &= H_0 - J_0 x \quad \text{on} \quad \Gamma. && (2.1.31) \end{aligned}$$

Then, clearly one may choose $\mathbf{A}_0 = \mathbf{a}_0$. We note that this $\mathbf{A}_0$ solves the leading order system (2.1.25), satisfies (2.1.27), and in addition, is time independent.

In fact, if we relax the $\mathbf{A}_0 \cdot \mathbf{n}$ gauge, we can solve explicitly for $\mathbf{A}_0$. For example, if we choose

$$\mathbf{A}_0 = \mathbf{a}_0 = \left(0, H_0 x - J_0 \frac{x^2}{2}\right)^T, \tag{2.1.32}$$

then both the system (2.1.13)-(2.1.15) and the property (2.1.27) are satisfied. However, the essential boundary condition (2.1.21) imposed in the gauge does not hold. Thus, if we want to obtain $\mathbf{A}_0$ in the $\mathbf{A}_0 \cdot \mathbf{n}$ gauge, one must solve (2.1.28)-(2.1.31).

In sum, we have shown that, using the formal asymptotic expansions (2.1.7)-(2.1.10), fixing the gauge according to (2.1.20) and (2.1.21), and choosing the initial data $\mathbf{a}_0$ to satisfy (2.1.29) and (2.1.30) one arrives at the following linear time independent leading order system for $\mathbf{A}$

$$\mathbf{curl}\,\mathrm{curl}\,\mathbf{A} = (0, J)^T \text{ in } \Omega, \tag{2.1.33}$$

$$\mathbf{A}\cdot\mathbf{n} = 0 \text{ on } \Gamma, \tag{2.1.34}$$

$$\mathrm{curl}\,\mathbf{A} = H - Jx \text{ on } \Gamma, \tag{2.1.35}$$

where we have dropped all subscripts.

Let us proceed with the derivation of the leading order system for the order parameter. As for the equation for the magnetic potential we substitute the expansions (2.1.7)-(2.1.12), into (2.1.4)-(2.1.6) to obtain

$$\begin{aligned}
&\frac{\partial\psi_0}{\partial t} + \left(\frac{l}{\lambda}\right)^2 \frac{\partial\psi_1}{\partial t} + i\left(\Phi_0 + \left(\frac{l}{\lambda}\right)^2 \Phi_1\right)\left(\psi_0 + \left(\frac{l}{\lambda}\right)^2 \psi_1\right) \\
- &\ \ \psi_0 + \left(\frac{l}{\lambda}\right)^2 \psi_1 + \left[|\psi_0|^2 + \left(\frac{l}{\lambda}\right)^2 (\psi_0\psi_1^* + \psi_0^*\psi_1)\right]\left[\psi_0 + \left(\frac{l}{\lambda}\right)^2 \psi_1\right] \\
+ &\ \ \left[i\left(\frac{\xi}{l}\right)\nabla + \mathbf{A}_0 + \left(\frac{l}{\lambda}\right)^2 \mathbf{A}_1\right]^2 \left(\psi_0 + \left(\frac{l}{\lambda}\right)^2 \psi_1\right) \\
+ &\ \ O\left(\left(\frac{l}{\lambda}\right)^4\right) = 0 \text{ in } \Omega \times [0,\infty),
\end{aligned}$$

$$\begin{aligned}
&\left\{ i\left(\frac{\xi}{l}\right)\nabla\psi_0 + i\left(\frac{\xi}{l}\right)\left(\frac{l}{\lambda}\right)^2 \nabla\psi_1 + \left(\frac{l}{\lambda}\right)\left[\left(\frac{\lambda}{l}\right)\mathbf{A}_0 + \left(\frac{l}{\lambda}\right)\mathbf{A}_1\right]\left[\psi_0 + \left(\frac{l}{\lambda}\right)^2 \psi_1\right]\right\}\cdot\mathbf{n} \\
&\qquad + O\left(\left(\frac{l}{\lambda}\right)^4\right) = 0 \text{ on } \Gamma \times [0,\infty),
\end{aligned}$$

$$\psi_0(0) + \left(\frac{l}{\lambda}\right)^2 \psi_1(0) + O\left(\left(\frac{l}{\lambda}\right)^4\right) = \psi_0^0 + \left(\frac{l}{\lambda}\right)^2 \psi_1^0 + O\left(\left(\frac{l}{\lambda}\right)^4\right) \text{ in } \Omega.$$

Collecting all leading order terms we arrive at the following nonlinear time-dependent leading order system for ψ_0

$$\frac{\partial\psi_0}{\partial t} + i\Phi_0\psi_0 - \psi_0 + |\psi_0|^2\psi_0 + \left(i\left(\frac{\xi}{l}\right)\nabla + \mathbf{A}_0\right)^2\psi_0 \quad = \quad 0 \text{ in } \Omega \times [0,\infty), \tag{2.1.36}$$

$$\left(i\left(\frac{\xi}{l}\right)\nabla\psi_0 + \mathbf{A}_0\psi_0\right)\cdot\mathbf{n} \quad = \quad 0 \text{ on } \Gamma \times [0,\infty), \tag{2.1.37}$$

$$\psi_0(0) \quad = \quad \psi^0 \text{ in } \Omega. \tag{2.1.38}$$

We recall that the leading order time independent linear system for the magnetic potential $\mathbf{A}$ decouples from the leading order nonlinear time dependent system for the order parameter ψ. Hence, one may first solve (2.1.33)-(2.1.35) for $\mathbf{A}$ and then substitute the solution into the system for ψ_0. We note that by using the divergence free property of $\mathbf{A}$, see (2.1.27), and the boundary condition (2.1.34), it is easy to see that the leading order system (2.1.36)-(2.1.38) can be written in the following equivalent form

$$\begin{aligned} \frac{\partial\psi}{\partial t} - \left(\frac{\xi}{l}\right)^2\Delta\psi + |\mathbf{A}|^2\psi + (i\Phi - 1)\psi \quad &+ \quad |\psi|^2\psi \\ +2i\left(\frac{\xi}{l}\right)\mathbf{A}\cdot\nabla\psi \quad &= \quad 0 \quad \text{on} \quad \Omega \times [0,\infty), \qquad (2.1.39) \\ \nabla\psi\cdot\mathbf{n} \quad &= \quad 0 \quad \text{on} \quad \Gamma \times [0,\infty), \qquad (2.1.40) \\ \psi(0) \quad &= \quad \psi^0 \quad \text{in} \quad \Omega, \qquad (2.1.41) \end{aligned}$$

where we have dropped all subscripts.

2.2 Weak Formulations

The first step in applying the finite element method is to write a weak formulation of our problems. In this section we present weak forms of the leading order systems for the magnetic potential $\mathbf{A}$ and the order parameter ψ, see (2.1.33)-(2.1.35) and (2.1.39)-(2.1.41), respectively. We show that if the weak solutions possess sufficient regularity, then standard integration by parts yields that they also satisfy the strong equations.

Let $(\cdot,\cdot)$ denote the standard $\mathbf{L}^2$ inner product. Recall that $\mathbf{H}^1_\mathbf{n}(\Omega)$ represents the space of all functions $\mathbf{Q} \in \mathbf{H}^1(\Omega)$ satisfying the boundary condition $\mathbf{Q}\cdot\mathbf{n} = 0$, see (1.4.6). The solution $\mathbf{A}$ of the leading order system (2.1.33)-(2.1.35) satisfies the following weak formulation.

Seek $\mathbf{A} \in \mathbf{H}^1_\mathbf{n}(\Omega)$ such that

$$\bar{a}(\mathbf{A},\tilde{\mathbf{A}}) = F(\tilde{\mathbf{A}}) \ \ \forall\, \tilde{\mathbf{A}} \in \mathbf{H}^1_\mathbf{n}(\Omega), \tag{2.2.1}$$

where $\bar{a}(\cdot,\cdot)$ is the bilinear form

$$\bar{a}(\mathbf{A},\tilde{\mathbf{A}}) = (\text{curl }\mathbf{A},\text{curl }\tilde{\mathbf{A}}) + (\text{div }\mathbf{A},\text{div }\tilde{\mathbf{A}}) \tag{2.2.2}$$

and $F(\cdot)$ is the linear functional

$$F(\tilde{\mathbf{A}}) = (\bar{f}(x),\text{curl }\tilde{\mathbf{A}}) \tag{2.2.3}$$

where $\bar{f}(x)$ is the infinitely differentiable function

$$\bar{f}(x) = H - Jx. \tag{2.2.4}$$

We now show that if $\mathbf{A}$ is sufficiently smooth, we can recover both (2.1.33) and (2.1.35). Using definitions (2.2.2), (2.2.3) and (2.2.4), equation (2.2.1) becomes

$$(\text{curl }\mathbf{A},\text{curl }\tilde{\mathbf{A}}) + (\text{div }\mathbf{A},\text{div }\tilde{\mathbf{A}}) = (H - Jx,\text{curl }\tilde{\mathbf{A}}) \ \ \forall\, \tilde{\mathbf{A}} \in \mathbf{H}^1_n(\Omega).$$

Provided that the weak solution $\mathbf{A}$ is sufficiently smooth we can integrate by parts to remove all derivatives from the test function $\tilde{\mathbf{A}}$. Let us first take a divergence free test function $\tilde{\mathbf{A}}$, that is we consider $\tilde{\mathbf{A}} \in \mathbf{H}^1_\mathbf{n}(\text{div};\Omega)$. Then equation (2.2.1) reduces to:

$$(\text{curl }\mathbf{A},\text{curl }\tilde{\mathbf{A}}) = (H - Jx,\text{curl }\tilde{\mathbf{A}}) \ \ \forall\, \tilde{\mathbf{A}} \in \mathbf{H}^1_\mathbf{n}(\Omega).$$

Using standard integration by parts we have that

$$(\text{curl } \mathbf{A}, \text{curl } \tilde{\mathbf{A}}) = (\mathbf{curl} \text{ curl } \mathbf{A}, \tilde{\mathbf{A}}) - \int_\Gamma \text{curl } \mathbf{A}(\tilde{\mathbf{A}} \times \mathbf{n}) \, d\Gamma, \tag{2.2.5}$$

and

$$\begin{aligned}(H - Jx, \text{curl } \tilde{\mathbf{A}}) &= \int_\Omega (H - Jx)\text{curl } \tilde{\mathbf{A}} \, d\Omega \\ &= J \int_\Omega \tilde{\mathbf{A}}_2 \, d\Omega + \int_\Gamma (H - Jx)(\mathbf{n} \times \tilde{\mathbf{A}}) \, d\Gamma. \end{aligned} \tag{2.2.6}$$

Hence

$$\begin{aligned}&\left(\mathbf{curl} \text{ curl } \mathbf{A}, \tilde{\mathbf{A}}\right) = \\ &\qquad \int_\Gamma (\text{curl } \mathbf{A} - (H - Jx)) (\tilde{\mathbf{A}} \times \mathbf{n}) \, d\Gamma \;\; \forall \, \tilde{\mathbf{A}} \in \mathbf{H}^1_\mathbf{n}(\Omega)\end{aligned} \tag{2.2.7}$$

and by choosing $\tilde{\mathbf{A}} \in \mathbf{H}^1_\mathbf{n}(\Omega)$ satisfying $\tilde{\mathbf{A}} = 0$ on Γ we will get that

$$\left(\mathbf{curl} \text{ curl } \mathbf{A}, \tilde{\mathbf{A}}\right) = \left((0, J)^T, \tilde{\mathbf{A}}\right) \;\; \forall \, \tilde{\mathbf{A}} \in \mathbf{H}^1_\mathbf{n}(\Omega).$$

Therefore we arrive at

$$\mathbf{curl} \text{ curl } \mathbf{A} = (0, J)^T \quad \text{a.e. in} \quad \Omega.$$

Next, consider a test function $\tilde{\mathbf{A}}$ with curl $\tilde{\mathbf{A}} = 0$. Then (2.2.1) yields

$$(\text{div } \mathbf{A}, \text{div } \tilde{\mathbf{A}}) = 0$$

for all such test functions. Therefore div $\mathbf{A} = 0$.

Finally, to recover the boundary condition we consider $\tilde{\mathbf{A}} \in \mathbf{H}^1_\mathbf{n}(\Omega)$. Taking into account that div $\mathbf{A} = 0$ and **curl** curl $\mathbf{A} = (0, J)^T$ it follows that

$$\int_\Gamma (\text{curl } \mathbf{A} - (H - Jx)) (\tilde{\mathbf{A}} \times \mathbf{n}) d\Gamma = 0 \;\; \forall \, \tilde{\mathbf{A}} \in \mathbf{H}^1_\mathbf{n}(\Omega),$$

or equivalently

$$\text{curl } \mathbf{A} = H - Jx \quad \text{a.e. on} \quad \Gamma.$$

Thus, assuming sufficient regularity for the solution of the weak problem (2.2.1), we recovered the strong equation (2.1.33) and the natural boundary condition (2.1.35).

We proceed with introducing a weak formulation for the order parameter ψ. Recall that the space $\mathcal{V}$ is defined in (1.4.16) and that $V = \mathcal{H}^1$, see (1.4.17). The strong solution ψ of the time-dependent nonlinear leading order system (2.1.39)-(2.1.41) satisfies the following weak formulation.

Seek $\psi \in \mathcal{V}$ such that

$$\begin{aligned}(\psi_t, v) + \left(\frac{\xi}{l}\right)^2 (\nabla\psi, \nabla v) + (\psi, v) + 2i\left(\frac{\xi}{l}\right)(\mathbf{A}\cdot\nabla\psi, v) = \\ - \quad \left((i\Phi - 2 + |\psi|^2 + |\mathbf{A}|^2)\psi, v\right) \quad \forall v \in V, t \geq 0, \qquad (2.2.8) \\ \psi(0) = \psi^0.\end{aligned}$$

Note that we have replaced the notation $\frac{\partial\psi}{\partial t}$ with ψ_t.

Again, standard integration by parts can be used to show that if the above weak problem has a sufficiently regular solution ψ then it also satisfies both the strong leading order equation (2.1.39) and the natural BC (2.1.40). Assuming enough regularity for ψ, say $\psi \in \mathcal{H}^2(\Omega)$, we integrate by parts to remove all derivatives from the test function v. We have

$$\left(\frac{\xi}{l}\right)^2 (\nabla\psi, \nabla v) = -\left(\frac{\xi}{l}\right)^2 (\Delta\psi, v) + \int_\Gamma (\nabla\psi\cdot\mathbf{n})\, v\, d\Gamma \quad \forall v \in V, t \geq 0, \qquad (2.2.9)$$

hence

$$\begin{aligned}\left(\psi_t - \left(\frac{\xi}{l}\right)^2 \Delta\,\psi + 2i\left(\frac{\xi}{l}\right)\mathbf{A}\cdot\nabla\psi + i\Phi\psi - \psi + |\psi|^2\psi + |\mathbf{A}|^2\psi, v\right) \\ + \quad \int_\Gamma (\nabla\psi\cdot\mathbf{n}) v\, d\Gamma = 0 \quad \forall v \in V, t \geq 0. \qquad (2.2.10)\end{aligned}$$

If we take $v \in V$ with $v = 0$ on Γ then we get

$$\psi_t - \left(\frac{\xi}{l}\right)^2 \Delta \psi + 2i\left(\frac{\xi}{l}\right) \mathbf{A} \cdot \nabla\psi + i\Phi\psi - \psi + |\psi|^2\psi + |\mathbf{A}|^2\psi = 0 \quad \text{a.e. in} \quad \Omega,\ t \geq 0.$$

So far, starting from the weak form (2.2.8) we have recovered the strong equation (2.1.33). For any $v \in V$ we arrive at

$$\int_\Gamma (\nabla\psi \cdot \mathbf{n})\, v\, d\Gamma \quad \forall v \in V, t \geq 0,$$

or equivalently

$$\nabla\psi \cdot \mathbf{n} = 0 \quad \text{a.e. on} \quad \Gamma. \tag{2.2.11}$$

Thus, we have shown that indeed (2.2.1) and (2.2.8) represent weak forms of the leading order systems for $\mathbf{A}$ and ψ, see (2.1.33)-(2.1.35) and (2.1.39)-(2.1.41), respectively.

The weak problem (2.2.8) can be written in the following form.

Seek $\psi \in \mathcal{V}$ such that

$$\begin{aligned} (\psi_t, v) + a(\psi, v) + b(\mathbf{A}, \psi, v) &= (f(\psi), v) \quad \text{for all} \quad v \in V, t \geq 0, \\ \psi(0) &= \psi^0, \end{aligned} \tag{2.2.12}$$

where $a(\cdot,\cdot)$ is the following bilinear form

$$a(\psi, v) = \left(\frac{\xi}{l}\right)^2 (\nabla\psi, \nabla v) + (\psi, v), \tag{2.2.13}$$

$b(\cdot,\cdot,\cdot)$ is the trilinear form

$$b(\mathbf{A}, \psi, v) = 2i\left(\frac{\xi}{l}\right)(\mathbf{A} \cdot \nabla\psi, v), \tag{2.2.14}$$

$f(\cdot)$ denotes the nonlinear function

$$f(\psi) \;=\; \left(2 - i\Phi - |\psi|^2 - |\mathbf{A}|^2\right)\psi, \tag{2.2.15}$$

and Φ is the following given function

$$\Phi \;=\; -\left(\frac{l^2 J}{\sigma\xi\lambda}\right) y.$$

The results collected in the following Lemma, see [76], will be used later on in the derivation of the optimal error estimates for the fully discrete order parameter problem.

Lemma 2.1 *For all $u, v \in V$ and $\mathbf{A} \in \mathbf{H}^1_n(div\,;\Omega)$ we have*

$$a(u,u) \;\geq\; C_l\|u\|_1^2, \tag{2.2.16}$$

$$a(u,v) \;\leq\; C_u\|u\|_1\|v\|_1, \tag{2.2.17}$$

$$b(\mathbf{A},u,v) \;=\; -b(\mathbf{A},v,u), \tag{2.2.18}$$

$$b(\mathbf{A},u,u) \;=\; 0. \tag{2.2.19}$$

Proof

The bilinear form $a(\cdot,\cdot)$ is coercive. Indeed,

$$a(u,u) = \left(\frac{\xi}{l}\right)^2 \|\nabla u\|_0^2 + \|u\|_0^2 \geq C_l\|u\|_1^2,$$

where $C_l = \min\left\{\left(\frac{\xi}{l}\right)^2, 1\right\}$ and we have used the definition of $\|\cdot\|_1$.

The continuity of the bilinear form $a(\cdot,\cdot)$ follows easily. Indeed, using Cauchy's inequality, see (1.3.8), one has

$$\begin{aligned}
&a(u,v) \leq a(u,u)^{1/2}\, a(v,v)^{1/2} \\
&= \left[\left(\frac{\xi}{l}\right)^2 (\nabla u, \nabla u) + (u,u)\right]^{1/2} \left[\left(\frac{\xi}{l}\right)^2 (\nabla v, \nabla, v) + (v,v)\right]^{1/2} \\
&\leq C_u\left[(\nabla u, \nabla u) + (u,u)\right]^{1/2} \left[(\nabla v, \nabla v) + (v,v)\right]^{1/2} \\
&\leq C_u\|u\|_1\|v\|_1,
\end{aligned}$$

where $C_u = \max\left\{\left(\frac{\xi}{l}\right), 1\right\}$.

In order to show the third property we integrate by parts and use the fact that $\mathbf{A} \in \mathbf{H}^1_n(\text{div}\,;\Omega)$. Then

$$b(\mathbf{A}, u, v) = -\int_\Omega u \operatorname{div}(\mathbf{A}v)\ d\Omega + \int_\Gamma u\,(v\mathbf{A}\cdot\mathbf{n})\ d\Gamma = -b(\mathbf{A}, v, u).$$

Now, (2.2.18) automatically implies (2.2.19). □

Using (2.2.18), one may rewrite the weak form (2.2.12) in the following equivalent form, which shall be used throughout this work.

Seek $\psi \in \mathcal{V}$ such that

$$\begin{aligned} (\psi_t, v) + a(\psi, v) - b(\mathbf{A}, v, \psi) &= (f(\psi), v) \quad \text{for all} \quad v \in V, t \geq 0, \\ \psi(0) &= \psi^0. \end{aligned} \tag{2.2.20}$$

The reason for using the weak formulation (2.2.20) will be discussed later when we consider discretizations in space and introduce the discrete problem for the magnetic potential.

2.3 Existence and Uniqueness for the Weak Solution A

We recall the weak problem for $\mathbf{A}$, see (2.2.1).

Seek $\mathbf{A} \in \mathbf{H}^1_\mathbf{n}(\Omega)$ such that

$$\bar{a}(\mathbf{A}, \tilde{\mathbf{A}}) = F(\tilde{\mathbf{A}}) \ \forall\, \tilde{\mathbf{A}} \in \mathbf{H}^1_\mathbf{n}(\Omega). \tag{2.3.1}$$

We will show that $\bar{a}(\mathbf{A}, \tilde{\mathbf{A}})$ and $F(\tilde{\mathbf{A}})$ defined in (2.2.2) and (2.2.3), respectively, satisfy all the hypotheses in the Lax-Milgram Lemma, see Lemma 1.2. Then Lax-Milgram guarantees the existence and uniqueness of the weak solution $\mathbf{A}$. In order to apply Lax-Milgram we will need the following equivalence result.

Lemma 2.2 *Assume that Ω is simply connected domain in $\mathbb{R}^d, d = 2, 3$. Assume that the boundary Γ is Lipschitz-continuous. Then, for all functions in $\mathbf{H}_n^1(\Omega)$ there exist positive constants C_1, C_2 such that*

$$C_1\|\mathbf{v}\|_1 \leq (\|\text{div } \mathbf{v}\|_0 + \|\text{curl } \mathbf{v}\|_0) \leq C_2\|\mathbf{v}\|_1. \tag{2.3.2}$$

The proof of Lemma 2.2 can be found in [45]. We continue with the existence and uniqueness for the weak solution $\mathbf{A}$ which follow standard elliptic finite element theory.

Lemma 2.3 *There exists a unique solution $\mathbf{A} \in \mathbf{H}_n^1(\Omega)$ to the weak problem (2.2.1).*

Proof

Using the Cauchy-Schwarz inequality, see (1.3.8), and Lemma 2.2 one can derive the continuity of the bilinear form $\bar{a}(\cdot,\cdot)$. Indeed,

$$\begin{aligned}
\bar{a}(\mathbf{A}, \tilde{\mathbf{A}}) = (\text{curl } \mathbf{A}, \text{curl } \tilde{\mathbf{A}}) + (\text{div } \mathbf{A}, \text{div } \tilde{\mathbf{A}}) & \\
\leq \ & \|\text{curl } \mathbf{A}\|_0\|\text{curl } \tilde{\mathbf{A}}\|_0 + \|\text{div } \mathbf{A}\|_0\|\text{div } \tilde{\mathbf{A}}\|_0 \\
\leq \ & \frac{1}{2}\left(\|\text{curl } \mathbf{A}\|_0^2 + \|\text{div } \mathbf{A}\|_0^2 + \|\text{curl } \tilde{\mathbf{A}}\|_0^2 + \|\text{div } \tilde{\mathbf{A}}\|_0^2\right) \\
\leq \ & \frac{C_2}{2}\|\mathbf{A}\|_1\|\tilde{\mathbf{A}}\|_1 \ \ \forall\, \tilde{\mathbf{A}}, \mathbf{A} \in \mathbf{H}_\mathbf{n}^1(\Omega).
\end{aligned}$$

Lemma 2.2 also implies the coercivity of the bilinear form $\bar{a}(\cdot,\cdot)$

$$\bar{a}(\mathbf{A}, \mathbf{A}) = \|\text{curl } \mathbf{A}\|_0^2 + \|\text{div } \mathbf{A}\|_0^2 \geq C_1\|\mathbf{A}\|_1^2 \ \ \forall\, \mathbf{A} \in \mathbf{H}_\mathbf{n}^1(\Omega).$$

It is left to show that the linear functional $F(\cdot)$, see (2.2.3), is continuous. Indeed

$$\begin{aligned}
|F(\tilde{\mathbf{A}})| &= |(\bar{f}(x), \text{curl } \tilde{\mathbf{A}})| \\
&\leq \|\bar{f}\|_0\|\text{curl } \tilde{\mathbf{A}}\|_0 \leq \|\bar{f}\|_0\|\text{curl } \tilde{\mathbf{A}}\|_0 + \|\text{div } \tilde{\mathbf{A}}\|_0 \\
&\leq C_{\bar{f}}(\|\text{curl } \tilde{\mathbf{A}}\|_0 + \|\text{div } \tilde{\mathbf{A}}\|_0) \leq C_{\bar{f}}\|\tilde{\mathbf{A}}\|_1 \ \ \forall\, \tilde{\mathbf{A}} \in \mathbf{H}_\mathbf{n}^1(\Omega),
\end{aligned}$$

where $C_{\bar{f}} = \max\{||\bar{f}||_0, 1\}$, and we recall that $\bar{f}(x)$ is defined in (2.2.4).

Hence, applying the Lax-Milgram Lemma the proof is completed. □

2.4 Existence and Uniqueness for the Weak Solution ψ

We continue with the existence and uniqueness of the weak solution ψ. We recall the weak problem (2.2.20).

Seek $\psi \in \mathcal{V}$ such that

$$\begin{aligned} (\psi_t, v) + a(\psi, v) - b(\mathbf{A}, v, \psi) &= (f(\psi), v) \quad \text{for all} \quad v \in V, t \geq 0, \\ \psi(0) &= \psi^0. \end{aligned}$$

The existence, uniqueness, and convergence of the time-dependent weak solution ψ are proved in [37]. Below we only state some of the results relevant to our presentation; in particular, we give a result demonstrating that the order parameter ψ is bounded in $L^\infty(0, T; \mathcal{H}^1(\Omega))$.

Lemma 2.4 *Let ψ be the solution of (2.2.20). Let the initial condition satisfy $||\psi^0(\mathbf{x})||_\infty \leq 1$ in Ω. Then one has*

$$||\psi(\mathbf{x}, t)||_\infty \leq 1 \quad in \quad \Omega \times (0, T). \tag{2.4.1}$$

In [37] this result is used to establish continuous dependence on the initial data over a finite time which also implies the uniqueness of the weak solution ψ. Next in [37] a global existence result for the weak solution ψ is proved. Finally, a convergence result is presented which guarantees that the sequence $\{(\psi_k, \frac{1}{\kappa}\mathbf{A}_k)\}$ converges to the unique solution $(\psi, \mathbf{A})$ with order of convergence $\mathcal{O}(\kappa^{-2})$. This implies that the solutions of the leading order systems (2.1.33)-(2.1.35) and (2.1.39)-(2.1.41), provide a good approximation to the solution of the full G-L problem (1.2.22)-(1.2.25 for moderate values of the G-L parameter κ.

Chapter 3

Finite Element Approximations

The goal of this chapter is to introduce the finite element spaces used throughout this work and present the discrete problems corresponding to the weak formulations (2.2.1) and (2.2.20). This chapter is organized in three sections.

In the first section we recall some well known aspects of the finite element method. The reader may consult any of the many available texts on finite elements; see , e.g., [14], [22], [23], [45], [55], [68] and [83].

In the second section we define the particular finite element spaces used in the derivations of the optimal error estimates for the magnetic potential and the order parameter. In particular, we list all their properties which will be needed for our theoretical purposes. As an example we consider biquadratic and bilinear finite element spaces which will be used in our numerical experiments.

In the third section we formulate a discrete problem for the magnetic potential. Then we present a semi-discrete and a fully-discrete problem for the order parameter. Throughout this work we study two different schemes for discretizing the time variable in the order parameter system. They result in two different fully-discrete problems for the order parameter having, respectively, first and second order accuracy in time. In order to keep our notation as simple as possible we denote solutions of both the Backward-Euler-Galerkin and Crank-Nicolson-Galerkin problems by Ψ^n.

3.1 Introduction

Recall that $\Omega \subset \mathbb{R}^d$ is a bounded domain with a Lipschitz continuous boundary Γ. We consider the numerical solution of initial boundary value problems. In particular, in this work we are concerned with the approximations for the nonlinear problem for the order parameter given in (2.2.1). To obtain approximate solutions we use standard Galerkin spatial discretizations and two different discretizations in time which have first and second order of accuracy. One of the most commonly used methods for solving partial differential equations (PDE's) is the finite element method (FEM). From a practical point of view the FEM has some advantages over other methods for solving PDE's, e.g., the finite difference method. Most notably it easily handles complex geometries. The FEM yields a system of algebraic equations for the unknown parameters; the coefficient matrix is sparse and has a banded structure.

If the PDE admits an equivalent representation as an extremal problem then one may use the Ritz method to obtain approximate solutions. The FEM can be considered as a special case of the Ritz method with a particular choice for the basis functions. If the PDE does not correspond to an extremal problem then one may use variational formulations based on the PDE itself. One such method is the Galerkin method which is a generalization of the Ritz method and is applicable to a wider class of problems including PDE's with no equivalent extremal formulation. The FEM can be considered as a particular example of the Galerkin method.

We continue with a brief discussion of the Galerkin method. Starting with the elliptic BVP one first derives an equivalent formulation known as a variational (weak) formulation. The weak problem is an infinite dimensional problem posed on a suitable functional space

V. To define a conforming Galerkin method we first choose a finite dimensional subspace $V^h \subset V$. Then we define a discrete variational problem by restricting the original weak problem to the space V^h. Solution of this variational problem, known as the approximate solution, can be expressed as a finite linear combination of the basis functions with unknown coefficients. Substitution of this solution into the weak formulation leads to a system of algebraic equations for the coefficients. From a numerical point of view efficiency of the Galerkin method largely depends on the suitable choice of the basis $\phi_1, ..., \phi_d$. For instance, the FEM results from a particular choice of the basis $\phi_1, ..., \phi_d$.

As a result the FEM may be viewed as a systematic method for generating basis functions on arbitrary regions $\Omega \subset \mathbb{R}^d$. Let $\bar{\Omega}$ denote the closure of Ω. The first step of the FEM is to subdivide (triangulate) the set $\bar{\Omega}$ into a finite number of subsets $\mathcal{K}$, called finite elements. By a finite element (FE) we shall mean the following ordered triple

$$(\mathcal{K}, P(\mathcal{K}), \Sigma_{\mathcal{K}}), \tag{3.1.1}$$

where

- $\mathcal{K}$ is a geometrical object, e.g. triangle, rectangle, etc.,
- $P(\mathcal{K})$ is a finite dimensional linear space of functions defined on $\mathcal{K}$,
- $\Sigma_{\mathcal{K}}$ is a set of degrees of freedom such that a function in $P(\mathcal{K})$ is uniquely determined by $\Sigma_{\mathcal{K}}$.

We denote the triangulation by $\mathcal{T}_h$ and require it to satisfy the following properties.

1. $\bar{\Omega} = \cup_{\mathcal{K} \in \mathcal{T}_h} \mathcal{K}$.
2. For each $\mathcal{K} \in \mathcal{T}_h$, the set $\mathcal{K}$ is closed and the interior $\mathcal{K}^0$ is nonempty.

3. For each distinct $\mathcal{K}_1, \mathcal{K}_2 \in \mathcal{T}_h$, one has $\mathcal{K}_1^0 \cap \mathcal{K}_2^0 = \emptyset$.

4. For each $\mathcal{K} \in \mathcal{T}_h$, the boundary $\partial\mathcal{K}$ is Lipschitz continuous.

5. Any face of any $\mathcal{K}_1 \in \mathcal{T}_h$ is either a subset of Γ, or a face of another $\mathcal{K}_2 \in \mathcal{T}_h$.

Once a triangulation $\mathcal{T}_h$ is established over the set $\bar{\Omega}$, one defines a finite element space V^h. A notable property of V^h is that the space $P(\mathcal{K}) = \{v_{h|\mathcal{K}} : v_h \in V^h\}$ contains polynomials, or functions "close" to polynomials. The third basic aspect of the FEM is that the space V^h has at least one "canonical" basis with basis functions having "small" support.

3.2 Finite Element Spaces

The goal of this section is to introduce the finite element spaces and their properties used throughout this work. As an example of particular finite elements we consider d-simplices in $\mathbb{R}^d$. Following [45], we introduce some standard definitions and results.

Let us recall that the convex hull of $(d+1)$ points $(a_j)_{j=1}^d \in \mathbb{R}^d$, which are not all located in a single hyperplane, is called an **d-simplex** in $\mathbb{R}^d$ and will be denoted by $\mathcal{K}$. For example, a 2-simplex is a triangle and a 3-simplex is a tetrahedron. The points a_j are called **vertices** of the d-simplex. For any integer m with $0 \le m \le d$, an **m-face** of the d-simplex $\mathcal{K}$ is any m-simplex whose $(m+1)$ vertices are also vertices of $\mathcal{K}$. The size and shape of a d-simplex $\mathcal{K}$ are specified by its diameter, denoted by $h_{\mathcal{K}}$, and by the diameter of the largest ball inscribed in $\mathcal{K}$, denoted by $\rho_{\mathcal{K}}$. Let $\mathcal{T}_h$ be a triangulation of $\bar{\Omega}$ consisting of closed simplices $\mathcal{K}$, whose diameters are bounded by h. We assume that any two simplices from the triangulation $\mathcal{T}_h$ are either disjoint or have at most a common face. We say that an affine family of triangulations $\{\mathcal{T}_h\}$ of d-simplices $\mathcal{K}$ is **regular** if the following two conditions are satisfied.

1. There exists a positive constant σ, independent of h and $\mathcal{K}$, such that

$$\sigma_{\mathcal{K}} = \frac{h_{\mathcal{K}}}{\rho_{\mathcal{K}}} \leq \sigma \quad \forall\, \mathcal{K} \in \mathcal{T}_h.$$

2. h approaches zero.

A regular family $\{\mathcal{T}_h\}$ is called **uniformly regular** (or quasi uniform), if there exists a positive constant τ such that

$$\tau h \leq h_{\mathcal{K}} \leq \ \sigma \rho_{\mathcal{K}} \quad \forall\, \mathcal{K} \in \mathcal{T}_h.$$

Given a nonnegative integer r we denote by P_r the space of all polynomials on $\mathbb{R}^d$ of degree less than or equal to r.

Definition 3.1 *Given a triangulation $\mathcal{T}_h$ of $\bar{\Omega}$ and a fixed integer $r \geq 1$, we define the standard finite element space*

$$S_r^h = \{v_h \in C^0(\bar{\Omega});\ v_h|_{\mathcal{K}} \in P_r \ \ \forall\, \mathcal{K} \in \mathcal{T}_h\}. \tag{3.2.1}$$

Similarly, one can define the corresponding standard complex finite element space $\mathcal{S}_r^h$ and the standard vector finite element space $\mathbf{S}_r^h$.

The finite element spaces defined in (3.2.1) satisfy the following **best approximation property** which will be used repeatedly throughout this work, see [45].

Lemma 3.1 *Let $\mathcal{T}_h$ be regular triangulation of $\bar{\Omega}$. Let s be a real number with $1 \leq s \leq r$. Then, for $m = 0, 1$ there exists an element $v_h \in S_r^h$, such that*

$$|v_h - v|_{m,q} \leq C h^{s+1-m} |v|_{s+1,q} \quad \forall\, v \in W^{s+1,q}(\Omega), \tag{3.2.2}$$

where C is a positive constant independent of h and v. $\square$

However, for an affine family of triangulations which is not necessary regular instead of (3.2.2) we have the weaker result

$$|v_h - v|_{m,q} \leq C\frac{h^{s+1}}{\rho^m}.$$

In what follows, we shall need to convert between $W^{m,p}$ and $W^{m,q}$ norms of finite element functions, as well as to replace stronger norms by weaker norms. This can be accomplished by means of the inverse inequalities given below, see [45].

Lemma 3.2 *Let r and p be real numbers with $1 \leq q,\ p \leq \infty$ and let $m = 0, 1$. Let us assume that $\mathcal{T}_h$ is a uniformly regular triangulation of $\bar{\Omega}$. Then there exist constants $C_1 > 0$ and $C_2 > 0$, independent of h, such that*

$$|v_h|_{1,q} \leq C_1 h^{-1+min(0,d/q-d/p)}\|v_h\|_{0,p} \quad \forall\, v_h \in S_r^h \tag{3.2.3}$$

and

$$|v_h|_{m,q} \leq C_2 h^{min(0,d/q-d/p)}|v_h|_{m,p} \quad \forall\, v_h \in S_r^h. \tag{3.2.4}$$

In addition, if $q \leq p$ then (3.2.4) holds for $\mathcal{T}_h$ that is regular. □

We continue with definitions of the particular finite element spaces used throughout this work. Let $\psi(t)$ and $\mathbf{A}$ be the solutions of the weak problems given in (2.2.20) and (2.2.1), respectively. For the approximation of the order parameter ψ we consider the following standard complex finite element space

$$V^h = \mathcal{S}_r^h, \tag{3.2.5}$$

and for the approximation of the magnetic potential $\mathbf{A}$ we consider the space

$$\mathbf{W}^h = \mathbf{S}_r^h \cap \mathbf{H}_n^1(\Omega). \tag{3.2.6}$$

Throughout this work the above notation will be reserved for the approximation spaces for the order parameter and the magnetic potential.

If the hypotheses of Lemma 3.1 hold, then the following best approximation properties are valid for V^h and $\mathbf{W}^h$ and there exists an element $v_h \in V^h$ such that

$$|v_h - v|_{m,q} \leq Ch^{s+1-m}|v|_{s+1,q} \quad \forall\, v \in W^{s+1,q}(\Omega) \tag{3.2.7}$$

and an element $\mathbf{w}_h \in \mathbf{W}^h$ such that

$$|\mathbf{w}_h - \mathbf{w}|_{m,q} \leq Ch^{s+1-m}|\mathbf{w}|_{s+1,q} \quad \forall\, \mathbf{w} \in W^{s+1,q}(\Omega). \tag{3.2.8}$$

Similarly, if the hypotheses of Lemma 3.2 hold, then the following inverse inequalities are valid for V^h and W^h

$$||\mathbf{w}_h||_\infty \leq Ch^{-\frac{d}{2}}||\mathbf{w}_h||_0 \quad \forall\, \mathbf{w}_h \in \mathbf{W}^h, \tag{3.2.9}$$

and

$$||v_h||_\infty \leq Ch^{-\frac{d}{2}}||v_h||_0 \quad \forall\, v_h \in V^h. \tag{3.2.10}$$

These inequalities are used repeatedly throughout this work.

Finally we assume that for sufficiently smooth $\psi(t)$ and $\mathbf{A}$ the finite element spaces V^h and $\mathbf{W}^h$ satisfy

$$\lim_{h\to 0}\left(\sup_{t\in[0,T]}\inf_{v_h\in V^h}\left(||\psi(t) - v_h||_\infty + h^{-\frac{d}{2}}||\psi(t) - v_h||_0\right)\right) = 0 \tag{3.2.11}$$

and

$$\lim_{h\to 0}\left(\inf_{\mathbf{w}_h\in \mathbf{W}^h}\left(||\mathbf{A} - \mathbf{w}_h||_\infty + h^{-\frac{d}{2}}||\mathbf{A} - \mathbf{w}_h||_0\right)\right) = 0, \tag{3.2.12}$$

respectively.

Following [5] we note that (3.2.11) follows from (3.2.7) and (3.2.10) while (3.2.12) follows from (3.2.8) and (3.2.9) provided that there exist interpolation operators of smooth functions into V^h and $\mathbf{W}^h$, respectively, with reasonable L^∞ approximation properties.

For the sake of generality we have introduced finite element spaces using a triangulation of $\bar{\Omega}$ based on d-simplices in $\mathbb{R}^d$. We note that in $\mathbb{R}^2$ a 2-simplex is a triangle. On the other hand, finite element spaces can also be constructed using triangulations based on regions other than simplices. For example, a triangulation $\mathcal{T}_h$ and a polynomial finite element space in two dimensions can be defined using suitably chosen functions on rectangles instead of triangles. As an example of such a space let us consider the biquadratic finite element space $Q_2(\mathcal{K})$. In terms of (3.1.1), Q_2 consists of a rectangle $\mathcal{K}$, $P(\mathcal{K}) = Q_2(\mathcal{K})$, where Q_2 denotes the set of functions which are polynomials of degree less than or equal to 2 in each coordinate direction, and the number of degrees of freedom is 9. Let $\tilde{\mathcal{K}}$ be the reference element with vertices $\tilde{\mathbf{x}}^1, \tilde{\mathbf{x}}^2, \tilde{\mathbf{x}}^3, \tilde{\mathbf{x}}^4$. Let us choose the following nine nodal points $\mathbf{x}^{1,1} = (0,0)$, $\mathbf{x}^{2,1} = (1/2,0)$, $\mathbf{x}^{3,1} = (1,0)$, $\mathbf{x}^{1,2} = (0,1/2)$, $\mathbf{x}^{2,2} = (1/2,1/2)$, $\mathbf{x}^{3,2} = (1,1/2)$, $\mathbf{x}^{1,3} = (0,1)$, $\mathbf{x}^{2,3} = (1/2,1)$ and $\mathbf{x}^{3,3} = (1,1)$. The biquadratic functions on $\tilde{\mathcal{K}}$ are polynomials in $\tilde{\mathbf{x}}$ of degree ≤ 2 with respect to each variable. They are defined by taking the the nine direct products of the 1-dimensional quadratic basis functions on the interval $[0,1]$

$$\theta_1(t) = (1-t)(1-2t),$$

$$\theta_2(t) = t(1-2t),$$

$$\theta_3(t) = 4t(1-t).$$

Thus the basis $\tilde{\phi}_{i,j}(\tilde{\mathbf{x}})$, $i,j = 1,2,3$ for Q_2 on a reference rectangle $\tilde{\mathcal{K}}$ is defined by

$$\tilde{\phi}_{i,j}(\tilde{\mathbf{x}}) = \theta_i(\tilde{x}_1)\,\theta_j(\tilde{x}_2) \quad \text{for} \quad i,j = 1,2,3.$$

The function space spanned by the basis functions $\tilde{\phi}_{i,j}, i = 1,2,3$ is the space of biquadratic functions on $\tilde{\mathcal{K}}$ and is denoted by $Q_2(\tilde{\mathcal{K}})$.

In order to determine the basis functions on an arbitrary straight-sided element $\mathcal{K}$ with vertices $\mathbf{x}^1, \mathbf{x}^2, \mathbf{x}^3, \mathbf{x}^4$ let us define a mapping $F_{\mathcal{K}}$ from $\tilde{\mathcal{K}}$ onto $\mathcal{K}$ by

$$\mathbf{x} = F_{\mathcal{K}}(\tilde{\mathbf{x}}) = \sum_{i=1}^{4} \mathbf{x}^i \tilde{\phi}_i(\tilde{\mathbf{x}}). \tag{3.2.13}$$

Given $\tilde{\phi}_i$ one may use $F_{\mathcal{K}}$ defined in (3.2.13) to obtain the basis functions ϕ_i for an arbitrary rectangle $\mathcal{K}$ with nodal points $\mathbf{x}^1, \mathbf{x}^2, ..., \mathbf{x}^9$ as follows

$$\phi_{i,j}(\mathbf{x}) = \tilde{\phi}_{i,j}\left(F_{\mathcal{K}}^{-1}(\mathbf{x})\right) \quad \text{for} \quad \mathbf{x} \in \mathcal{K}, \quad \text{and} \quad i = 1,2,3.$$

It also is possible to define the mapping $F_{\mathcal{K}}$ so that it maps the reference element $\tilde{\mathcal{K}}$ onto a curved-sided element $\mathcal{K}$. Our numerical calculations are limited to the case of a square domain Ω having sides parallel to the coordinate axes.

In a similar way one can define the space Q_1 of all functions which are polynomials of degree less than or equal to one in each coordinate direction. We note that basis for Q_1 on a reference rectangle has only four elements of the form $\phi_{i,j} = \theta_i \theta_j$ for $i,j = 1,2$, where θ_i denote the linear 1−dimensional basis functions.

We construct approximate solutions of the weak problems given in (2.2.1) and (2.2.20) using quasi uniform triangulation. Hence the finite element spaces V^h and $\mathbf{W}^h$ used in this work satisfy all necessary properties.

Let $\mathcal{T}_h$ be a quasi-uniform partition of Ω into rectangles $\mathcal{K}$ having sides parallel to the coordinate axis in $\mathbb{R}^2$. Here h is the maximal length of a side of a rectangle $\mathcal{K}$ in $\mathcal{T}_h$. For $i = 1,2$ let us define the following two finite element subspaces of $\mathcal{H}^1(\Omega)$ and $\mathbf{H}^1_n(\Omega)$, respectively.

$$V^h = \{v \in C^0(\bar{\Omega}) \mid v(\mathcal{K}) \in Q_i(\mathcal{K}) \;\; \forall\, \mathcal{K} \in \mathcal{T}_h\}, \tag{3.2.14}$$

$$\mathbf{W}^h \quad = \quad \{\mathbf{w} \in \mathbf{C}^0(\bar{\Omega}) \mid \mathbf{w}(\mathcal{K}) \in \mathbf{Q}_i(\mathcal{K}) \ \forall\, \mathcal{K} \in \mathcal{T}_h, \ \ \mathbf{w} \cdot \mathbf{n} = 0 \ \text{ on } \ \Gamma\}. \qquad (3.2.15)$$

When $i = 1$ the spaces V^h and $\mathbf{W}^h$ correspond to bilinear finite elements and for $i = 2$, V^h and $\mathbf{W}^h$ are determined using biquadratic finite elements. Numerical results presented in Chapter 9 will be computed by finite element codes in which we will use the above discrete spaces defined in (3.2.14) and (3.2.15)..

3.3 Discretization

The goal of this section is to formulate a discrete problem for the magnetic potential $\mathbf{A}$ as well as semidiscrete and fully-discrete problems for the order parameter ψ. We discretize the continuous equations (2.2.1) and (2.2.20) in space by the standard Galerkin method. To this end, we choose finite dimensional subspaces $\mathbf{W}^h \subset \mathbf{H}^1_n(\Omega)$ and $V^h \subset \mathcal{H}^1(\Omega)$, consisting of continuous functions. Then, we seek approximations $\mathbf{A}_h \in \mathbf{W}^h$ and $\psi_h \in V^h$ of the weak solutions $\mathbf{A}$ of (2.2.1) and ψ of (2.2.20). Since the weak problem for ψ is time dependent, for a given T with $0 < T < \infty$, one seeks approximations ψ_h for $0 \le t \le T$.

Throughout this work, we assume that the finite dimensional spaces V^h and $\mathbf{W}^h$ satisfy all of the properties stated in Section 3.2.

Let us recall the weak problem for $\mathbf{A}$ given in (2.2.1).

Seek $\mathbf{A} \in \mathbf{H}^1_\mathbf{n}(\Omega)$ such that

$$\bar{a}(\mathbf{A}, \tilde{\mathbf{A}}) = F(\tilde{\mathbf{A}}) \ \ \forall\, \tilde{\mathbf{A}} \in \mathbf{H}^1_\mathbf{n}(\Omega).$$

Then we consider the following discrete problem for $\mathbf{A}_h$.

Seek $\mathbf{A}_h \in \mathbf{W}^h$ such that

$$\bar{a}(\mathbf{A}_h, \tilde{\mathbf{A}}_\mathbf{h}) = F(\tilde{\mathbf{A}}_\mathbf{h}) \ \ \forall\, \tilde{\mathbf{A}}_\mathbf{h} \in \mathbf{W}^h, \qquad (3.3.1)$$

where $\bar{a}(\cdot,\cdot)$ and $F(\cdot)$ are defined in (2.2.2) and (2.2.3), respectively.

Let us recall the weak problem for ψ, see (2.2.20).

Seek $\psi \in \mathcal{V}$ such that

$$\begin{aligned}(\psi_t, v) + a(\psi, v) - b(\mathbf{A}, v, \psi) &= (f(\psi), v) \quad \forall v \in V, t \geq 0,\\ \psi(0) &= \psi^0.\end{aligned}$$

Then we consider the following semi-discrete problem for ψ_h.

Seek $\psi_h : [0, T] \longrightarrow V^h$ such that

$$\begin{aligned}(\frac{d}{dt}\psi_h, v_h) + a(\psi_h, v_h) - b(\mathbf{A}_h, v_h, \psi_h) &= (f_h(\psi_h), v_h) \quad \forall v_h \in V^h, 0 \leq t \leq T,\\ \psi_h(0) &= \tilde{\psi}^0,\end{aligned} \tag{3.3.2}$$

where $a(\cdot,\cdot)$, $b(\cdot,\cdot,\cdot)$ are defined in (2.2.13), (2.2.14), respectively,

$$f_h(\psi) = \left(2 - i\Phi - |\psi|^2 - |\mathbf{A}_h|^2\right)\psi, \tag{3.3.3}$$

and $\tilde{\psi}^0$ is an approximation of ψ^0 in V^h.

We note that the semidiscrete problem (3.3.2) is, in fact, a system of nonlinear ODE's since we have discretized the space variable only.

We now proceed with discretizing the time variable in the semidiscrete problem (3.3.2). As a result, we will arrive at the fully discrete problem for the order parameter in which both the space and the time variables are discretized. In the rest of this work we are concerned with two fully discrete schemes. First, we consider the Backward-Euler-Galerkin scheme which is first-order accurate in time. Then, we present the Crank-Nicolson-Galerkin scheme which is second-order accurate in time. We denote the fully-discrete solution for both the Backward-Euler-Galerkin and Crank-Nicolson-Galerkin problems by Ψ^n.

Let $k > 0$ be the time step. Throughout this work we assume that the time step is fixed. All results can be easily generalized to the case of a variable time step. We denote $t_n = nk$, for $0 \leq n \leq N$ and $T = Nk$.

Let $\Psi^n \in V^h$ be the fully discrete approximation of $\psi(t_n)$ in V^h at time t_n. We first consider the Backward-Euler method in which we replace the time derivative of ψ_h by the backward difference quotient

$$\frac{\tilde{d}}{dt}\Psi^n = \frac{\Psi^n - \Psi^{n-1}}{k}. \tag{3.3.4}$$

The Backward-Euler-Galerkin discretization of (2.2.20) is as follows

Seek $\Psi^n \in V^h$ such that

$$\begin{aligned} (\frac{\tilde{d}\Psi^n}{dt}, v_h) + a(\Psi^n, v_h) - b(\mathbf{A}_h, v_h, \Psi^n) &= (f_h(\Psi^n), v_h) \forall v_h \in V^h\ , \ \ 1 \leq n \leq N, \\ \Psi^0 &= \tilde{\psi}^0. \end{aligned} \tag{3.3.5}$$

In addition to the Backward Euler scheme we also consider the popular Crank-Nicolson type scheme often used in the literature, see, e.g., [5], [34], [77]. There are different names associated with this second order scheme, for example, Crank-Nicolson method, one-stage Gauss-Legendre implicit Runge-Kutta scheme, one-leg multi-step method. For the sake of simplicity we refer to this scheme as the Crank-Nicolson scheme. Since we are concerned with the numerical approximation of a dynamical problem the use of such a higher order scheme may be beneficial from a computational viewpoint. For example, if variable steps in time are used in a higher order scheme this may result in reaching the steady state configuration of the model system much faster than with a first order scheme. In addition, the use of higher order schemes may also give better resolution of the initial transient period.

We recall that the implicit Crank-Nicolson method for the general nonlinear problem

$$y\prime(t) \ = \ F(y(t)) \quad \text{for} \quad t \in (t_0, T)$$

$$y(t_0) \quad = \quad y_0$$

reads

$$y_n = y_{n-1} + kF\left(\frac{y_n + y_{n-1}}{2}\right).$$

The Crank-Nicolson-Galerkin discretization of (2.2.20) can be stated as follows.

Seek $\Psi^n \in V^h$ such that

$$\begin{aligned} (\frac{\tilde{d}\Psi^n}{dt}, v_h) + a(\bar{\Psi}^n, v_h) - b(\mathbf{A}_h, \bar{\Psi}^n, v_h) &= (f_h(\bar{\Psi}^n), v_h)\, \forall v_h \in V^h,\ 1 \le n \le N, \\ \Psi^0 &= \tilde{\psi}^0, \end{aligned} \tag{3.3.6}$$

where $\frac{\tilde{d}}{dt}$ is defined by (3.3.4) and we have used the notation

$$\bar{\Psi}^n = \frac{\Psi^n + \Psi^{n-1}}{2}. \tag{3.3.7}$$

Chapter 4

Approximation Results for the Magnetic Potential

This chapter is devoted to the finite element approximations for the magnetic potential. It consists of two sections.

In the first section we prove existence, uniqueness and derive optimal $\mathbf{L}^2$ and $\mathbf{H}^1$ error estimates for the solution $\mathbf{A}_h$ of the discrete problem (3.3.1). The derivation of the error estimates for the discrete problem for $\mathbf{A}_h$ is standard and follows directly from the steady state finite element theory for elliptic equations.

In the second section we show that under certain smoothness requirements for the weak solution $\mathbf{A}$ the infinity norm of both the weak solution $\mathbf{A}$ and the discrete solution $\mathbf{A}_h$ are bounded independently of the discretization parameter h. These results will be used repeatedly in the derivation of the optimal $\mathcal{L}^2$ and $\mathcal{H}^1$ error estimates for the order parameter.

From now on let us assume that $\Omega \subset \mathbb{R}^d$, for $d = 2, 3$. Let $\mathbf{A}$ and $\psi(t_n)$ denote the unique solutions of the weak problems given in (2.2.1) and (2.2.20), respectively. Finally, let C denote a generic positive constant, different at different places, which is independent of the discretization parameter h and the time step k.

4.1 Existence, Uniqueness and Optimal $\mathbf{H}^1$ and $\mathbf{L}^2$ Error Estimates

We recall the problems for $\mathbf{A}$ and $\mathbf{A}_h$, see (2.2.1) and (3.3.1), respectively.

Seek $\mathbf{A} \in \mathbf{H}^1_n(\Omega)$ such that

$$a(\mathbf{A}, \tilde{\mathbf{A}}) = F(\tilde{\mathbf{A}}) \ \ \forall\, \tilde{\mathbf{A}} \in \mathbf{H}^1_n(\Omega).$$

Seek $\mathbf{A}_h \in \mathbf{W}^h \subset \mathbf{H}^1_n(\Omega)$ such that

$$a(\mathbf{A}_h, \tilde{\mathbf{A}}_h) = F(\tilde{\mathbf{A}}_h) \ \ \forall\, \tilde{\mathbf{A}}_h \in \mathbf{W}^h.$$

Let us define the error $\mathbf{E}_h$ in the discrete problem (3.3.1), by

$$\mathbf{E}_h = \mathbf{A} - \mathbf{A}_h. \tag{4.1.1}$$

A direct application of Cea's Lemma 1.3 gives us the following optimal estimate for the error $\mathbf{E}_h$.

Lemma 4.1 *Let* $\mathbf{A} \in \mathbf{H}^1_n(\Omega)$ *be the unique solution to (2.2.1) which is guaranteed by Lemma 2.3. Then there exists a unique solution* $\mathbf{A}_h \in \mathbf{W}^h$ *to the discrete problem (3.3.1). Moreover, the following optimal estimate holds*

$$||\mathbf{E}_h||_1 \leq C h^m ||\mathbf{A}||_{m+1}, \ \ \textit{provided}\ \ \mathbf{A} \in \mathbf{H}^1_n(\Omega) \cap \mathbf{H}^{m+1}(\Omega). \tag{4.1.2}$$

Proof

The existence and uniqueness of the discrete solution $\mathbf{A}_h \in \mathbf{W}^h$ follows directly by noting that $\mathbf{W}^h \subset \mathbf{H}^1_n(\Omega)$ and applying Lax-Milgram Lemma.

To obtain the estimate (4.1.2) let us recall that $F(\tilde{\mathbf{A}}_h)$ is a bounded linear functional on $\mathbf{H}^1_n(\Omega)$ and $\bar{a}(\cdot,\cdot)$ is a bilinear form on $\mathbf{H}^1_n(\Omega) \times \mathbf{H}^1_n(\Omega)$ which is continuous and coercive. Since all the hypotheses in the Cea's Lemma 1.3, are satisfied, one immediately obtains the following abstract error estimate

$$||\mathbf{E}_h||_1 \leq C \inf_{\tilde{\mathbf{A}}_h \in \mathbf{W}^h} ||\mathbf{A} - \tilde{\mathbf{A}}_h||_1.$$

Hence, we have reduced the problem of estimating the $\mathbf{H}^1$ norm of the error $\mathbf{E}_h$ to an approximation problem. Thus, using the best approximation property of $\mathbf{W}^h$, see (3.2.2), we obtain the desired result

$$\|\mathbf{E}_h\|_1 \le Ch^m \|\mathbf{A}\|_{m+1} \text{ provided } \mathbf{A} \in \mathbf{H}^1_n(\Omega) \cap \mathbf{H}^{m+1}(\Omega). \quad \square$$

Under an additional assumption on the dual problem, see (1.3.15), one can derive the following optimal $\mathbf{L}^2$ estimate.

Lemma 4.2 *Let* $\mathbf{A}$ *and* $\mathbf{A}_h$ *denote the unique solutions to the weak (2.2.1) and discrete (3.3.1) problems. Let us assume that the dual problem corresponding to (2.2.1) is regular. Then we have the optimal estimate*

$$\|\mathbf{E}_h\|_0 \le Ch^{m+1} \|\mathbf{A}\|_{m+1} \textit{ provided } \mathbf{A} \in \mathbf{H}^1_n(\Omega) \cap \mathbf{H}^{m+1}(\Omega). \tag{4.1.3}$$

Proof

To prove the $\mathbf{L}^2$ error estimate we need to assume that the dual problem given below is regular; that is, if $\varphi \in \mathbf{L}^2(\Omega)$ is arbitrary function and ϕ is the solution of

$$\bar{a}(\tilde{\mathbf{A}}, \phi) = (\varphi, \tilde{\mathbf{A}}) \quad \forall\, \tilde{\mathbf{A}} \in \mathbf{H}^1_n(\Omega), \tag{4.1.4}$$

then $\phi \in \mathbf{H}^2(\Omega) \cap \mathbf{H}^1_n(\Omega)$.

We recall that all hypotheses of Cea's Lemma 1.3 are satisfied in the present setting. We also recall the compact imbedding (1.4.12) which implies that in both two and three space dimensions we have

$$\mathbf{H}^1_n(\Omega) \subset \mathbf{L}^2(\Omega). \tag{4.1.5}$$

It follows that all the hypotheses in the Aubin-Nitsche Lemma, see Lemma 1.4, are satisfied. Hence applying the Aubin-Nitsche Lemma we arrive at the desired optimal $\mathbf{L}^2$ error estimate

$$\|\mathbf{E}_h\|_0 \le Ch^{m+1} \|\mathbf{A}\|_{m+1} \;, \text{ provided } \mathbf{A} \in \mathbf{H}^1_n(\Omega) \cap \mathbf{H}^{m+1}(\Omega). \quad \square \tag{4.1.6}$$

4.2 Uniform estimates for $\mathbf{A}$ and $\mathbf{A}_h$

The goal of this section is to derive several preliminary estimates for the solutions of the weak and the approximate problems for the magnetic potential. More precisely, we prove that the L^∞-norms of both the weak and discrete solutions $\mathbf{A}$ and $\mathbf{A}_h$ are bounded independently of the discretization parameter h. The decoupling of the leading order magnetic potential system from the leading order system for the order parameter plays an important role in the derivation of such uniform estimates. It allows us to derive uniform estimates for the magnetic potential and then use them in order to bound optimally all terms in the order parameter system. The results derived in this section are crucial for the derivation of the optimal fully discrete $\mathcal{L}^2$ and $\mathcal{H}^1$ error estimates and will be used extensively throughout this work.

As a direct application of the Sobolev Imbedding Theorem we have that if $\mathbf{w} \in \mathbf{H}^2$ then in both two and three dimensions $\|\mathbf{w}\|_\infty$ is bounded. This is summarized in the following lemma.

Lemma 4.3 *Let $\Omega \subset \mathbb{R}^d$ for $d = 2, 3$. Let m be a positive integer such that $m + 1 > d/2$. If $\mathbf{w} \in \mathbf{H}^{m+1}(\Omega)$ then we have the estimate*

$$\|\mathbf{w}\|_\infty \;\leq\; C, \tag{4.2.1}$$

where C is a generic constant independent of the discretization parameter h.

Proof

Let us recall, see Lemma 1.1, that for $d = 2,\ 3$ the following imbedding holds

$$\mathbf{W}^{m+1,2}(\Omega) \hookrightarrow C^0(\Omega), \tag{4.2.2}$$

provided that $m+1>d/2$. By the continuity of the imbedding (4.2.2) we have

$$\|\mathbf{w}\|_\infty \leq C\|\mathbf{w}\|_{m+1} \leq C,$$

provided $\mathbf{w} \in \mathbf{H}^{m+1}(\Omega)$. This concludes the proof of (4.2.1). $\square$

In particular, we may apply Lemma 4.3 to obtain an equivalent result for the solution of the weak problem (2.2.1). In order to derive optimal error estimates it is customary to require additional smoothness for the weak solution. In particular, we shall assume that $\mathbf{A} \in \mathbf{H}^1_n(\Omega) \cap \mathbf{H}^{m+1}(\Omega)$. Then Lemma 4.3 yields

$$\|\mathbf{A}\|_\infty \ \leq \ C, \tag{4.2.3}$$

provided that $m+1>d/2$.

We define a **projection** $\bar{\mathbf{P}}\mathbf{A}$ of the weak solution $\mathbf{A}$ onto the finite element space $\mathbf{W}^h$ by

$$\bar{a}(\bar{\rho}, \mathbf{w}_h) = 0 \quad \forall\, \mathbf{w}_h \in \mathbf{W}^h, \tag{4.2.4}$$

where

$$\bar{\rho} = \bar{\mathbf{P}}\mathbf{A} - \mathbf{A} \tag{4.2.5}$$

and the bilinear form $\bar{a}(\cdot,\cdot)$ is defined in (2.2.2).

Lemma 4.4 *Let $\Omega \subset \mathbb{R}^d$ for $d=2,3$. Let m be a positive integer such that $m+1>d/2$. Let $\mathbf{A} \in \mathbf{H}^1_n(\Omega) \cap \mathbf{H}^{m+1}(\Omega)$ be the weak solution of problem (2.2.1). Then, we have the estimate*

$$\|\mathbf{A} - \bar{\mathbf{P}}\mathbf{A}\|_0 \leq C\, h^{m+1}, \tag{4.2.6}$$

where C is a generic constant independent of the discretization parameter h.

Proof

According to (4.2.4), $\bar{\mathbf{P}}\mathbf{A}$ solves the problem

$$\bar{a}(\bar{\mathbf{P}}\mathbf{A}, \mathbf{w}_h) = \bar{a}(\mathbf{A}, \mathbf{w}_h) \quad \forall\, \mathbf{w}_h \in \mathbf{W}^h. \tag{4.2.7}$$

We note that $\bar{a}(\mathbf{A}, \mathbf{w}_h)$ defines a bounded linear functional on $\mathbf{H}_n^1(\Omega)$ and that $\bar{a}(\cdot,\cdot)$ is a continuous and coercive bilinear form on $\mathbf{H}_n^1(\Omega) \times \mathbf{H}_n^1(\Omega)$. Hence by the Lax-Milgram Lemma there exists a unique $\bar{\mathbf{P}}\mathbf{A}$ solving (4.2.7).

Now, we let $\varphi \in L^2(\Omega)$ be arbitrary and assume that the solution ϕ of the dual problem

$$\bar{a}(\mathbf{w}, \phi) = (\varphi, \mathbf{w})$$

is regular. Then, using the continuous imbedding, (4.1.5), the Aubin-Nitshe Lemma and the regularity of the dual problem we get the desired $\mathbf{L}^2$ estimate (4.2.6). □

Lemma 4.5 *Let $\Omega \subset \mathbb{R}^d$ for $d = 2, 3$. Let $\mathbf{A} \in \mathbf{H}_n^1(\Omega) \cap \mathbf{H}^{m+1}(\Omega)$ be the weak solution of problem (2.2.1), where $m + 1 > d/2$. Let us assume that the dual problem corresponding to (2.2.1) is regular. Let $\mathbf{A}_h \in \mathbf{W}^h$ be the finite element approximation to $\mathbf{A}$ which satisfies (3.2.12). Then*

$$\|\mathbf{A}_h\|_\infty \;\; \leq \;\; C \quad \textit{for sufficiently small } h, \tag{4.2.8}$$

where C is a generic constant independent of the discretization parameter h.

Proof

In order to show that $\|\mathbf{A}_h\|_\infty$ can be bounded independently of h we first estimate $\|\mathbf{A}_h\|_\infty - \|\mathbf{A}\|_\infty$ and then use the fact that $\|\mathbf{A}\|_\infty \leq C$.

One may use the optimal estimates (4.1.3), (4.2.6) and the inverse inequality for $\mathbf{W}^h$, see (3.2.9), to get that $\|\mathbf{A}_h\|_\infty - \|\mathbf{A}\|_\infty \leq C\ h^{m+1-\frac{d}{2}}$. To show this we first add and subtract

$\mathbf{A}$ as well as an arbitrary element $\mathbf{w}_h \in \mathbf{W}^h$. Applying the triangle inequality we get

$$\begin{aligned} \|\mathbf{A}_h\|_\infty - \|\mathbf{A}\|_\infty &\le \|\mathbf{A}_h - \mathbf{A}\|_\infty \\ &\le (\|\mathbf{A}_h - \bar{\mathbf{P}}\mathbf{A}\|_\infty + \|\bar{\mathbf{P}}\mathbf{A} - \mathbf{w}_h\|_\infty) + \|\mathbf{A} - \mathbf{w}_h\|_\infty. \end{aligned}$$

Next we use the inverse inequality (3.2.9) to obtain

$$\|\mathbf{A}_h\|_\infty - \|\mathbf{A}\|_\infty \le C\, h^{-\frac{d}{2}} (\|\mathbf{A}_h - \bar{\mathbf{P}}\mathbf{A}\|_0 + \|\bar{\mathbf{P}}\mathbf{A} - \mathbf{w}_h\|_0) + \|\mathbf{A} - \mathbf{w}_h\|_\infty.$$

We proceed by adding and subtracting $\mathbf{A}$ and using the triangle inequality to get

$$\begin{aligned} &\|\mathbf{A}_h\|_\infty - \|\mathbf{A}\|_\infty \\ &\le C\, h^{-\frac{d}{2}} (\|\mathbf{A}_h - \mathbf{A}\|_0 + 2\|\mathbf{A} - \bar{\mathbf{P}}\mathbf{A}\|_0 + \|\mathbf{A} - \mathbf{w}_h\|_0) + \|\mathbf{A} - \mathbf{w}_h\|_\infty \\ &\le C\, h^{-\frac{d}{2}} (\|\mathbf{A}_h - \mathbf{A}\|_0 \|\mathbf{A} - \bar{\mathbf{P}}\mathbf{A}\|_0) + C\, h^{-\frac{d}{2}} \|\mathbf{A} - \mathbf{w}_h\|_0 + \|\mathbf{A} - \mathbf{w}_h\|_\infty. \end{aligned}$$

Using the optimal error estimates for $\|\mathbf{A}_h - \mathbf{A}\|_0$ and $\|\mathbf{A} - \bar{\mathbf{P}}\mathbf{A}\|_0$ and the property (3.2.12) of the finite element space $\mathbf{W}^h$ one has

$$\begin{aligned} \|\mathbf{A}_h\|_\infty - \|\mathbf{A}\|_\infty &\le \|\mathbf{A}_h - \mathbf{A}\|_\infty \\ &\le C\, h^{m+1-\frac{d}{2}} + \left(C\, h^{-\frac{d}{2}} \|\mathbf{A} - \mathbf{w}_h\|_0 + \|\mathbf{A} - \mathbf{w}_h\|_\infty\right) \qquad (4.2.9) \\ &\le C\, h^{m+1-\frac{d}{2}}. \end{aligned}$$

Thus, using (4.2.3) it follows that

$$\|\mathbf{A}_h\|_\infty \le \|\mathbf{A}\|_\infty + C\, h^{m+1-\frac{d}{2}} \le C,$$

provided that $m+1 > d/2$ and h is sufficiently small. □

Note that in both two and three space dimensions it suffices to have $\mathbf{A} \in \mathbf{H}^2(\Omega)$.

Chapter 5

Existence and Uniqueness for the Auxiliary Problems

Proving optimal estimates for the fully discrete approximation of the order parameter is a much more complicated task than proving estimates for the magnetic potential since it does not follow standard finite element theory. There are two main difficulties. First, the nonlinear function $f_h(\cdot)$ appearing in the fully-discrete problems (3.3.5) and (3.3.6) is only locally Lipschitz. To circumvent this difficulty we follow the approach of [5] and consider an auxiliary problem whose solutions satisfy the same equation as Ψ^n except that the locally Lipschitz function $f_h(\cdot)$ on the right hand side is replaced by a globally Lipschitz function $f_h^\delta(\cdot)$. The function $f_h^\delta(\cdot)$ is defined in such a way that it agrees with $f_h(\cdot)$ on a set M^δ, see also [77]. The second difficulty is in handling the trilinear form $b(\cdot,\cdot,\cdot)$. From its definition (2.2.14) we note that $b(\cdot,\cdot,\cdot)$ has essentially the same structure as the nonlinear term in the Navier-Stokes equations, see e.g., [23], [45], [51], [76]. However, in our model the trilinear form $b(\cdot,\cdot,\cdot)$ depends not only on the weak solution for the order parameter but also on the weak and the discrete solutions for the magnetic potential. The uniform estimates for $\mathbf{A}$ and $\mathbf{A}_h$ derived in Chapter 4 will allow for optimal estimates of all terms involving the trilinear form $b(\cdot,\cdot,\cdot)$.

This chapter consists of four sections. The first section starts with a short discussion of the need to introduce the auxiliary fully discrete problems. Then we define the auxiliary problems corresponding to both the Backward-Euler-Galerkin and Crank-Nicolson-Galerkin problems. As before, we use Ψ_δ^n to denote the solution to both auxiliary problems.

In the second section we collect several preliminary results used in the proof of the existence and uniqueness for Ψ_δ^n. We start with a derivation of estimates for the terms in the auxiliary problems involving the trilinear form $b(\cdot,\cdot,\cdot)$ and the globally Lipschitz continuous function $f_h^\delta(\cdot)$. Next, we state a Brower-type fixed point result whose proof may be found in [5].

In the third and fourth sections we prove existence and uniqueness results for the fully discrete solutions. Later on, in Chapter 8, we will combine these results to obtain existence and uniqueness results and optimal error estimates for the fully discrete problems.

5.1 The Auxiliary Problems

For the purpose of our analysis one needs to derive "optimal" upper bounds for all terms involving the nonlinear functions $f(\cdot)$ and $f_h(\cdot)$ defined in (2.2.15) and (3.3.3), respectively. As stated before we follow the approach which has been applied in [5] to a problem having the same type of cubic nonlinearity. One may also consult [77] for a short discussion of the idea.

Let us recall that $\mathbf{A}_h$ denotes the solution of the discrete problem (3.3.1) for the magnetic potential. Let us also recall that for any $v \in V$ we define $f_h(v) = (2 - i\Phi - |v|^2 - |\mathbf{A}_h|^2)\, v$, where Φ is the leading order scalar electric potential defined in (2.1.22). Note that due to the cubic nonlinearity, in general, the function $f_h(\cdot)$ fails to be globally Lipschitz continuous. In order to obtain optimal estimates for all terms involving the nonlinear function $f_h(\cdot)$ we either need to have $f_h(\cdot)$ globally Lipschitz, or we have to resort to a different technique than the standard one presented in [77]. This leads to one of the main ideas implemented in this work. It involves the introduction of a globally Lipschitz continuous function $f_h^\delta(\cdot)$ which coincides with the locally Lipschitz function $f_h(\cdot)$ on a set M^δ. This set is defined as an appropriate δ-neighborhood of the weak solution ψ. Using $f_h^\delta(\cdot)$ we introduce a new function Ψ_δ^n which solves an auxiliary problem obtained by replacing $f_h(\cdot)$ in the fully-discrete problem by the globally Lipschitz function $f_h^\delta(\cdot)$.

Specifically, we proceed with the following definition of the set M^δ.

Definition 5.1 *Let us fix $\delta > 0$ and define*

$$M^\delta = \{z \in \mathbf{C} : \exists (\mathbf{x}, t) \in \Omega \times [0, T],\ |z - \psi(\mathbf{x}, t)| < \delta\}, \tag{5.1.1}$$

where ψ is the solution of the weak problem (2.2.20).

Then f_h^δ is defined as follows.

Definition 5.2 *Let $f_h^\delta : \mathbf{C} \to \mathbf{C}$ be a globally Lipschitz continuous function such that*

$$f_h^\delta(z) = f_h(z) \quad \forall\, z \in M^\delta. \tag{5.1.2}$$

Let L^δ be the Lipschitz constant for f_h^δ. Using f_h^δ one may define the following auxiliary problem.

Seek $\Psi_\delta^n \in V^h$ such that

$$\begin{aligned}
(\frac{\tilde{d}\Psi_\delta^n}{dt}, v_h) + a(\Psi_\delta^n, v_h) - b(\mathbf{A}_h, \Psi_\delta^n, v_h) &= \left(f_h^\delta(\Psi_\delta^n), v_h\right) \forall\, v_h \in V^h\ ,\ \ 1 \leq n \leq N, \\
\Psi_\delta^0 &= \tilde{\psi}^0.
\end{aligned} \tag{5.1.3}$$

We note that Ψ_δ^n solves a problem identical to the original fully discrete problem (3.3.5) with the only exception that $f_h(\cdot)$ is replaced by $f_h^\delta(\cdot)$.

Using the definition of M^δ given in (5.1.1), let us define the auxiliary problem corresponding to the fully-discrete Crank-Nicolson-Galerkin problem (3.3.6).

Seek $\Psi_\delta^n \in V^h$ such that

$$\begin{aligned}(\frac{\tilde{d}\Psi_\delta^n}{dt}, v_h) + a(\bar{\Psi}_\delta^n, v_h) + b(\mathbf{A}_h, \bar{\Psi}_\delta^n, v_h) &= \left(f_h^\delta(\bar{\Psi}_\delta^n), v_h\right) \forall\, v_h \in V^h\ 1 \le n \le N, \\ \Psi^0 &= \tilde{\psi}^0, \end{aligned} \tag{5.1.4}$$

where we have used the notation

$$\bar{\Psi}_\delta^n = \frac{\Psi_\delta^n + \Psi_\delta^{n-1}}{2}.$$

5.2 Preliminary Results

We can derive the following preliminary estimate used in the existence and uniqueness proofs for the solutions of (5.1.3) and (5.1.4).

Lemma 5.1 *Let $\Omega \subset \mathbb{R}^d$ for $d = 2, 3$. Let $\mathbf{A} \in \mathbf{H}_n^1(\Omega) \cap \mathbf{H}^{m+1}(\Omega)$ be the weak solution of problem (2.2.1), where $m + 1 > d/2$. Let us assume that the dual problem corresponding to (2.2.1) is regular. Let $\mathbf{A}_h \in \mathbf{W}^h$ be the finite element approximation to $\mathbf{A}$ which satisfies (3.2.12). Then for $f_h^\delta(\cdot)$ defined in (5.1.2) we have*

$$|(f_h^\delta(v_h), v_h)| \le C_\delta \left(\|v_h\|_0^2 + \|v_h\|_0\right) \quad \forall\ v_h \in V^h, \tag{5.2.1}$$

where C is a generic constant which depends on δ and is independent of the spatial discretization parameter h.

Proof

Let ψ be the solution of the weak problem (2.2.20). Using the triangle inequality and the global Lipschitz continuity of $f_h^\delta(\cdot)$ we get

$$\begin{aligned}|(f_h^\delta(v_h), v_h)| &= |(f_h^\delta(v_h) - f_h^\delta(\psi) + f_h^\delta(\psi), v_h)| \\ &\le |(f_h^\delta(v_h) - f_h^\delta(\psi), v_h)| + |(f_h^\delta(\psi), v_h)| \\ &\le L^\delta \|v_h - \psi\|_0 \|v_h\|_0 + |(f_h^\delta(\psi), v_h)|. \end{aligned} \tag{5.2.2}$$

Note that definitions (5.1.1) and (5.1.2) imply that if ψ is the weak solution of (2.2.20) then $\psi \in M^\delta$ and hence

$$f_h^\delta(\psi) = f_h(\psi).$$

Thus one may use the definition of $f_h(\psi)$, see (3.3.3), to write

$$\begin{aligned} |(f_h(\psi), v_h)| &= \left|\left((2 - i\Phi - |\mathbf{A}_h|^2 - |\psi|^2)\psi, v_h\right)\right| \\ &\le \left(C + \|\psi\|_\infty^2 + \|\mathbf{A}_h\|_\infty^2\right) \|\psi\|_0 \|v_h\|_0. \end{aligned}$$

Using the fact that $\|\psi\|_\infty \le 1$ which was proved in Lemma 2.4 and the uniform bound for $\mathbf{A}_h$ derived in Lemma 4.5, we have

$$|(f_h^\delta(\psi), v_h)| \le C\|v_h\|_0. \tag{5.2.3}$$

Combining (5.2.2) and (5.2.3) we have

$$\begin{aligned} |(f_h^\delta(v_h), v_h)| &\le L^\delta \|v_h - \psi\|_0 \|v_h\|_0 + C\|v_h\|_0 \\ &\le L^\delta \|v_h\|_0^2 + L^\delta \|\psi\|_0 \|v_h\|_0 + C\|v_h\|_0 \\ &\le C_\delta \left(\|v_h\|_0^2 + \|v_h\|_0\right), \end{aligned}$$

where we have used the fact that $\|\psi\|_0 \le C_1$ and the notation $C_\delta = \max\{L^\delta, L^\delta C_1 + C\}$. This concludes the proof of Lemma 5.1. □

We continue with deriving one more preliminary result which will be used repeatedly in the proofs of the optimal error estimates for the order parameter.

Lemma 5.2 *Let $\Omega \subset \mathbb{R}^d$ for $d = 2, 3$. Let $\mathbf{A} \in \mathbf{H}_n^1(\Omega) \cap \mathbf{H}^{m+1}(\Omega)$ be the weak solution of problem (2.2.1), where $m + 1 > d/2$. Let us assume that the dual problem corresponding to*

(2.2.1) is regular. Let $\mathbf{A}_h \in \mathbf{W}^h$ *be the finite element approximation to* $\mathbf{A}$ *which satisfies (3.2.12). Then for any* $v, w \in \mathcal{H}^1(\Omega)$ *and for arbitrary* $v_h \in V^h$ *the following estimates hold*

$$|b(\mathbf{A}, v, w)| \leq C\|w\|_0\|v\|_1 \tag{5.2.4}$$

and

$$|b(\mathbf{A}_h, v_h, v_h)| \leq Ch^{m-d/2}\|v_h\|_0^2. \tag{5.2.5}$$

Proof

Using the definition of the trilinear form $b(\cdot,\cdot,\cdot)$, the uniform bound for $\mathbf{A}$, and the Cauchy-Schwarz inequality we have the estimate

$$|b(\mathbf{A}, v, w)| = |(\mathbf{A}\cdot\nabla v, w)| \leq \|\mathbf{A}\|_\infty|(\nabla v, w)| \leq \|\mathbf{A}\|_\infty\|\nabla v\|_0\|w\|_0 \leq C\|v\|_1\|w\|_0.$$

To show (5.2.5) we proceed as follows. First, we use the property (2.2.19) and the Cauchy-Schwarz inequality to get

$$\begin{aligned} |b(\mathbf{A}_h, v_h, v_h)| &= |b(\mathbf{A}_h - \mathbf{A}, v_h, v_h)| \\ &\leq \|\mathbf{A}_h - \mathbf{A}\|_0\|v_h\|_1\|v_h\|_\infty. \end{aligned}$$

Then we use the optimal error estimate (4.1.3), the inverse inequality (3.2.10) valid in V^h and the standard inverse inequality $\|v_h\|_1 \leq h^{-1}\|v_h\|_0$ to estimate $b(\mathbf{A}_h, v_h, v_h)$ as follows

$$|b(\mathbf{A}_h, v_h, v_h)| \leq Ch^{m+1}h^{-1}\|v_h\|_0 h^{-d/2}\|v_h\|_0 = Ch^{m-d/2}\|v_h\|_0^2. \quad \Box$$

To prove existence for the solution Ψ_δ^n of the auxiliary problem (5.1.3), we will use the following complex valued version of a well known Brower-type fixed point result, see [5].

Lemma 5.3 *Let* $(H, (\cdot,\cdot))$ *be a finite dimensional inner product space with associated norm* $\|\cdot\|$. *Let* $g : H \longrightarrow H$ *be continuous and assume that there exists* $\alpha > 0$ *such that for every*

$z \in H$ with $\|z\| = \alpha$ there holds $Re(g(z), z) \geq 0$. Then, there exists a $z^* \in H$ such that $g(z^*) = 0$ and $\|z^*\| \leq \alpha$.

5.3 Existence and Uniqueness for the Auxiliary Backward-Euler-Galerkin Problem

The goal of this section is to prove an existence and uniqueness result for the auxiliary Backward-Euler-Galerkin problem (5.1.3). In Chapter 6 we will use the results for Ψ_δ^n to derive the desired global existence and uniqueness of the fully discrete solution Ψ^n.

The idea here is to apply Lemma 5.3 in order to prove the following existence result.

Theorem 5.1 *Let $\Omega \subset \mathbb{R}^d$ for $d = 2, 3$. Let $\mathbf{A} \in \mathbf{H}_n^1(\Omega) \cap \mathbf{H}^{m+1}(\Omega)$ be the weak solution of problem (2.2.1), where $m \geq d/2$. We assume that the dual problem corresponding to (2.2.1) is regular. Let $\mathbf{A}_h \in \mathbf{W}^h$ be the finite element approximation to $\mathbf{A}$ which satisfies (3.2.12). Then for sufficiently small k there exists a solution $\Psi_\delta^n \in V^h$ to the auxiliary problem (5.1.3).*

Proof

Let us recall the auxiliary problem for the Backward-Euler scheme given in (5.1.3),

$$\begin{aligned} (\frac{\tilde{d}\Psi_\delta^n}{dt}, v_h) + a(\Psi_\delta^n, v_h) - b(\mathbf{A}_h, v_h, \Psi_\delta^n) &= \left(f_h^\delta(\Psi_\delta^n), v_h\right) \forall\, v_h \in V^h\ ,\ \ 1 \leq n \leq N, \\ \Psi_\delta^0 &= \tilde{\psi}^0. \end{aligned}$$

For a given $w_h \in V^h$ let us define $\Upsilon : V^h \longrightarrow V^h$ by

$$(\Upsilon(w_h), v_h) = -a(w_h, v_h) + b(\mathbf{A}_h, v_h, w_h) + (f_h^\delta(w_h), v_h) \quad \forall\, v_h \in V^h. \tag{5.3.1}$$

It follows that

$$(\frac{\tilde{d}\Psi_\delta^n}{dt}, v_h) = -a(\Psi_\delta^n, v_h) + b(\mathbf{A}_h, v_h, \Psi_\delta^n) + \left(f_h^\delta(\Psi_\delta^n), v_h\right) \forall\, v_h \in V^h\ ,\ \ 1 \leq n \leq N.$$

Since $\Psi_\delta^n \in V^h$ one has

$$(\frac{\tilde{d}\Psi_\delta^n}{dt}, v_h) = (\Upsilon(\Psi_\delta^n), v_h) \forall\, v_h \in V^h \ , \ \ 1 \le n \le N.$$

Using the fact that the above equation holds for all $v_h \in V^h$ and the definition of $\tilde{d}/dt$ one can rewrite the auxiliary problem (5.1.3) in the following form

$$\Psi_\delta^n = \Psi_\delta^{n-1} + k\Upsilon(\Psi_\delta^n),\ 1 \le n \le N. \tag{5.3.2}$$

Given $\Psi_\delta^{n-1} \in V^h$, let us define $\Pi : V^h \longrightarrow V^h$ for $v_h \in V^h$ by

$$\Pi(v_h) = v_h - \Psi_\delta^{n-1} - k\Upsilon(v_h). \tag{5.3.3}$$

Our goal is to show that $\Pi(\cdot)$ is continuous and satisfies $Re(\Pi(v_h), v_h) \ge 0$ for $v_h \in V^h$ with $||v_h||_0 = \alpha > 0$. The desired result will then follow from Lemma 5.3.

Clearly, $\Pi(\cdot)$ is continuous, since $a(\cdot,\cdot)$, $b(\cdot,\cdot,\cdot)$, and $f_h^\delta(\cdot)$ are continuous on $V^h \times V^h$, $W^h \times V^h \times V^h$ and V^h, respectively. On the other hand, from the definition of Υ, the coercivity of $a(\cdot,\cdot)$, proved in Lemma 2.1, and the bounds for $|b(\mathbf{A}_h, v_h, v_h)|$ and $|(f_h^\delta(v_h), v_h)|$ given in (5.2.5) and (5.2.1), respectively, we get that for any $v_h \in V^h$ the following holds

$$\begin{aligned} -kRe(\Upsilon(v_h), v_h) &= -kRe\left(-a(v_h, v_h) + b(\mathbf{A}_h, v_h, v_h) + (f_h^\delta(v_h), v_h)\right) \\ &\ge -k|b(\mathbf{A}_h, v_h, v_h)| - k|(f_h^\delta(v_h), v_h)| \\ &\ge -kCh^{m-d/2}||v_h||_0^2 - kC_\delta\left(||v_h||_0^2 + ||v_h||_0\right) \\ &\ge -k\left(Ch^{m-d/2} + C_\delta\right)||v_h||_0^2 - kC_\delta||v_h||_0. \end{aligned}$$

Thus using the definition of the operator Π given in (5.3.3) we arrive at

$$\begin{aligned} Re(\Pi(v_h), v_h) &= ||v_h||_0^2 - Re(\Psi_\delta^{n-1}, v_h) - kRe(\Upsilon(v_h), v_h) \\ &\ge ||v_h||_0^2 - ||\Psi_\delta^{n-1}||_0\, ||v_h||_0 - k\left(Ch^{m-d/2} + C_\delta\right)||v_h||_0^2 - kC_\delta||v_h||_0 \\ &= \left(\left[1 - k\left(Ch^{m-d/2} + C_\delta\right)\right]||v_h||_0 - \left(||\Psi_\delta^{n-1}||_0 + kC_\delta\right)\right)||v_h||_0. \end{aligned}$$

Then for sufficiently small k and for every $v_h \in V^h$ such that

$$\|v_h\|_0 = \frac{\|\Psi_\delta^{n-1}\|_0 + kC_\delta}{1 - k\left(Ch^{m-d/2} + C_\delta\right)} + 1,$$

the following holds

$$Re(\Pi(v_h), v_h) > 0.$$

Applying Lemma 5.3, there exists a $v_h^* \in V^h$ such that $\Pi(v_h^*) = 0$. Equivalently, there exists a Ψ_δ^n satisfying the auxiliary problem (5.1.3) . □

We proceed with establishing the uniqueness for the auxiliary problem (5.1.3).

Theorem 5.2 *Let $\Omega \subset \mathbb{R}^d$ for $d = 2, 3$. Let $\mathbf{A} \in \mathbf{H}_n^1(\Omega) \cap \mathbf{H}^{m+1}(\Omega)$ be the weak solution of problem (2.2.1), where $m \geq d/2$. We assume that the dual problem corresponding to (2.2.1) is regular. Let $\mathbf{A}_h \in \mathbf{W}^h$ be the finite element approximation to $\mathbf{A}$ which satisfies (3.2.12). Then for sufficiently small k the solution Ψ_δ^n of the auxiliary problem (5.1.3) is unique.*

Proof

We suppose that there exist $\Psi_{\delta,1}^n, \Psi_{\delta,2}^n \in V^h$ of the auxiliary problem (5.1.3). According to (5.3.2) they satisfy

$$\Psi_{\delta,1}^n = \Psi_\delta^{n-1} + k\Upsilon(\Psi_{\delta,1}^n)$$

and

$$\Psi_{\delta,2}^n = \Psi_\delta^{n-1} + k\Upsilon(\Psi_{\delta,2}^n).$$

Subtracting these representations for $\Psi_{\delta,1}^n$ and $\Psi_{\delta,2}^n$ and using the definition of Υ we have

$$\begin{aligned}
\|\Psi_{\delta,1}^n - \Psi_{\delta,2}^n\|_0^2 &= (\Psi_{\delta,1}^n - \Psi_{\delta,2}^n, \Psi_{\delta,1}^n - \Psi_{\delta,2}^n) = k\left(\Upsilon(\Psi_{\delta,1}^n) - \Upsilon(\Psi_{\delta,2}^n), \Psi_{\delta,1}^n - \Psi_{\delta,2}^n\right) \\
&= k\left(-a(\Psi_{\delta,1}^n - \Psi_{\delta,2}^n, \Psi_{\delta,1}^n - \Psi_{\delta,2}^n) + b(\mathbf{A}_h, \Psi_{\delta,1}^n - \Psi_{\delta,2}^n, \Psi_{\delta,1}^n - \Psi_{\delta,2}^n)\right) \\
&+ k\left(f_h^\delta(\Psi_{\delta,1}^n) - f_h^\delta(\Psi_{\delta,2}^n), \Psi_{\delta,1}^n - \Psi_{\delta,2}^n\right)
\end{aligned}$$

The coercivity of the bilinear form $a(\cdot,\cdot)$, the bound (5.2.5) for the trilinear form $b(\cdot,\cdot,\cdot)$, and the global Lipschitz continuity of f_h^δ imply

$$\begin{aligned}\|\Psi_{\delta,1}^n - \Psi_{\delta,2}^n\|_0^2 &\leq k|b(\mathbf{A}_h, \Psi_{\delta,1}^n - \Psi_{\delta,2}^n, \Psi_{\delta,1}^n - \Psi_{\delta,2}^n)| + kL^\delta\|\Psi_{\delta,1}^n - \Psi_{\delta,2}^n\|_0^2 \\ &\leq kCh^{m-d/2}\|\Psi_{\delta,1}^n - \Psi_{\delta,2}^n\|_0^2 + kL^\delta\|\Psi_{\delta,1}^n - \Psi_{\delta,2}^n\|_0^2 \\ &\leq L^\delta k\|\Psi_{\delta,1}^n - \Psi_{\delta,2}^n\|_0^2,\end{aligned}$$

provided that $k > 0$ is sufficiently small and $m \geq d/2$.

Thus, if $k > 0$ is sufficiently small, e.g., $k < \frac{1}{L^\delta}$ it follows that

$$\|\Psi_{\delta,1}^n - \Psi_{\delta,2}^n\|_0^2 < \|\Psi_{\delta,1}^n - \Psi_{\delta,2}^n\|_0^2,$$

which is a contradiction and hence $\Psi_{\delta,1}^n = \Psi_{\delta,2}^n$. □

5.4 Existence and Uniqueness for the Auxiliary Crank-Nicolson-Galerkin Problem

In this section we prove an existence and uniqueness result for the Crank-Nicolson-Galerkin problem given in (5.1.4). The proof follows closely the corresponding results for the Backward-Euler-Galerkin problem proved in the previous section.

Theorem 5.3 *Let $\Omega \subset \mathbb{R}^d$ for $d = 2, 3$. Let $\mathbf{A} \in \mathbf{H}_n^1(\Omega) \cap \mathbf{H}^{m+1}(\Omega)$ be the weak solution of problem (2.2.1), where $m \geq d/2$. We assume that the dual problem corresponding to (2.2.1) is regular. Let $\mathbf{A}_h \in \mathbf{W}^h$ be the finite element approximation to $\mathbf{A}$ which satisfies (3.2.12). Then for sufficiently small k there exists a solution $\Psi_\delta^n \in V^h$ to the auxiliary problem (5.1.4).*

Proof

Recall the auxiliary problem, see (5.1.4)

$$\begin{aligned}(\frac{\tilde{d}\Psi_\delta^n}{dt}, v_h) + a(\bar{\Psi}_\delta^n, v_h) + b(\mathbf{A}_h, \bar{\Psi}_\delta^n, v_h) &= \left(f_h^\delta(\bar{\Psi}_\delta^n), v_h\right) \forall\ v_h \in V^h\ 1 \le n \le N, \\ \Psi_\delta^0 &= \tilde{\psi}^0.\end{aligned}$$

We note that the definition of $\bar{\Psi}_\delta^n$ given in (3.3.7) implies

$$\Psi_\delta^n = 2\bar{\Psi}_\delta^n - \Psi_\delta^{n-1}. \tag{5.4.1}$$

Hence we can rewrite the auxiliary problem (5.1.4) in the following equivalent form

$$\begin{aligned}&(\bar{\Psi}_\delta^n, v_h) = (\Psi_\delta^{n-1}, v_h) \\ +\ &\frac{k}{2}\left[-a(\bar{\Psi}_\delta^n, v_h) - b(\mathbf{A}_h, \bar{\Psi}_\delta^n, v_h) + \left(f_h^\delta(\bar{\Psi}_\delta^n), v_h\right)\right] \forall v_h \in V^h\ 1 \le n \le N \\ &\Psi_\delta^0 = \tilde{\psi}^0.\end{aligned}$$

In preparation for applying Lemma 5.3, for a given $w_h \in V^h$ we define $\Upsilon : V^h \longrightarrow V^h$ by

$$(\Upsilon(w_h), v_h) = \frac{1}{2}\left[-a(w_h, v_h) - b(\mathbf{A}_h, v_h, w_h) + \left(f_h^\delta(w_h, v_h)\right)\right] \quad \forall\ v_h,\ w_h \in V^h. \tag{5.4.2}$$

As before, since $\bar{\Psi}_\delta^n \in V^h$ one can rewrite the auxiliary problem (5.1.4) in the following form

$$\bar{\Psi}_\delta^n = \Psi_\delta^{n-1} + k\Upsilon(\bar{\Psi}_\delta^n) \quad 1 \le n \le N. \tag{5.4.3}$$

Given $\Psi_\delta^{n-1} \in V^h$, let us define $\Pi : V^h \longrightarrow V^h$ for $v_h \in V^h$ by

$$\Pi(v_h) = v_h - \Psi_\delta^{n-1} - k\Upsilon(v_h). \tag{5.4.4}$$

As in the proof for Backward-Euler scheme our goal is to show that $\Pi(\cdot)$ is continuous and satisfies $Re(\Pi(v_h), v_h) \ge 0$ for $v_h \in V^h$. Then, the desired result will follow from Lemma 5.3.

Clearly, $\Pi(\cdot)$ is continuous. Also

$$\begin{aligned} Re\,(\Pi(v_h), v_h) &= Re\left(v_h - \Psi_\delta^{n-1} - k\Upsilon(v_h), v_h\right) \\ &\geq \|v_h\|_0^2 - \|\Psi_\delta^{n-1}\|_0 \|v_h\|_0 - -kRe\,(\Upsilon(v_h), v_h)\,. \end{aligned}$$

On the other hand, exactly as in the proof of Theorem 5.1, one may use (5.4.2), the coercivity of the bilinear form $a(\cdot,\cdot)$, (5.2.5) and (5.2.1) to show that for any $v_h \in V^h$ we have

$$\begin{aligned} -kRe(\Upsilon(v_h), v_h) &= -\frac{k}{2}Re\left(-a(v_h, v_h) + b(\mathbf{A}_h, v_h, v_h) + (f_h^\delta(v_h), v_h)\right) \\ &\geq -\frac{k}{2}\left(Ch^{m-d/2} + C_\delta\right)\|v_h\|_0^2 - \frac{k}{2}C_\delta\|v_h\|_0. \end{aligned}$$

Thus using (5.4.4) and proceeding analogously to the proof of Lemma 5.1 one has that for sufficiently small $k > 0$ and for every $v_h \in V^h$ satisfying

$$\|v_h\|_0 = \frac{\|\Psi_\delta^{n-1}\|_0 + \frac{k}{2}C_\delta}{1 - \frac{k}{2}\left(Ch^{m-d/2} + C_\delta\right)} + 1,$$

the condition $Re(\Pi(v_h), v_h) > 0$ holds. Hence Lemma 5.3 implies that there exists a $v_h^* \in V^h$ such that $\Pi(v_h^*) = 0$. Equivalently, given Ψ_δ^{n-1} there exists a $\bar{\Psi}_\delta^n$ satisfying (5.4.3). Finally, (5.4.1) implies that there exists a $\Psi_\delta^n = 2\bar{\Psi}_\delta^n - \Psi_\delta^{n-1}$ satisfying the auxiliary problem (5.1.4). $\square$

The uniqueness result for the auxiliary problem (5.1.4) may be proved in a manner analogous to the proof of the uniqueness for the auxiliary problem (5.1.3). We present this proof for the sake of completeness.

Theorem 5.4 *Let $\Omega \subset \mathbb{R}^d$ for $d = 2, 3$. Let $\mathbf{A} \in \mathbf{H}_n^1(\Omega) \cap \mathbf{H}^{m+1}(\Omega)$ be the weak solution of problem (2.2.1), where $m \geq d/2$. We assume that the dual problem corresponding to (2.2.1) is regular. Let $\mathbf{A}_h \in \mathbf{W}^h$ be the finite element approximation to $\mathbf{A}$ which satisfies (3.2.12). Then for sufficiently small k the solution Ψ_δ^n of the auxiliary problem (5.1.4) is unique.*

Proof

We suppose that for a given $\Psi_\delta^{n-1} \in V^h$ there exist two different solutions $\Psi_{\delta,1}^n, \Psi_{\delta,2}^n \in V^h$ of the auxiliary problem (5.1.4). Then (5.4.1) implies that there exist $\bar{\Psi}_{\delta,1}^n, \bar{\Psi}_{\delta,2}^n$ with

$$\bar{\Psi}_{\delta,1}^n = \Psi_\delta^{n-1} + k\Upsilon(\bar{\Psi}_{\delta,1}^n)$$

and

$$\bar{\Psi}_{\delta,2}^n = \Psi_\delta^{n-1} + k\Upsilon(\bar{\Psi}_{\delta,2}^n).$$

Similar to the proof of Lemma 5.2 one may use the coercivity of the bilinear form $a(\cdot,\cdot)$, the global Lipschitz continuity of f_h^δ and (5.2.5) to get

$$\begin{aligned}
\|\bar{\Psi}_{\delta,1}^n - \bar{\Psi}_{\delta,2}^n\|_0^2 &= (\bar{\Psi}_{\delta,1}^n - \Psi_{\delta,2}^n, \bar{\Psi}_{\delta,1}^n - \bar{\Psi}_{\delta,2}^n) = k\left(\Upsilon(\bar{\Psi}_{\delta,1}^n) - \Upsilon(\bar{\Psi}_{\delta,2}^n), \bar{\Psi}_{\delta,1}^n - \bar{\Psi}_{\delta,2}^n\right) \\
&= \frac{k}{2}\left[-a(\bar{\Psi}_{\delta,1}^n - \Psi_{\delta,2}^n, \bar{\Psi}_{\delta,1}^n - \bar{\Psi}_{\delta,2}^n) + b(\mathbf{A}_h, \bar{\Psi}_{\delta,1}^n - \bar{\Psi}_{\delta,2}^n, \bar{\Psi}_{\delta,1}^n - \bar{\Psi}_{\delta,2}^n)\right] \\
&\leq \frac{k}{2}Ch^{m-d/2}\|\bar{\Psi}_{\delta,1}^n - \Psi_{\delta,2}^n\|_0^2 + \frac{k}{2}L^\delta\|\bar{\Psi}_{\delta,1}^n - \bar{\Psi}_{\delta,2}^n\|_0^2 \\
&\leq k\frac{L^\delta}{2}\|\bar{\Psi}_{\delta,1}^n - \Psi_{\delta,2}^n\|_0^2,
\end{aligned}$$

provided that $k > 0$ is sufficiently small and $m \geq d/2$. Thus if $k > 0$ is sufficiently small, for example, $k < \frac{2}{L^\delta}$ then

$$\|\bar{\Psi}_{\delta,1}^n - \bar{\Psi}_{\delta,2}^n\|_0^2 \leq \|\bar{\Psi}_{\delta,1}^n - \bar{\Psi}_{\delta,2}^n\|_0^2.$$

This contradicts our assumption and implies that $\bar{\Psi}_{\delta,1}^n = \bar{\Psi}_{\delta,2}^n$. Finally, (5.4.1) gives $\Psi_{\delta,1}^n = \Psi_{\delta,2}^n$ and concludes the proof. $\square$

Chapter 6

Error Estimates for the Auxiliary Backward-Euler-Galerkin Problem

In this chapter we derive optimal error estimates for the $\mathcal{L}^2$ and $\mathcal{H}^1$ norms of the error in the Backward-Euler-Galerkin problem (5.1.3).

We start with a short discussion of the main ideas used in the proofs of the optimal error estimates. We use a well-known technique for deriving error estimates for evolution problems. An excellent source describing this technique is the monograph [77]. One may also consult one of the many available references, e.g., [5], [29], [30], [39], [51], [76], and [80].

Specifically, let ψ denote the solution of the weak problem (2.2.20) and let Ψ_δ^n be the solution of the auxiliary Backward-Euler-Galerkin problem (5.1.3) and the auxiliary Crank-Nicolson-Galerkin problem (5.1.4) then we split the error e_δ^n as $e_\delta^n = \Psi_\delta^n - \psi(t_n) = \theta_\delta^n + \rho^n$, where $\theta_\delta^n = \Psi_\delta^n - P\psi(t_n) \in V^h$ and $\rho^n = P\psi(t_n) - \psi(t_n)$. Here $P\psi(t_n) \in V^h$ represents the standard projection of the weak solution ψ onto the finite element space V^h. Using standard finite element theory one can derive optimal estimates for ρ^n. The main part of this chapter is devoted to the derivation of optimal estimates for the discrete function θ_δ^n. Our approach will be to derive an appropriate equation which is satisfied by θ_δ^n and then use this equation in order to estimate θ_δ^n.

6.1 Preliminary Estimates

Let us recall the weak problem for the order parameter (2.2.20) and the corresponding auxiliary Backward-Euler-Galerkin problem (5.1.3).

Seek $\psi \in V$ such that

$$\begin{aligned}(\psi_t, v) + a(\psi, v) - b(\mathbf{A}, v, \psi) &= (f(\psi), v) \quad \forall v \in V, t \geq 0\\ \psi(0) &= \psi^0.\end{aligned}$$

Seek $\Psi_\delta^n \in V^h$ such that

$$(\frac{\tilde{d}\Psi_\delta^n}{dt}, v_h) + a(\Psi_\delta^n, v_h) - b(\mathbf{A}_h, v_h, \Psi_\delta^n) = \left(f_h^\delta(\Psi_\delta^n), v_h\right) \quad \forall\, v_h \in V^h\,,\quad 1 \leq n \leq N,$$
$$\Psi_\delta^0 = \tilde{\psi}^0,$$

where $\tilde{d}/dt$ is defined in (3.3.4).

Let us define the **error** at the n-th time level in this auxiliary problem by

$$e_\delta^n = \Psi_\delta^n - \psi(t_n). \tag{6.1.1}$$

The **projection** $P\psi(t_n)$ of $\psi(t_n)$ onto V^h is defined in the usual manner by

$$a(\rho^n, v_h) = 0 \quad \forall\, v_h \in V^h, \tag{6.1.2}$$

where

$$\rho^n = P\psi(t_n) - \psi(t_n) \tag{6.1.3}$$

and the bilinear form $a(\cdot,\cdot)$ is defined in (2.2.13).

Let us consider the following splitting of the error e_δ^n

$$e_\delta^n = \theta_\delta^n + \rho^n, \tag{6.1.4}$$

where

$$\theta_\delta^n \;=\; \Psi_\delta^n - P\psi(t_n) \tag{6.1.5}$$

and ρ^n is defined in (6.1.3).

We begin our preliminary estimates with the following three standard results, see e.g. [77].

Lemma 6.1 *Let the weak solution of (2.2.20) satisfy $\psi \in \mathcal{V}$ with $\psi(\cdot, \mathrm{x}) \in \mathcal{H}^{m+1}(\Omega)$. Let ρ^n be defined in (6.1.3) for $n \geq 0$. Then the following optimal estimate holds*

$$\|\rho^n\|_0 + h\|\rho^n\|_1 \leq Ch^{m+1}, \tag{6.1.6}$$

where C is a generic constant independent of the spatial discretization parameter h.

Proof

Let us fix $n \geq 0$. The definition of ρ^n given in equation (6.1.3) and (6.1.2) imply that the projection $P\psi(t_n)$ satisfies the equation

$$a(P\psi(t_n), v_h) = a(\psi(t_n), v_h) \quad \forall\, v_h \in V^h. \tag{6.1.7}$$

We recall that $a(\cdot,\cdot)$ is a continuous and coercive bilinear form on $\mathcal{H}^1(\Omega) \times \mathcal{H}^1(\Omega)$, see Lemma 2.1. Thus it follows that $a(\psi(t_n), v_h)$ defines a bounded linear functional on $\mathcal{H}^1(\Omega)$. Since all hypotheses in the Lax-Milgram Lemma 1.2 are satisfied, we can apply it to find that for a given $n \geq 0$ there exists a unique solution $P\psi(t_n) \in V^h$ to the problem (6.1.7). Further, application of Cea's Lemma 1.3 with $v_h = P\psi(t_n) \in V^h$ yields the optimal error estimate

$$\|\rho^n\|_1 \leq Ch^m, \tag{6.1.8}$$

provided that the weak solution satisfies $\psi \in \mathcal{H}^{m+1}(\Omega)$.

Using the continuity of the imbedding (4.1.5) and applying the Aubin-Nitsche Lemma 1.4, we arrive at the desired optimal $\mathcal{L}^2$ estimate

$$||\rho^n||_0 \le Ch^{m+1}, \tag{6.1.9}$$

provided that $\psi \in \mathcal{H}^{m+1}(\Omega)$. Combining (6.1.8) and (6.1.9), the proof is completed. $\square$

Let us define ρ_t^n as follows

$$\rho_t^n = P\psi_t(t_n) - \psi_t(t_n). \tag{6.1.10}$$

Then the proof of the following optimal estimate for ρ_t^n can be derived in complete analogy with proof of Lemma 6.1.

Lemma 6.2 *Under the hypotheses of Lemma 6.1 we have*

$$||\rho_t^n||_0 + h||\rho_t^n||_1 \le Ch^{m+1}. \qquad \square \tag{6.1.11}$$

One may use Lemma 6.1 to estimate the following optimal estimate for $||\theta^0||_0$.

Lemma 6.3 *Let $\psi(0) \in \mathcal{H}^{m+1}(\Omega)$. Denote $e^0 = \tilde{\psi}^0 - \psi^0$. If the initial conditions in (2.2.20) and (5.1.3) satisfy*

$$||e^0||_0 \le Ch^{m+1}, \tag{6.1.12}$$

then we obtain the following optimal estimate

$$||\theta^0||_0 \le Ch^{m+1}. \tag{6.1.13}$$

Proof

Using the splitting of the error given by (6.1.4) and the triangle inequality one has

$$||\theta^0||_0 = ||e^0 - \rho^0||_0 \le ||e^0||_0 + ||\rho^0||_0.$$

Our assumption on the initial condition (6.1.12) together with Lemma 6.1 implies

$$||\theta_\delta^0||_0 \leq C_\delta\, h^{m+1}. \quad \square$$

Following [77], one can derive the following two standard results which we will use in the proof of the optimal estimate for θ_δ^n.

Lemma 6.4 *If the weak solution of (2.2.20) satisfy $\psi \in \mathcal{V}$ with $\psi(\cdot, \mathbf{x}) \in \mathcal{H}^{m+1}(\Omega)$, then for $\frac{\tilde{d}}{dt}$ defined in (3.3.4) we have the following optimal estimate*

$$||\frac{\tilde{d}}{dt}\rho^n||_0 \leq Ch^{m+1}\ , \quad n = 1, 2, ..., N. \tag{6.1.14}$$

Proof

Let us recall that $t_n = nk$, where $k > 0$ is the constant time step. Then one may use (3.3.4) and Lemma 6.2 to estimate $\frac{\tilde{d}}{dt}\rho^n$ as follows

$$\begin{aligned} ||\frac{\tilde{d}}{dt}\rho^n||_0 &= \left\|\frac{1}{k}\int_{t_{n-1}}^{t_n} \rho_t(s)ds\right\|_0 \\ &\leq \frac{1}{k}\int_{(n-1)k}^{nk} ||\rho_t(s)||_0 ds \\ &\leq \frac{1}{k}Ch^{m+1}k = Ch^{m+1}, \end{aligned}$$

provided that $\psi \in \mathcal{H}^{m+1}(\Omega)$. $\square$

It is easy to derive an $\mathcal{L}^2$ estimate for the difference of the time derivative ψ_t of the weak solution and its approximation $\frac{\tilde{d}}{dt}\psi$; see, e.g., [77].

Lemma 6.5 *We assume that the solution ψ to the weak problem (2.2.20) satisfies $||\psi_{tt}||_0 \leq C$. Then the following estimate holds*

$$\left\|\frac{\tilde{d}}{dt}\psi(t_n) - \psi_t(t_n)\right\|_0 \leq Ck, \quad \textit{for} \quad n = 1, 2 ..., N\ , \tag{6.1.15}$$

Proof

Since by definition (3.3.4) $\tilde{d}/dt$ represents the backward difference operator one can write

$$\begin{aligned} \left\| \frac{\tilde{d}}{dt}\psi(t_n) - \psi_t(t_n) \right\|_0 &= \left\| \frac{\psi(t_n) - \psi(t_{n-1})}{k} - \psi_t(t_n) \right\|_0 \\ &= \left\| \frac{1}{k} \int_{t_{n-1}}^{t_n} (s - t_{n-1}) \psi_{tt}(s) ds \right\|_0 \\ &\leq Ck, \quad \text{for} \quad n = 1, 2 ..., N \ , \end{aligned}$$

provided that $||\psi_{tt}||_0 \leq C$. $\Box$

Let us recall from Lemma 2.4 that $||\psi(\mathbf{x}, t)||_\infty \leq 1$ in $\Omega \times (0, T)$. We now show that for the projection $P\psi$ one has $||P\psi(t_n)||_\infty \leq 1 + C$. This result will be used later on in the derivation of the optimal fully discrete $\mathcal{L}^2$ error estimate.

Lemma 6.6 *For $\Omega \subset \mathbb{R}^d$ for $d = 2, 3$ and for a positive integer m satisfying $m + 1 > d/2$ we assume that the weak solution of (2.2.20) satisfies $\psi \in \mathcal{V}$ with $\psi(\cdot, \mathbf{x}) \in \mathcal{H}^{m+1}(\Omega)$. If the finite element space V^h satisfy (3.2.11) then for sufficiently small h we have the estimate*

$$||P\psi(t_n)||_\infty \leq 1 + C \quad in \quad \Omega \quad for \quad 1 \leq n \leq N, \tag{6.1.16}$$

where C is a generic constant independent of h.

Proof

The proof of Lemma 6.6 depends on several of our previous results and assumptions. We proceed by noting that by the definition of the projection $P\psi(t_n)$ and the triangle inequality we have

$$||P\psi(t_n)||_\infty \leq ||\psi(t_n)||_\infty + ||\rho^n||_\infty. \tag{6.1.17}$$

Since we already know that $||\psi(t_n)||_\infty \leq 1$ it is left to show that $||\rho^n||_\infty \leq C$.

Using the definition of ρ^n, see (6.1.3), and the triangle inequality we have that for any $v_h \in V^h$ the following holds

$$\begin{aligned} \|\rho^n\|_\infty &= \|P\psi(t_n) - \psi(t_n)\|_\infty \\ &\leq \|P\psi(t_n) - v_h\|_\infty + \|\psi(t_n) - v_h\|_\infty. \end{aligned}$$

Using the inverse inequality (3.2.10) and the triangle inequality one has

$$\begin{aligned} \|\rho^n\|_\infty &\leq Ch^{-\frac{d}{2}}\|P\psi(t_n) - v_h\|_0 + \|\psi(t_n) - v_h\|_\infty \\ &\leq Ch^{-\frac{d}{2}}\left(\|\rho^n\|_0 + \|\psi(t_n) - v_h\|_0\right) + \|\psi(t_n) - v_h\|_\infty, \end{aligned} \tag{6.1.18}$$

where we have added and subtracted $\psi(t_n)$ to get the last result. Substituting the estimate for $\|\rho^n\|_0$ given in Lemma 6.1 into (6.1.18) we get that

$$\|\rho^n\|_\infty \leq Ch^{-\frac{d}{2}}h^{m+1} + \left(Ch^{-\frac{d}{2}}\|\psi(t_n) - v_h\|_0 + \|\psi(t_n) - v_h\|_\infty\right).$$

For a fixed $\delta > 0$ appearing in the definition of M^δ one may use our assumptions on the approximation properties of the finite element space V^h, see (3.2.11), in order to get the estimate

$$\|\rho^n\|_\infty \leq \frac{\delta}{4}, \tag{6.1.19}$$

provided that h is sufficiently small and $m + 1 > d/2$.

Thus (6.1.17) and (6.1.19) imply that

$$\|P\psi(t_n)\|_\infty \leq \|\psi(t_n)\|_\infty + \|\rho^n\|_\infty \leq 1 + C,$$

for sufficiently small h and for $m + 1 > d/2$. $\square$

Recall that we want to derive optimal error estimates for the error e_δ^n in the auxiliary problem (5.1.3). Since we have already derived optimal estimates for ρ^n it remains only to derive optimal estimates for the $\theta_\delta^n \in V^h$.

We define

$$\omega^n = \omega_1^n + \omega_2^n, \tag{6.1.20}$$

where we have used the notation

$$\omega_1^n = \frac{\tilde{d}}{dt}\rho^n \tag{6.1.21}$$

and

$$\omega_2^n = \frac{\tilde{d}}{dt}\psi(t_n) - \psi_t(t_n). \tag{6.1.22}$$

An initial step in proving estimates for θ_δ^n is to derive an appropriate equation which is satisfied by θ_δ^n. Such an equation is derived in the following lemma.

Lemma 6.7 *Let ψ and Ψ_δ^n be the solutions of the weak (2.2.20) and auxiliary (5.1.3) problems. Then $\theta_\delta^n = \Psi_\delta^n - P\psi(t_n)$ satisfies the following equation:*

$$\begin{aligned}
&(\frac{\tilde{d}}{dt}\theta_\delta^n, \theta_\delta^n) + a(\theta_\delta^n, \theta_\delta^n) \\
&\quad = \left(f_h^\delta(\Psi_\delta^n) - f(\psi(t_n)), \theta_\delta^n) - (\omega^n, \theta_\delta^n\right) \\
&\quad + b(\mathbf{A}_h, \theta_\delta^n, \theta_\delta^n) - b(\mathbf{A} - \mathbf{A}_h, \theta_\delta^n, P\psi(t_n)) + b(\mathbf{A}, \theta_\delta^n, \rho^n),
\end{aligned} \tag{6.1.23}$$

where ρ^n is defined in (6.1.3) and ω^n is given in (6.1.20).

Proof

Recalling that $V^h \subset V$ one may subtract the weak equation (2.2.20) from the auxiliary equation (5.1.3) to get

$$\begin{aligned}
\left(\frac{\tilde{d}}{dt}\Psi_\delta^n - \psi_t(t_n), v_h\right) &+ a(e_\delta^n, v_h) - b(\mathbf{A}_h, v_h, \Psi_\delta^n) + b(\mathbf{A}, v_h, \psi(t_n)) \\
&= \left(f_h^\delta(\Psi_\delta^n\right) - f(\psi(t_n)), v_h) \ \forall \ v_h \in V^h,
\end{aligned}$$

where $e_\delta^n = \Psi_\delta^n - \psi(t_n)$ is the error in the auxiliary problem (5.1.3) which we ultimately want to estimate. Adding and subtracting $(\frac{\tilde{d}}{dt}P\psi(t_n), v_h)$, $a(P\psi(t_n), v_h)$ and $b(\mathbf{A}_h, v_h, P\psi(t_n))$ we get

$$\begin{aligned}
\left(\frac{\tilde{d}}{dt}\theta_\delta^n, v_h\right) &+ \left(\frac{\tilde{d}}{dt}P\psi(t_n) - \psi_t(t_n), v_h\right) \\
&+ \quad a(\theta_\delta^n, v_h) + a(\rho^n, v_h) - b(\mathbf{A}_h, v_h, \theta_\delta^n) \qquad (6.1.24) \\
&- \quad b(\mathbf{A}_h, v_h, P\psi(t_n)) + b(\mathbf{A}, v_h, \psi(t_n)) \\
&= \quad \left(f_h^\delta(\Psi_\delta^n) - f(\psi(t_n)), v_h\right) \;\; \forall \;\; v_h \in V^h,
\end{aligned}$$

where we have used the definitions of ρ^n and θ^n given in (6.1.3) and (6.1.5), respectively.

Using the definitions of ω^n and ρ^n given in (6.1.20) and (6.1.3) respectively, we can write

$$\begin{aligned}
\frac{\tilde{d}}{dt}P\psi(t_n) - \psi_t(t_n) &= (\frac{\tilde{d}}{dt}\rho^n) + \left(\frac{\tilde{d}}{dt}\psi(t_n) - \psi_t(t_n)\right) \\
&= \omega_1^n + \omega_2^n = \omega^n. \qquad (6.1.25)
\end{aligned}$$

Adding and subtracting $b(\mathbf{A}, v_h, P\psi(t_n))$, using the definition of the projection given in (6.1.2), and (6.1.25) we get

$$\begin{aligned}
&(\frac{\tilde{d}}{dt}\theta_\delta^n, v_h) + a(\theta_\delta^n, v_h) \\
&\quad - \quad b(\mathbf{A}_h, v_h, \theta_\delta^n) + b(\mathbf{A}_h - \mathbf{A}, v_h, P\psi(t_n)) - b(\mathbf{A}, v_h, \rho^n) \qquad (6.1.26) \\
&\quad = \quad \left(f_h^\delta(\Psi_\delta^n) - f(\psi(t_n)), v_h\right) - (\omega^n, v_h) \quad \text{for all} \quad v_h \in V^h.
\end{aligned}$$

We choose $v_h = \theta_\delta^n \in V^h$ to obtain the θ_δ^n-equation given in (6.1.23). $\square$

Before proceeding with the estimate for $\|\theta_\delta^n\|_0$ we briefly explain why we prefer to work with the weak form (2.2.20) in which the derivative in the trilinear form $b(\cdot,\cdot,\cdot)$ is on the test function $v \in V$, instead of using the weak form (2.2.12). The reason is that if we use (2.2.12) we would have to derive an "optimal" estimate for the term $|b(\mathbf{A} - \mathbf{A}_h, P\psi(t_n), \theta_\delta^n)|$.

To estimate this term using Lemma 6.6 one would need to integrate by parts and move the derivative from $P\psi(t_n)$ to θ_δ^n. Unfortunately, such an integration will produce an extra term due to the fact that $\mathbf{A}_h$ is not necessarily divergence free i.e. $(\text{div } \mathbf{A}_h, v_h) \neq 0$ for $v_h \in V^h$. Thus one would need to require that the finite element subspace $\mathbf{W}^h \subset \mathbf{H}_n^1(\Omega)$ has the property

$$\text{for} \quad \mathbf{A}_h \in \mathbf{W}^h \quad (\text{div } \mathbf{A}_h, v_h) = 0 \quad \forall \ v_h \in V^h. \tag{6.1.27}$$

However, we would like to avoid such condition (6.1.27) on $\mathbf{W}^h$ because in practice it is difficult to construct divergence free finite element spaces.

In order to estimate $\|\theta_\delta^n\|_0$, we first note that

$$\begin{aligned} (\frac{\tilde{d}}{dt}\theta_\delta^n, \theta_\delta^n) &= \frac{1}{2}\frac{\tilde{d}}{dt}\|\theta_\delta^n\|_0^2 + \frac{k}{2}\|\frac{\tilde{d}}{dt}\theta_\delta^n\|_0^2 \\ &\geq \frac{1}{2}\frac{\tilde{d}}{dt}\|\theta_\delta^n\|_0^2. \end{aligned} \tag{6.1.28}$$

Hence we begin by estimating the terms on the right-hand-side of (6.1.23). Clearly,

$$\begin{aligned} |(\omega^n, \theta_\delta^n)| &\leq |(\omega_1^n, \theta_\delta^n)| + |(\omega_2^n, \theta_\delta^n)| \\ &\leq \frac{1}{2}\|\omega_1^n\|_0^2 + \frac{1}{2}\|\omega_2^n\|_0^2 + \|\theta_\delta^n\|_0^2 \qquad (6.1.29) \\ &\leq \frac{1}{2}\|\frac{\tilde{d}}{dt}\rho^n\|_0^2 + \frac{1}{2}\|\frac{\tilde{d}}{dt}\psi(t_n) - \psi_t(t_n)\|_0^2 + \|\theta_\delta^n\|_0^2. \qquad (6.1.30) \end{aligned}$$

Applying Lemmas 6.4 and 6.5 we get

$$|(\omega^n, \theta_\delta^n)| \leq Ch^{2m+2} + Ck^2 + \|\theta_\delta^n\|_0^2. \tag{6.1.31}$$

The estimates for the rest of the terms in the right-hand side of equation (6.1.23) are presented as separate lemmas.

We may use (5.2.4), (6.1.16) and (6.1.6) in order to show the following.

Lemma 6.8 *For $\Omega \subset \mathbb{R}^d$ for $d = 2,3$ and for a positive integer m satisfying $m+1 > d/2$ we assume that the weak solution of problem (2.2.1) satisfies $\mathbf{A} \in \mathbf{H}_n^1(\Omega) \cap \mathbf{H}^{m+1}(\Omega)$. We also assume that the dual problem corresponding to (2.2.1) is regular and that $\mathbf{A}_h \in \mathbf{W}^h$ is the finite element approximation to $\mathbf{A}$, where $\mathbf{W}^h$ satisfies (3.2.12). If the weak solution of (2.2.20) satisfy $\psi \in \mathcal{V}$ with $\psi(\cdot, \mathbf{x}) \in \mathcal{H}^{m+1}(\Omega)$, Ψ_δ^n is the solution of the auxiliary problem (5.1.3), and if the finite element space V^h satisfy (3.2.11), then for any $\epsilon > 0$ we obtain the following estimate*

$$\begin{aligned} &|b(\mathbf{A} - \mathbf{A}_h, \theta_\delta^n, P\psi(t_n)| + |b(\mathbf{A}, \theta_\delta^n, \rho^n)| + |b(\mathbf{A}_h, \theta_\delta^n, \theta_\delta^n)| \\ &\quad \leq \; C_{b,\epsilon}^\delta \left(h^{2m+2} + \|\theta_\delta^n\|_0^2 \right) + \epsilon \|\theta_\delta^n\|_1^2, \end{aligned} \tag{6.1.32}$$

where $C_{b,\epsilon}^\delta$ is a generic constant which depends on δ and ϵ and is independent of the spatial and time discretization parameters h and k.

Proof

Let us fix arbitrary $\epsilon_i > 0$, $\quad i = 1,2,3$. Using (5.2.4) and the estimate for $\|\rho^n\|_0$ given in Lemma 6.1 we get

$$\begin{aligned} |b(\mathbf{A}, \theta_\delta^n, \rho^n)| \; &\leq \; C \|\theta_\delta^n\|_1 \|\rho^n\|_0 \\ &\leq \; C_1 h^{m+1} \|\theta_\delta^n\|_1 \leq C_{1,\epsilon_1} h^{2m+2} + \epsilon_1 \|\theta_\delta^n\|_1^2. \end{aligned}$$

On the other hand, Lemma 4.2 and Lemma 6.6 imply

$$\begin{aligned} |b(\mathbf{A} - \mathbf{A}_h, \theta_\delta^n, P\psi(t_n))| \; &\leq \; \|\mathbf{A} - \mathbf{A}_h\|_0 \|P\psi(t_n)\|_\infty \|\theta_\delta^n\|_1 \\ &\leq \; C_{2,\epsilon_2} h^{2m+2} + \epsilon_2 \|\theta_\delta^n\|_1^2. \end{aligned} \tag{6.1.33}$$

Finally, using Lemma 4.5 we arrive at

$$\begin{aligned} |b(\mathbf{A}_h, \theta_\delta^n, \theta_\delta^n)| \; &\leq \; \|\mathbf{A}_h\|_\infty \|\theta_\delta^n\|_1 \|\theta_\delta^n\|_0 \\ &\leq \; C_{3,\epsilon_3} \|\theta_\delta^n\|_0^2 + \epsilon_3 \|\theta_\delta^n\|_1^2. \end{aligned}$$

By letting $\epsilon = \max\{\epsilon_1, \epsilon_2, \epsilon_3\}$ and $C_{b,\epsilon} = \max\{C_{1,\epsilon_1} + C_{2,\epsilon_2}, C_{3,\epsilon_3}\}$ the proof is completed. $\square$

We continue with deriving estimates for the terms in the θ_δ^n-equation (6.1.23) which involve the nonlinear functions $f(\cdot)$ and $f_h^\delta(\cdot)$. In particular, we seek upper estimates involving only terms of the form h^{2m+2} and $||\theta_\delta^n||_0^2$.

We recall that Ψ_δ^n is the solution to the auxiliary problem (5.1.3) and that the existence and uniqueness of Ψ_δ^n has been proved in Theorems 5.1 and 5.2, respectively.

We have the following estimate.

Lemma 6.9 *Under the same hypotheses as in Lemma 6.8 we obtain the following estimate*

$$\left|\left(f_h^\delta(\Psi_\delta^n) - f(\psi(t_n)), v_h\right)\right| \leq C_f^\delta \left(h^{m+1} + ||\theta_\delta^n||_0\right) ||v_h||_0 \quad \forall \ v_h \in V^h. \tag{6.1.34}$$

Proof

Using the triangle inequality, the definition of M^δ, the global Lipschitz continuity of $f_h^\delta(\cdot)$ and the definitions (2.2.15) and (3.3.3) of $f(\cdot)$ and $f_h(\cdot)$ we have

$$\begin{aligned}
&\left|\left(f_h^\delta(\Psi_\delta^n) - f(\psi(t_n)), v_h\right)\right| \\
&\quad \leq \left|\left(f_h^\delta(\Psi_\delta^n) - f_h^\delta(\psi(t_n)), v_h\right)\right| + \left|\left(f_h^\delta(\psi(t_n)) - f(\psi(t_n)), v_h\right)\right| \\
&\quad \leq L^\delta ||e_\delta^n||_0 ||v_h||_0 + |(f_h(\psi(t_n)) - f(\psi(t_n)), v_h)| \\
&\quad \leq L^\delta ||e_\delta^n||_0 |||v_h||_0 + \left|\left((|\mathbf{A}_h|^2 - |\mathbf{A}|^2)\psi(t_n), v_h\right)\right|.
\end{aligned}$$

To conclude the proof one may use the splitting of $||e_\delta^n||_0$ defined in (6.1.4), Lemma 6.1, Lemma 4.3, Lemma 4.5, Lemma 4.2 and Lemma 2.4. We get

$$\begin{aligned}
&\left|\left(f_h^\delta(\Psi_\delta^n) - f(\psi(t_n)), v_h\right)\right| \\
&\quad \leq L^\delta ||\rho^n + \theta_\delta^n||_0 ||v_h||_0 + |((|\mathbf{A}_h| + |\mathbf{A}|)(|\mathbf{A}_h| - |\mathbf{A}|)\psi(t_n), v_h)| \\
&\quad \leq L^\delta ||\rho^n||_0 ||v_h||_0 + L^\delta ||\theta_\delta^n||_0 ||v_h||_0 + (||\mathbf{A}_h||_\infty + ||\mathbf{A}||_\infty) ||\psi(t_n)||_\infty |(|\mathbf{A}_h - \mathbf{A}|, v_h)|
\end{aligned}$$

$$
\begin{aligned}
&\leq L^\delta C h^{m+1}\|v_h\|_0 + L^\delta\|\theta_\delta^n\|_0\|v_h\|_0 + C_1\|\mathbf{A}_h - \mathbf{A}\|_0\|v_h\|_0 \\
&\leq \left(CL^\delta h^{m+1} + L^\delta\|\theta_\delta^n\|_0 + C_2 h^{m+1}\right)\|v_h\|_0 \\
&\leq C_f^\delta\left(h^{m+1} + \|\theta_\delta^n\|_0\right)\|v_h\|_0\,,
\end{aligned}
$$

where we have used the notation $C_f^\delta = \max\left\{L^\delta, C_2 + CL^\delta\right\}$. $\square$

In particular, if we choose $v_h = \theta_\delta^n \in V^h$ then equation (6.1.34) reads

$$
\begin{aligned}
\left|\left(f_h^\delta(\Psi_\delta^n) - f(\psi(t_n)), \theta_\delta^n\right)\right| &\leq C_f^\delta\left(h^{m+1}\|\theta_\delta^n\|_0 + \|\theta_\delta^n\|_0^2\right) \\
&\leq \frac{C_f^\delta}{2}\left(h^{2m+2} + 3\|\theta_\delta^n\|_0^2\right) \qquad (6.1.35) \\
&\leq \tilde{C}_f^\delta\left(h^{2m+2} + \|\theta_\delta^n\|_0^2\right)\,,
\end{aligned}
$$

where $\tilde{C}_f^\delta = \left(\frac{3}{2}\right)C_f^\delta$.

6.2 Optimal $\mathcal{L}^2$ Error Estimates

In this section we use the preliminary results established in the previous section to prove optimal $\mathcal{L}^2$ error estimates for the auxiliary Backward-Euler-Galerkin problem (5.1.3). Let us recall that $\Omega \subset \mathbb{R}^d$ where $d = 2, 3$ and C denotes a positive constant independent of h and k.

Lemma 6.10 *Let $\mathbf{A}$ and $\mathbf{A}_h$ denote the solutions of the weak (2.2.1) and approximate (3.3.1) problems. For $1 \leq n \leq N$ let $\psi(t_n)$ and Ψ_δ^n denote the solutions of the weak (2.2.20) and the auxiliary problems (5.1.3) at the n-th time level. For a positive integer m with $m+1 > d/2$ we assume that $\mathbf{A} \in \mathbf{H}_n^1(\Omega) \cap \mathbf{H}^{m+1}(\Omega)$ and $\psi \in \mathcal{V}$ with $\psi(\cdot, \mathbf{x}) \in \mathcal{H}^{m+1}(\Omega)$ and $\|\psi_{tt}\|_0 \leq C$. If the initial conditions satisfy (6.1.12) then for sufficiently small h and k the following optimal $\mathcal{L}^2$ estimate holds*

$$
\|\theta_\delta^n\|_0 \leq C_\delta(h^{m+1} + k), \qquad (6.2.1)
$$

where C_δ is a generic constant which depends on δ and is independent of the discretization parameters h and k.

Proof

Let us recall the θ_δ^n-equation (6.1.23)

$$(\frac{\tilde{d}}{dt}\theta_\delta^n, \theta_\delta^n) + a(\theta_\delta^n, \theta_\delta^n) = \left(f_h^\delta(\Psi_\delta^n) - f(\psi(t_n)), \theta_\delta^n\right) - (\omega^n, \theta_\delta^n)$$
$$+ \quad b(\mathbf{A}_h, \theta_\delta^n, \theta_\delta^n) - b(\mathbf{A} - \mathbf{A}_h, \theta_\delta^n, P\psi(t_n)) + b(\mathbf{A}, \theta_\delta^n, \rho^n).$$

Using the coercivity of $a(\cdot,\cdot)$ proved in Lemma 2.1, the lower bound (6.1.28), and the triangle inequality we have

$$\begin{aligned}
&\frac{1}{2}\frac{\tilde{d}}{dt}||\theta_\delta^n||_0^2 + C_a||\theta_\delta^n||_1^2 \\
&\leq \quad \left|\left(f_h^\delta(\Psi_\delta^n) - f(\psi(t_n)), \theta_\delta^n\right)\right| + |(\omega^n, \theta_\delta^n)| \\
&+ \quad |b(\mathbf{A}_h, \theta_\delta^n, \theta_\delta^n)| + |b(\mathbf{A} - \mathbf{A}_h, \theta_\delta^n, P\psi(t_n))| + |b(\mathbf{A}, \theta_\delta^n, \rho^n)|\,.
\end{aligned}$$

Further, substituting the estimate given in (6.1.31) we obtain

$$\begin{aligned}
&\frac{1}{2}\frac{\tilde{d}}{dt}||\theta_\delta^n||_0^2 + C_a||\theta_\delta^n||_1^2 \leq C\left(h^{2m+2} + k^2\right) + ||\theta_\delta^n||_0^2 \\
&+ \quad \left|\left(f_h^\delta(\Psi_\delta^n) - f(\psi(t_n)), \theta_\delta^n\right)\right| \\
&+ \quad |b(\mathbf{A}_h, \theta_\delta^n, \theta_\delta^n)| + |b(\mathbf{A} - \mathbf{A}_h, \theta_\delta^n, P\psi(t_n))| + |b(\mathbf{A}, \theta_\delta^n, \rho^n)|\,.
\end{aligned}$$

Applying Lemma 6.8 and using the estimate (6.1.35) we have

$$\begin{aligned}
\frac{1}{2}\frac{\tilde{d}}{dt}||\theta_\delta^n||_0^2 + C_a||\theta_\delta^n||_1^2 \quad &\leq \quad C\left(h^{2m+2} + k^2\right) + ||\theta_\delta^n||_0^2 \\
&+ \quad \tilde{C}_f^\delta h^{2m+2} + \tilde{C}_f^\delta||\theta_\delta^n||_0^2 \\
&+ \quad C_{b,\epsilon}^\delta\left(h^{2m+2} + ||\theta_\delta^n||_0^2\right) + \epsilon||\theta_\delta^n||_1^2.
\end{aligned}$$

Choosing, for example, $\epsilon = \frac{C_a}{2}$ we can guarantee that $C_a - \epsilon > 0$. In this case we get

$$\frac{\tilde{d}}{dt}\|\theta_\delta^n\|_0^2 \leq C_\delta\left(h^{2m+2} + k^2 + \|\theta_\delta^n\|_0^2\right).$$

We denote

$$R_0 = h^{2m+2} + k^2. \tag{6.2.2}$$

Using this notation we arrive at

$$\frac{\tilde{d}}{dt}\|\theta_\delta^n\|_0^2 \leq C_\delta\left(R_0 + \|\theta_\delta^n\|_0^2\right). \tag{6.2.3}$$

Using the definition of $\tilde{d}/dt$ given in (3.3.4) we can rewrite (6.2.3) in the following equivalent form

$$(1 - C_\delta k)\|\theta_\delta^n\|_0^2 \leq \|\theta_\delta^{n-1}\|_0^2 + C_\delta k R_0. \tag{6.2.4}$$

Following [77], we pick k sufficiently small, say $k \leq \tilde{C_\delta}^{-1}$, where $\tilde{C_\delta} > C_\delta$. Then one may expand $1/(1 - C_\delta k)$ in powers of k to get

$$\|\theta_\delta^n\|_0^2 \leq (1 + \tilde{C_\delta} k)\|\theta_\delta^{n-1}\|_0^2 + C_\delta k R_0, \tag{6.2.5}$$

for sufficiently small $k > 0$. After repeated applications of the inequality (6.2.5) we have that for $1 \leq n \leq N$

$$\|\theta_\delta^n\|_0^2 \leq \left(1 + \tilde{C_\delta} k\right)^n \|\theta_\delta^0\|_0^2 + C_\delta k n R_0. \tag{6.2.6}$$

Since $\tilde{C_\delta} > 0$ it follows that $\left(1 + \tilde{C_\delta} k\right)^n \leq e^{\tilde{C_\delta} k n}$ and hence

$$\|\theta_\delta^n\|_0^2 \leq C_\delta\left(\|\theta_\delta^0\|_0^2 + h^{2m+2} + k^2\right), \tag{6.2.7}$$

where $C_\delta = \max\{e^{\tilde{C_\delta} k n}, C_\delta k n\}$. Using the fact that the initial data satisfies (6.1.12) and the estimate (6.1.13) for $\|\theta_\delta^0\|_0$ we obtain

$$\|\theta_\delta^n\|_0 \leq C_\delta(h^{m+1} + k),$$

where we keep the same notation for C_δ after taking the square root. This concludes the proof of Lemma 6.10. $\square$

To complete the derivation of the optimal $\mathcal{L}^2$ error estimate for the auxiliary problem (5.1.3) we combine Lemma 6.10 which gives an estimate for $||\theta_\delta^n||_0$ with the standard estimate for $||\rho^n||_0$ derived in Lemma 6.1.

Theorem 6.1 *Let the hypotheses of Lemma 6.10 hold. Then the following optimal $\mathcal{L}^2$ error estimate holds*

$$||e_\delta^n||_0 \leq C_\delta(h^{m+1} + k), \tag{6.2.8}$$

where C_δ is a generic constant which depends on δ and is independent of the discretization parameters h and k.

Proof

Let us recall the splitting of the error

$$||e_\delta^n||_0 = ||\Psi_\delta^n - \psi(t_n)||_0 \leq ||\theta_\delta^n||_0 + ||\rho^n||_0,$$

where Ψ_δ^n and $\psi(t_n)$ solve (5.1.3) and (2.2.20), respectively. Applying (6.1.6) and (6.2.1) we arrive at the desired optimal error estimate

$$||e_\delta^n||_0 \quad \leq \quad C_\delta(h^{m+1} + k). \quad \square$$

6.3 Optimal $\mathcal{H}^1$ Error Estimates

In this section we derive an optimal $\mathcal{H}^1$ error estimate for the auxiliary Backward-Euler-Galerkin problem (5.1.3).

Let us recall that according to Lemma 6.7 the fully-discrete function θ_δ^n satisfies equation (6.1.26) for any $v_h \in V^h$. In analogy with the proof of the optimal $\mathcal{L}^2$ error estimates for

θ_δ^n the goal is to derive a lower bound for the terms in the left-hand side of (6.1.26) and an upper bound for all terms in the right-hand side of the equation (6.1.26)

$$
\begin{aligned}
&(\frac{\tilde{d}}{dt}\theta_\delta^n, v_h) + a(\theta_\delta^n, v_h) \\
&- \quad b(\mathbf{A}_h, v_h, \theta_\delta^n) + b(\mathbf{A}_h - \mathbf{A}, v_h, P\psi(t_n)) - b(\mathbf{A}, v_h, \rho^n) \\
&= \quad \left(f_h^\delta(\Psi_\delta^n) - f(\psi(t_n)), v_h\right) - (\omega^n, v_h) \quad \text{for all} \quad v_h \in V^h.
\end{aligned}
$$

We begin with several preliminary lemmas in which we derive bounds for all terms in the above equation. We start with an upper bound for the terms in (6.1.26) involving the trilinear form $b(\cdot,\cdot,\cdot)$.

Lemma 6.11 *Under the hypotheses of Lemma 6.8 and the additional assumption that* $k = \mathbf{o}\left(h^{d/2}\right)$ *we have that, the following estimate holds for any* $v_h \in V^h$

$$
|b(\mathbf{A}, v_h, \psi(t_n)) - b(\mathbf{A}_h, v_h, \Psi_\delta^n)| \le C_{b,\bar{\epsilon}}\left(h^{2m} + \|\theta_\delta^n\|_1^2\right) + \bar{\epsilon}\|v_h\|_0^2. \qquad (6.3.1)
$$

Proof

As before we add and subtract $b\left(\mathbf{A}, v_h, P\psi(t_n)\right)$, and $b\left(\mathbf{A}_h, v_h, P\psi(t_n)\right)$ and use the definitions of θ_δ^n and ρ^n to obtain

$$
\begin{aligned}
&|b(\mathbf{A}, v_h, \psi(t_n)) - b(\mathbf{A}_h, v_h, \Psi_\delta^n)| \\
&\quad \le \quad |b(\mathbf{A}_h, v_h, \theta_\delta^n)| + |b(\mathbf{A}_h - \mathbf{A}, v_h, P\psi(t_n))| + |b(\mathbf{A}, v_h, \rho^n)|\,.
\end{aligned}
$$

Let us fix an arbitrary $\epsilon_1 > 0$. Using (4.2.3), (6.1.6), and the inverse inequality

$$
\|v_h\|_1 \le Ch^{-1}\|v_h\|_0 \quad \forall\, v_h \in V^h\,, \qquad (6.3.2)
$$

we have

$$
|b(\mathbf{A}, v_h, \rho^n)| \quad \le \quad \|\mathbf{A}\|_\infty\|\rho^n\|_0\|v_h\|_1 \qquad (6.3.3)
$$

$$\begin{aligned} &\leq C_1 h^{m+1}\|v_h\|_1 \leq C_1 h^m \|v_h\|_0 \\ &\leq \frac{C_1}{\epsilon_1} h^{2m} + \frac{1}{2}\epsilon_1 \|v_h\|_0^2. \end{aligned} \tag{6.3.4}$$

On the other hand for any $\epsilon_2 > 0$ one may use (6.1.16), Lemma 4.2 and (6.3.2) to get

$$\begin{aligned} |b(\mathbf{A}_h - \mathbf{A}, v_h, P\psi(t_n))| &\leq \|P\psi(t_n)\|_\infty \|\mathbf{A} - \mathbf{A}_h\|_0 \|v_h\|_1 \\ &\leq C_2 h^m \|v_h\|_0 \leq \frac{C_2}{\epsilon_2} h^{2m} + \frac{1}{2}\epsilon_2 \|v_h\|_0^2. \end{aligned} \tag{6.3.5}$$

Let us proceed with the estimate for the $|b(\mathbf{A}_h, v_h, \theta_\delta^n)|$ term. Using the triangle inequality and the Cauchy-Schwarz inequality one has

$$\begin{aligned} |b(\mathbf{A}_h, v_h, \theta_\delta^n)| &\leq |b(\mathbf{A} - \mathbf{A}_h, v_h, \theta_\delta^n)| + |b(\mathbf{A}, v_h, \theta_\delta^n)| \\ &\leq \|\mathbf{A} - \mathbf{A}_h\|_\infty \|v_h\|_1 \|\theta_\delta^n\|_0 + |b(\mathbf{A}, \theta_\delta^n, v_h)|. \end{aligned}$$

The estimate (4.2.9) for $\|\mathbf{A} - \mathbf{A}_h\|_\infty$, the inverse inequality (6.3.2), and the optimal estimate (6.2.1) for $\|\theta_\delta^n\|_0$ imply

$$\begin{aligned} |b(\mathbf{A}_h, v_h, \theta_\delta^n)| &\leq C h^{m+1-d/2} h^{-1} \|v_h\|_0 \left(h^{m+1} + k\right) + |b(\mathbf{A}, \theta_\delta^n, v_h)| \\ &= C\left(h^{m-d/2} h^{m+1} + h^{m-d/2} k\right) \|v_h\|_0 + |b(\mathbf{A}, \theta_\delta^n, v_h)|. \end{aligned} \tag{6.3.6}$$

On the other hand, the Cauchy-Schwarz inequality, (4.2.9), (6.3.2), (6.2.1) and (4.2.3) imply that one can estimate the last term in (6.3.6) as follows

$$\begin{aligned} |b(\mathbf{A}, v_h, \theta_\delta^n)| &\leq \|\mathbf{A}_h - \mathbf{A}\|_\infty \|v_h\|_1 \|\theta_\delta^n\|_0 + \|\mathbf{A}\|_\infty \|\theta_\delta^n\|_1 \|v_h\|_0 \\ &\leq C h^{m+1-d/2} h^{-1} \|v_h\|_0 \left(h^{m+1} + k\right) + C \|\theta_\delta^n\|_1 \|v_h\|_0 \\ &= C\left(h^{m-d/2+m+1} + h^{m-d/2} k + \|\theta_\delta^n\|_1\right) \|v_h\|_0. \end{aligned}$$

As a result it follows that

$$|b(\mathbf{A}, v_h, \theta_\delta^n)| \leq C\left(h^{2m-d/2+1} + h^{m-d/2} k + \|\theta_\delta^n\|_1\right) \|v_h\|_0.$$

Let us note that when $m+1 > d/2$ one has $h^{2m+1-d/2} < h^m$. On the other hand, for $k \le h^{d/2}$ one has $h^{m-d/2}k \le h^m$. Thus when $m+1 > d/2$ and $k = \mathbf{o}\left(h^{d/2}\right)$ it follows that

$$
\begin{aligned}
|b(\mathbf{A}, v_h, \theta_\delta^n)| &\le C\,(h^m + \|\theta_\delta^n\|_1)\,\|v_h\|_0 \\
&\le \frac{C_3}{\epsilon_3}\left(h^{2m} + \|\theta_\delta^n\|_1^2\right) + \epsilon_3\|v_h\|_0^2. \qquad (6.3.7)
\end{aligned}
$$

Combining (6.3.4), (6.3.5) and (6.3.7) yields

$$
|b(\mathbf{A}, v_h, \psi(t_n)) - b(\mathbf{A}_h, v_h, \Psi_\delta^n)| \le C_{b,\bar\epsilon}\left(h^{2m} + \|\theta_\delta^n\|_1^2\right) + \bar\epsilon\|v_h\|_0^2,
$$

where we have used the notations $C_{b,\bar\epsilon} = \sum_{i=1}^3 \frac{C_i}{\epsilon_i}$ and $\bar\epsilon = \sum_{i=1}^3 \epsilon_i$. This concludes the proof of Lemma 6.11. □

We proceed with the upper bound for the terms in (6.1.26) involving the nonlinear functions $f(\cdot)$ and $f_h^\delta(\cdot)$.

Lemma 6.12 *Let the hypotheses of Lemma 6.9 hold. Then for any $v_h \in V^h$ one has the following estimate:*

$$
\left|\left(f_h^\delta(\Psi_\delta^n) - f(\psi(t_n)), v_h\right)\right| \le C_{f,\tilde\epsilon}^\delta\left(h^{2m} + k^2\right) + \tilde\epsilon\|v_h\|_0^2. \qquad (6.3.8)
$$

Proof

Let us recall the inequality (6.1.34) derived in Lemma 6.9.

$$
\left|\left(f_h^\delta(\Psi_\delta^n) - f(\psi(t_n)), v_h\right)\right| \le C_f^\delta\left(h^{m+1} + \|\theta_\delta^n\|_0\right)\|v_h\|_0,
$$

which holds for any $v_h \in V^h$. Using the optimal estimate for $\|\theta_\delta^n\|_0$, see (6.2.1), one has

$$
\begin{aligned}
\left|\left(f_h^\delta(\Psi_\delta^n) - f(\psi(t_n)), v_h\right)\right| &\le C_f^\delta\left(h^{m+1} + Ch^{m+1} + Ck\right)\|v_h\|_0 \\
&\le \frac{C_f^\delta}{\tilde\epsilon}\left(h^{2m+2} + k^2\right) + \tilde\epsilon\|v_h\|_0^2 \\
&\le C_{f,\tilde\epsilon}^\delta\left(h^{2m} + k^2\right) + \tilde\epsilon\|v_h\|_0^2. \quad \square
\end{aligned}
$$

We proceed with the last preliminary result used in the proof of the optimal estimate for $\|\theta_\delta^n\|_1$.

Lemma 6.13 *For $\Omega \subset \mathbb{R}^d$ for $d = 2,3$ and for a positive integer m with $m+1 > d/2$ we assume that the weak solution of problem (2.2.1) satisfies $\mathbf{A} \in \mathbf{H}_n^1(\Omega) \cap \mathbf{H}^{m+1}(\Omega)$. In addition we assume that the dual problem corresponding to (2.2.1) is regular and $\mathbf{A}_h \in \mathbf{W}^h$ is the finite element approximation to $\mathbf{A}$ which satisfies (3.2.12). Let Ψ_δ^n be the solution of the auxiliary problem (5.1.3). If the weak solution of (2.2.20) satisfies $\psi \in \mathcal{V}$ with $\psi(\cdot,\mathbf{x}) \in \mathcal{H}^{m+1}(\Omega)$ and $\|\psi_{tt}\|_0 \le C$, and if the finite element space V^h satisfies (3.2.11), then θ_δ^n satisfies the following inequality:*

$$\left(\theta_\delta^n - \theta_\delta^{n-1}, v_h\right) + ka\left(\theta_\delta^n, v_h\right) \le kC_\epsilon^\delta\left(R_0 + \|\theta_\delta^n\|_1^2\right) + k\epsilon\|v_h\|_0^2 \quad \forall\, v_h \in V^h \tag{6.3.9}$$

for sufficiently small h and k such that $k = \mathbf{o}\left(h^{d/2}\right)$ and R_0 is defined by (6.2.2).

Proof

We recall equation (6.1.26).

$$\begin{aligned}
&(\frac{\tilde{d}}{dt}\theta_\delta^n, v_h) + a(\theta_\delta^n, v_h) - b(\mathbf{A}_h, v_h, \theta_\delta^n) + b(\mathbf{A}_h - \mathbf{A}, v_h, P\psi(t_n)) - b(\mathbf{A}, v_h, \rho^n) \\
&\quad = \left(f_h^\delta(\Psi_\delta^n) - f(\psi(t_n)), v_h\right) - (\omega^n, v_h) \;\; \forall\, v_h \in V^h.
\end{aligned}$$

Using the definition of $\tilde{d}/dt$ and multiplying by $k > 0$ we obtain

$$\begin{aligned}
\left(\theta_\delta^n - \theta_\delta^{n-1}, v_h\right) + ka\left(\theta_\delta^n, v_h\right) &\le k\left|b(\mathbf{A}_h, v_h, \theta_\delta^n) - b(\mathbf{A}_h - \mathbf{A}, v_h, P\psi(t_n)) + b(\mathbf{A}, v_h, \rho^n)\right| \\
&+ \;\; k\left|\left(f_h^\delta(\Psi_\delta^n) - f(\psi(t_n)), v_h\right)\right| + k\left|(\omega^n, v_h)\right| \;\; \forall\, v_h \in V^h.
\end{aligned}$$

Applying Lemma 6.11, Lemma 6.12, and the Cauchy-Schwarz inequality one has

$$\begin{aligned}
&\left(\theta_\delta^n - \theta_\delta^{n-1}, v_h\right) + ka\left(\theta_\delta^n, v_h\right) \le kC_{b,\bar{\epsilon}}\left(h^{2m} + \|\theta_\delta^n\|_1^2\right) + k\bar{\epsilon}\|v_h\|_0^2 \\
&+ \;\; kC_{f,\bar{\epsilon}}^\delta\left(h^{2m} + k^2\right) + k\bar{\epsilon}\|v_h\|_0^2 + \frac{k}{\epsilon}\|\omega^n\|_0^2 + k\epsilon\|v_h\|_0^2 \;\; \forall\, v_h \in V^h.
\end{aligned} \tag{6.3.10}$$

Using the definition of ω^n given in (6.1.20) and applying Lemmas 6.4 and 6.5 it follows that

$$\|\omega^n\|_0 \le \|\omega_1^n\|_0 + \|\omega_2^n\|_0 \le C\left(h^{m+1} + k\right). \tag{6.3.11}$$

In terms of the notation for R_0 given in (6.2.2), inequality (6.3.11) implies that

$$\|\omega^n\|_0^2 \le CR_0 \le C\left(h^{2m+2} + k^2\right).$$

Next we combine the like terms in (6.3.10) to arrive at

$$\left(\theta_\delta^n - \theta_\delta^{n-1}, v_h\right) + ka\left(\theta_\delta^n, v_h\right) \le k\bar{C}_\epsilon^\delta R_0 + kC_{b,\bar{\epsilon}}\|\theta_\delta^n\|_1^2 + k\epsilon\|v_h\|_0^2 \;\; \forall\, v_h \in V^h,$$

where $\epsilon = \bar{\epsilon} + \tilde{\epsilon} + \epsilon$ and $\bar{C}_\epsilon^\delta = \max\{C_{b,\bar{\epsilon}}, C_{f,\tilde{\epsilon}}^\delta, \epsilon^{-1}\}$. By denoting $C_\epsilon^\delta = \max\{\bar{C}_\epsilon^\delta, C_{b,\bar{\epsilon}}\}$ one arrives at the desired inequality

$$\left(\theta_\delta^n - \theta_\delta^{n-1}, v_h\right) + ka\left(\theta_\delta^n, v_h\right) \le kC_\epsilon^\delta\left(R_0 + \|\theta_\delta^n\|_1^2\right) + k\epsilon\|v_h\|_0^2. \quad \square$$

We first show that an application of the standard technique for deriving $\mathcal{H}^1$ estimates for θ_δ^n; see, e.g., [77], will result in an unsatisfactory bound for $\|\theta_\delta^n\|_1$. We choose the test function v_h in inequality (6.3.9) as follows: $v_h = \theta_\delta^n - \theta_\delta^{n-1} \in V^h$. Then

$$\left(\theta_\delta^n - \theta_\delta^{n-1}, \theta_\delta^n - \theta_\delta^{n-1}\right) + ka\left(\theta_\delta^n, \theta_\delta^n - \theta_\delta^{n-1}\right) \le kC_\epsilon^\delta\left(R_0 + \|\theta_\delta^n\|_1^2\right) + k\epsilon\|\theta_\delta^n - \theta_\delta^{n-1}\|_0^2.$$

Using the coercivity and continuity of the bilinear form $a(\cdot,\cdot)$ and collecting the like terms it follows that

$$(1 - k\epsilon)\|\theta_\delta^n - \theta_\delta^{n-1}\|_0^2 + kC_l\|\theta_\delta^n\|_1^2 \le kC_u\|\theta_\delta^n\|_1\|\theta_\delta^{n-1}\|_1 + kC_\epsilon^\delta R_0 + kC_\epsilon^\delta\|\theta_\delta^n\|_1^2,$$

where C_l and C_u are the coercivity and continuity constants for the bilinear form $a(\cdot,\cdot)$. Dropping the nonnegative term involving the L^2 norm in the left-hand side and dividing through by $k > 0$ gives the inequality

$$C_l\|\theta_\delta^n\|_1^2 \le \frac{C_u}{\epsilon}\|\theta_\delta^{n-1}\|_1^2 + C_{u,\epsilon}\|\theta_\delta^n\|_1^2 + C_\epsilon^\delta R_0 + C_\epsilon^\delta\|\theta_\delta^n\|_1^2,$$

or equivalently,

$$\left(C_l - C_{u,\epsilon} - C_\epsilon^\delta\right) ||\theta_\delta^n||_1^2 \le \frac{C_u}{\epsilon} ||\theta_\delta^{n-1}||_1^2 + C_\epsilon^\delta R_0. \tag{6.3.12}$$

We note that one doesn't know the sign of $\bar{C}_\epsilon^\delta = \left(C_l - C_{u,\epsilon} - C_\epsilon^\delta\right)$. Even if $\bar{C}_\epsilon^\delta > 0$ the inequality (6.3.12) will not lead to the desired optimal $\mathcal{H}^1$ estimate for θ_δ^n. The reason is that when we apply the inequality (6.3.12) repeatedly, one will arrive at an estimate of the form

$$||\theta_\delta^n||_1^2 \le \left(\frac{C_{u,\epsilon}}{\bar{C}_\epsilon^\delta}\right)^n ||\theta_\delta^0||_1^2 + nC_\epsilon^\delta R_0. \tag{6.3.13}$$

Note that the right-hand side of (6.3.13) approaches infinity as n goes to ∞. Consequently a straightforward application of standard techniques to our particular problem produces unsatisfactory estimates for $||\theta_\delta^n||_1$.

Below we develop an alternative approach for deriving an optimal H_1 estimate for θ_δ^n based on an idea from [51]. The bulk of this idea consists in defining a discrete analog $\Delta_h : V^h \longrightarrow V^h$ of the Laplacian operator Δ and then choosing the test function in the θ_δ^n-inequality as $v_h = -\Delta_h\, \theta_\delta^n$; see [51] and [77]. This approach allows us to get a term of the form $||\nabla\theta_\delta^n||_0^2$ on the left-hand side of the θ_δ^n-inequality without eliminating the time step k from this inequality. Since all terms on the right-hand side of the θ_δ^n-inequality are multiplied by k, for k sufficiently small one may collect the terms involving $||\nabla\theta_\delta^n||_0^2$ on the left-hand side in a term of the form $(1 - Ck)\, ||\nabla\theta_\delta^n||_0^2$. Then one can proceed analogously to the derivation of the optimal estimates for $||\theta_\delta^n||_0$ and obtain an optimal estimate for $||\nabla\theta_\delta^n||_0$.

Let us recall that equation (6.1.26) holds for any $v_h \in V^h$. For the purpose of deriving appropriate lower bounds for the terms on the left-hand side of (6.1.26) we introduce an operator $\Delta_h : V^h \longrightarrow V^h$.

Definition 6.1 *Given $v_h \in V^h$ let us define $\triangle_h$ by:*

$$(\triangle_h v_h, w_h) = -(\nabla v_h, \nabla w_h) \quad \forall \ w_h \in V^h. \tag{6.3.14}$$

Using the operator $\triangle_h$ one may derive the following lower estimate.

Lemma 6.14 *For θ_δ^n defined in (6.1.5) and $\triangle_h$ given in (6.3.14) we have the following lower estimate:*

$$\begin{aligned} &\left(\theta_\delta^n - \theta_\delta^{n-1}, -\triangle_h \theta_\delta^n\right) + ka\,(\theta_\delta^n, -\triangle_h \theta_\delta^n) \\ &\geq \frac{1}{2}\|\nabla\theta_\delta^n\|_0^2 + kC_a\|\triangle_h \theta_\delta^n\|_0^2 - \frac{1}{2}\|\nabla\theta_\delta^{n-1}\|_0^2. \end{aligned} \tag{6.3.15}$$

Proof

Using the symmetry of the L^2 inner product, the definition of $\triangle_h$ and the Cauchy-Schwarz inequality one has

$$\begin{aligned} \left(\theta_\delta^n - \theta_\delta^{n-1}, -\triangle_h \theta_\delta^n\right) &= \left(-\triangle_h \theta_\delta^n, \theta_\delta^n - \theta_\delta^{n-1}\right) \\ &= \left(\nabla\theta_\delta^n, \nabla\theta_\delta^n - \nabla\theta_\delta^{n-1}\right) \\ &\geq \|\nabla\theta_\delta^n\|_0^2 - \|\nabla\theta_\delta^n\|_0\|\nabla\theta_\delta^{n-1}\|_0 \\ &\geq \|\nabla\theta_\delta^n\|_0^2 - \frac{1}{2}\|\nabla\theta_\delta^n\|_0^2 - \frac{1}{2}\|\nabla\theta_\delta^{n-1}\|_0^2 \\ &= \frac{1}{2}\|\nabla\theta_\delta^n\|_0^2 - \frac{1}{2}\|\nabla\theta_\delta^{n-1}\|_0^2. \end{aligned} \tag{6.3.16}$$

On the other hand, using the definition of the bilinear form $a(\cdot,\cdot)$, its symmetry and the definition of $\triangle_h$ one can estimate the second term on the left-hand side of (6.3.15) as follows.

$$\begin{aligned} a\,(\theta_\delta^n, -\triangle_h \theta_\delta^n) &= C_a\,(\nabla\theta_\delta^n, \nabla(-\triangle_h \theta_\delta^n)) + (\theta_\delta^n, -\triangle_h \theta_\delta^n) \\ &= C_a\,(\triangle_h\theta_\delta^n, \triangle_h\theta_\delta^n) + (\theta_\delta^n, -\triangle_h \theta_\delta^n) \\ &= C_a\|\triangle_h \theta_\delta^n\|_0^2 + (\nabla\theta_\delta^n, \nabla\theta_\delta^n) \end{aligned} \tag{6.3.17}$$

$$
\begin{aligned}
&= C_a \| \triangle_h \theta_\delta^n \|_0^2 + \|\nabla \theta_\delta^n\|_0^2 \\
&\geq C_a \| \triangle_h \theta_\delta^n \|_0^2.
\end{aligned}
$$

Combining (6.3.16) and (6.3.17) together we have the desired lower bound

$$
\begin{aligned}
&\left(\theta_\delta^n - \theta_\delta^{n-1}, -\triangle_h \theta_\delta^n\right) + ka\left(\theta_\delta^n, -\triangle_h \theta_\delta^n\right) \\
&\quad \geq \frac{1}{2}\|\nabla \theta_\delta^n\|_0^2 + kC_a \| \triangle_h \theta_\delta^n\|_0^2 - \frac{1}{2}\|\nabla \theta_\delta^{n-1}\|_0^2 \quad \square.
\end{aligned}
$$

The central result of this section is contained in the next theorem.

Theorem 6.2 *Let* $\mathbf{A}$ *and* $\mathbf{A}_h$ *denote the solutions of the weak (2.2.1) and approximate (3.3.1) problems, respectively. For* $1 \leq n \leq N$ *let* $\psi(t_n)$ *and* Ψ_δ^n *denote the solutions of the weak (2.2.20) and the auxiliary problems (5.1.3) at the n-th time level. For a positive integer* m *satisfying* $m+1 > d/2$ *we assume that* $\mathbf{A} \in \mathbf{H}_n^1(\Omega) \cap \mathbf{H}^{m+1}(\Omega)$ *and* $\psi \in \mathcal{V}$ *with* $\psi(\cdot, \mathbf{x}) \in \mathcal{H}^{m+1}(\Omega)$ *and* $\|\psi_{tt}\|_0 \leq C$. *If the initial condition satisfies*

$$
\|e_\delta^0\|_1 \leq C_\delta h^m, \tag{6.3.18}
$$

then for sufficiently small h *and* k *with* $k = \mathbf{o}\left(h^{d/2}\right)$ *the following optimal* $\mathcal{H}^1$ *estimate hold*

$$
\|e_\delta^n\|_1 \leq C_\delta (h^m + k). \tag{6.3.19}
$$

Proof

Let us recall the inequality (6.3.9) derived in Lemma 6.13:

$$
\left(\theta_\delta^n - \theta_\delta^{n-1}, v_h\right) + ka\left(\theta_\delta^n, v_h\right) \leq kC_\epsilon^\delta \left(R_0 + \|\theta_\delta^n\|_1^2\right) + k\epsilon \|v_h\|_0^2 \quad \forall\, v_h \in V^h.
$$

We denote:

$$
R_1 = h^{2m} + k^2. \tag{6.3.20}
$$

We recall that $\triangle_h : V^h \longrightarrow V^h$ and consider the following choice for the test function: $v_h = -\triangle_h \theta_\delta^n \in V^h$. Then,

$$\left(\theta_\delta^n - \theta_\delta^{n-1}, -\triangle_h \theta_\delta^n\right) + ka\left(\theta_\delta^n, -\triangle_h \theta_\delta^n\right) \le kC_\epsilon^\delta\left(R_1 + \|\theta_\delta^n\|_1^2\right) + k\epsilon\|\triangle_h \theta_\delta^n\|_0^2;$$

and in combination with the lower estimate from Lemma 6.14 we obtain

$$\frac{1}{2}\|\nabla\theta_\delta^n\|_0^2 + kC_a\|\triangle_h \theta_\delta^n\|_0^2 - \frac{1}{2}\|\nabla\theta_\delta^{n-1}\|_0^2 \le kC_\epsilon^\delta\left(R_1 + \|\theta_\delta^n\|_1^2\right) + k\epsilon\|\triangle_h \theta_\delta^n\|_0^2.$$

Collecting like terms one has

$$\begin{aligned} &\frac{1}{2}\|\nabla\theta_\delta^n\|_0^2 + k\left(C_a - \epsilon\right)\|\triangle_h \theta_\delta^n\|_0^2 \\ &\quad\le \frac{1}{2}\|\nabla\theta_\delta^{n-1}\|_0^2 + kC_\epsilon^\delta R_1 + kC_\epsilon^\delta\left(\|\nabla\theta_\delta^n\|_0^2 + \|\theta_\delta^n\|_0^2\right). \end{aligned} \tag{6.3.21}$$

Let us recall that $R_0 = h^{2m+2} + k^2$ was defined in (6.2.2) and the estimate $\|\theta_\delta^n\|_0^2 \le CR_0$. As a result

$$\|\theta_\delta^n\|_0^2 \le CR_1, \tag{6.3.22}$$

where R_1 is given in (6.3.20). Choosing $\epsilon = \frac{C_a}{2}$ and multiplying the equation (6.3.21) by two we obtain

$$\|\nabla\theta_\delta^n\|_0^2 + kC_a\|\triangle_h \theta_\delta^n\|_0^2 \le \|\nabla\theta_\delta^{n-1}\|_0^2 + 4kC_\epsilon^\delta R_1 + 2kC_\epsilon^\delta\|\nabla\theta_\delta^n\|_0^2.$$

After dropping the nonnegative term $kC_a\|\triangle_h \theta_\delta^n\|_0^2$ on the left-hand side and collecting the like terms we obtain

$$\left(1 - 2kC_\epsilon^\delta\right)\|\nabla\theta_\delta^n\|_0^2 \le \|\nabla\theta_\delta^{n-1}\|_0^2 + 4kC_\epsilon^\delta R_1,$$

or equivalently,

$$\left(1 - k\bar{C}_\epsilon^\delta\right)\|\nabla\theta_\delta^n\|_0^2 \le \|\nabla\theta_\delta^{n-1}\|_0^2 + 2k\bar{C}_\epsilon^\delta R_1,$$

where $\bar{C}^{\delta}_{\epsilon} = 2C^{\delta}_{\epsilon}$.

Similar to the derivation of the optimal estimate for $||\theta^n_\delta||_0$ one has that for sufficiently small $k > 0$ the following holds

$$||\nabla\theta^n_\delta||^2_0 \leq (1 + \bar{C}_\delta k)\, ||\nabla\theta^{n-1}_\delta||^2_0 + k\bar{C}_\delta R_1.$$

After repeated applications of the above inequality it follows that

$$||\nabla\theta^n_\delta||^2_0 \leq (1 + \bar{C}_\delta k)^n\, ||\nabla\theta^0_\delta||^2_0 + nk\bar{C}_\delta R_1.$$

The initial condition (6.3.18) and the definition of R_1 imply

$$||\nabla\theta^n_\delta||^2_0 \leq \max\{e^{\bar{C}_\delta kn}, nk\bar{C}_\delta\}\left(h^{2m} + k^2\right).$$

Hence

$$||\nabla\theta^n_\delta||_0 \leq C^\delta\,(h^m + k)\,, \tag{6.3.23}$$

where $C^\delta = \left[\max\{e^{\bar{C}_\delta kn}, nk\bar{C}_\delta\}\right]^{1/2}$.

Combining the optimal estimate (6.2.1) for the $\mathcal{L}^2$ norm of θ^n_δ together with the optimal estimate (6.3.23) for the $\mathcal{H}^1$ seminorm we arrive at

$$||\theta^n_\delta||_1 \leq C_\delta(h^m + k). \tag{6.3.24}$$

Finally, using the splitting of the error given in (6.1.4) and combining (6.3.24) together with the standard $\mathcal{H}^1$ estimate for ρ^n derived in Lemma 6.1 we establish the desired optimal $\mathcal{H}^1$ estimate

$$||e^n_\delta||_1 \leq C_\delta\,(h^m + k)\,. \quad \square$$

This concludes the proof of Theorem 6.2. $\square$

Chapter 7

Error Estimates for the Auxiliary Crank-Nicolson-Galerkin Problem

In this chapter we derive optimal $\mathcal{L}^2$ and $\mathcal{H}^1$ error estimates for the auxiliary Crank-Nicolson-Galerkin problem (5.1.4). We follow essentially the same approach as in Chapter 6. However, since now we want to prove optimal estimates of order $\mathbf{O}\left(k^2\right)$ in time, it is necessary to derive an appropriate θ_δ^n-equation which allows for accurate time estimates. Thus, the main differences with Chapter 6 are in the derivation of the θ_δ^n-equation and in the estimates for the terms on the right-hand side of this equation.

7.1 Preliminary Estimates

In this section we collect several preliminary results used later on in the derivation of the optimal error estimates for the auxiliary Crank-Nicolson-Galerkin problem (5.1.4).

We begin with the results used in the derivation of the optimal $\mathcal{L}^2$ error estimates for (5.1.4). Let us define $P\psi(t_n)$, ρ^n, θ_δ^n and e_δ^n as before with the only difference being that now Ψ_δ^n solves (5.1.4). For these definitions we refer to (6.1.2), (6.1.3), (6.1.5) and (6.1.1), respectively.

We start with the derivation of an appropriate θ_δ^n-equation.

Lemma 7.1 *Let ψ and Ψ_δ^n be the solutions of the weak and auxiliary problem, see (2.2.20) and (5.1.4), respectively. If ψ satisfies $\psi \in \mathcal{V}$ with $\psi(\cdot, \mathbf{x}) \in \mathcal{H}^2(\Omega)$, then θ_δ^n satisfies the* *following equation*

$$\begin{aligned}\left(\frac{\tilde{d}}{dt}\theta_\delta^n, \bar{\theta}_\delta^n\right) &+ a\left(\bar{\theta}_\delta^n, \bar{\theta}_\delta^n\right) = -\left(\omega^n, \bar{\theta}_\delta^n\right) + \left(f_h^\delta(\bar{\Psi}_\delta^n) - f(\psi(t_{n-\frac{1}{2}})), \bar{\theta}_\delta^n\right) \\ &+ b\left(\mathbf{A}_h, \bar{\theta}_\delta^n, \bar{\theta}_\delta^n\right) + b\left(\mathbf{A}_h, \bar{\theta}_\delta^n, P\bar{\psi}^n - \psi(t_{n-\frac{1}{2}})\right) \\ &- b\left(\mathbf{A} - \mathbf{A}_h, \bar{\theta}_\delta^n, \psi(t_{n-\frac{1}{2}})\right).\end{aligned} \tag{7.1.1}$$

Proof

Subtracting (2.2.20) from (5.1.4) one has

$$\begin{aligned}(\frac{\tilde{d}}{dt}\Psi_\delta^n - \psi_t(t_n), v_h) + a\left(\bar{\Psi}_\delta^n - \psi(t_n), v_h\right) - b\left(\mathbf{A}_h, v_h, \bar{\Psi}_\delta^n\right) + b\left(\mathbf{A}, v_h, \psi(t_n)\right) \\ = \left(f_h^\delta(\bar{\Psi}_\delta^n), v_h\right) - \left(f(\psi(t_n)), v_h\right) \forall\, v_h \in V^h.\end{aligned}$$

Adding and subtracting $(\frac{\tilde{d}}{dt}P\psi(t_n), v_h)$, $\frac{1}{2}a(P\psi(t_n), v_h)$, $\frac{1}{2}a(P\psi(t_{n-1}), v_h)$ and $\frac{1}{2}a(\psi(t_{n-1}), v_h)$ to the left-hand side of the above equation and using the definitions of θ_δ^n and ρ^n we get

$$\begin{aligned}&\left(\frac{\tilde{d}}{dt}\theta_\delta^n, v_h\right) + \left(\frac{\tilde{d}}{dt}P\psi(t_n) - \psi_t(t_n), v_h\right) + a\left(\bar{\theta}_\delta^n, v_h\right) \\ &+ \frac{1}{2}a\left(\rho^n, v_h\right) + \frac{1}{2}a\left(\rho^{n-1}, v_h\right) - \frac{1}{2}a\left(\psi(t_n) - \psi(t_{n-1}), v_h\right) \\ &= b\left(\mathbf{A}_h, v_h, \bar{\Psi}_\delta^n\right) - b\left(\mathbf{A}, v_h, \psi(t_n)\right) + \left(f_h^\delta(\bar{\Psi}_\delta^n), v_h\right) - \left(f(\psi(t_n)), v_h\right) \forall\, v_h \in V^h,\end{aligned}$$

where we have used the notation

$$\bar{\theta}_\delta^n = \frac{\theta_\delta^n + \theta_\delta^{n-1}}{2}. \tag{7.1.2}$$

Using the definition of the projection operator given in (6.1.2) and (7.1.2) the above equation reduces to

$$\begin{aligned}&\left(\frac{\tilde{d}}{dt}\theta_\delta^n, v_h\right) + \left(\frac{\tilde{d}}{dt}P\psi(t_n) - \psi_t(t_n), v_h\right) + a\left(\bar{\theta}_\delta^n, v_h\right) - \frac{1}{2}a\left(\psi(t_n) - \psi(t_{n-1}), v_h\right) \\ &= b\left(\mathbf{A}_h, v_h, \bar{\Psi}_\delta^n\right) - b\left(\mathbf{A}, v_h, \psi(t_n)\right) + \left(f_h^\delta(\bar{\Psi}_\delta^n), v_h\right) - \left(f(\psi(t_n)), v_h\right) \forall\, v_h \in V^h.\end{aligned}$$

We recall that $t_{n-\frac{1}{2}} = \left(n - \frac{1}{2}\right) k$, where $k > 0$ is a constant time step. Adding and subtracting $(\frac{\tilde{d}}{dt}\psi(t_n), v_h)$, $(\psi_t(t_{n-\frac{1}{2}}), v_h)$ and $(f(\psi(t_{n-\frac{1}{2}}), v_h)$ to the right-hand side of the above equation we get

$$\begin{aligned}
\left(\frac{\tilde{d}}{dt}\theta^n, v_h\right) + a\left(\bar{\theta}^n_\delta, v_h\right) &= \left(\psi_t(t_n), v_h\right) - \left(\frac{\tilde{d}}{dt}P\psi(t_n), v_h\right) \\
+ \quad & a\left(\frac{\psi(t_n) - \psi(t_{n-1})}{2}, v_h\right) + b\left(\mathbf{A}_h, v_h, \bar{\Psi}^n_\delta\right) - b\left(\mathbf{A}, v_h, \psi(t_n)\right) \\
+ \quad & \left(\frac{\tilde{d}}{dt}\psi(t_n), v_h\right) - \left(\frac{\tilde{d}}{dt}\psi(t_n), v_h\right) + \left(\psi_t(t_{n-\frac{1}{2}}), v_h\right) - \left(\psi_t(t_{n-\frac{1}{2}}), v_h\right) \\
+ \quad & \left(f(\psi(t_{n-\frac{1}{2}}), v_h\right) - \left(f(\psi(t_{n-\frac{1}{2}}), v_h\right) + \left(f^\delta_h(\bar{\Psi}^n_\delta), v_h\right) - \left(f(\psi(t_n)), v_h\right) \forall\, v_h \in V^h.
\end{aligned}$$

Using the weak problem (2.2.20) and the definition of ρ^n given in (6.1.3) one has

$$\begin{aligned}
\left(\psi_t(t_n), v_h\right) - \left(f(\psi(t_n)), v_h\right) &= -a(\psi(t_n), v_h) + b\left(\mathbf{A}, v_h, \psi(t_n)\right), \\
\left(-\frac{\tilde{d}}{dt}P\psi(t_n) + \frac{\tilde{d}}{dt}\psi(t_n), v_h\right) &= -\left(\frac{\tilde{d}}{dt}\rho^n, v_h\right), \\
-\left(\psi_t(t_{n-\frac{1}{2}}), v_h\right) + \left(f(\psi(t_{n-\frac{1}{2}}), v_h\right) &= a(\psi(t_{n-\frac{1}{2}}), v_h) - b\left(\mathbf{A}, v_h, \psi(t_{n-\frac{1}{2}})\right).
\end{aligned}$$

Thus we arrive at

$$\begin{aligned}
\left(\frac{\tilde{d}}{dt}\theta^n, v_h\right) + a\left(\bar{\theta}^n_\delta, v_h\right) = -\left(\frac{\tilde{d}}{dt}\rho^n, v_h\right) &- a\left(\frac{\psi(t_n) + \psi(t_{n-1})}{2} - \psi(t_{n-\frac{1}{2}}), v_h\right) \\
+ \quad & \left(\psi_t(t_{n-\frac{1}{2}}) - \frac{\tilde{d}}{dt}\psi(t_n), v_h\right) + \left(f^\delta_h(\bar{\Psi}^n_\delta) - f(\psi(t_{n-\frac{1}{2}})), v_h\right) \\
+ \quad & b\left(\mathbf{A}_h, v_h, \bar{\Psi}^n_\delta\right) - b\left(\mathbf{A}, v_h, \psi(t_{n-\frac{1}{2}})\right) \forall\, v_h \in V^h.
\end{aligned}$$

We recall that

$$\omega^n_1 = \frac{\tilde{d}}{dt}\rho^n. \tag{7.1.3}$$

We redefine ω^n_2 as

$$\omega^n_2 = \frac{\tilde{d}}{dt}\psi(t_n) - \psi_t(t_{n-\frac{1}{2}}) \tag{7.1.4}$$

and set

$$\bar{\psi}^n = \frac{\psi(t_n) + \psi(t_{n-1})}{2}. \tag{7.1.5}$$

Collecting the like terms and using the notation (7.1.3)-(7.1.5) one has

$$\begin{aligned}
\left(\frac{\tilde{d}}{dt}\theta^n, v_h\right) + a\left(\bar{\theta}^n_\delta, v_h\right) &= -\left(\omega_1^n + \omega_2^n, v_h\right) \\
- \quad a\left(\bar{\psi}^n - \psi(t_{n-\frac{1}{2}}), v_h\right) &+ \left(f_h^\delta(\bar{\Psi}^n_\delta) - f(\psi(t_{n-\frac{1}{2}})), v_h\right) \\
+ \quad b\left(\mathbf{A}_h, v_h, \bar{\Psi}^n_\delta\right) &- b\left(\mathbf{A}, v_h, \psi(t_{n-\frac{1}{2}})\right) \forall\, v_h \in V^h.
\end{aligned} \tag{7.1.6}$$

For a sufficiently smooth weak solution ψ of (2.2.20) let us define

$$\omega_3^n = -\left(\bar{\psi}^n - \psi(t_{n-\frac{1}{2}})\right), \tag{7.1.7}$$

$$\omega_4^n = \left(\frac{\xi}{l}\right)^2 \Delta\left(\bar{\psi}^n - \psi(t_{n-\frac{1}{2}})\right) = -\left(\frac{\xi}{l}\right)^2 \Delta\,\omega_3^n. \tag{7.1.8}$$

The definition of the bilinear form $a(\cdot,\cdot)$ given in (2.2.13), together with the definition of ω_3^n given in (7.1.7), imply that for any $v_h \in V^h$

$$a\left(\bar{\psi}^n - \psi(t_{n-\frac{1}{2}}), v_h\right) = -a\left(\omega_3^n, v_h\right) = -\left(\frac{\xi}{l}\right)^2 \left(\nabla\omega_3^n, \nabla v_h\right) - \left(\omega_3^n, v_h\right).$$

Integrating by parts, accounting for the boundary condition (2.1.40), and using the definition of ω_4^n given in (7.1.8) we get

$$\begin{aligned}
a\left(\bar{\psi}^n - \psi(t_{n-\frac{1}{2}}), v_h\right) &= \left(\frac{\xi}{l}\right)^2 \left(\Delta\omega_3^n, v_h\right) - \left(\omega_3^n, v_h\right) \\
&= -\left(\omega_4^n, v_h\right) - \left(\omega_3^n, v_h\right) = -\left(\omega_3^n + \omega_4^n, v_h\right).
\end{aligned}$$

For simplicity we introduce the notation

$$\omega^n = \sum_{j=1}^{2} \omega_j^n - \sum_{j=3}^{4} \omega_j^n. \tag{7.1.9}$$

Then using (7.1.9) equation (7.1.6) transforms into

$$\left(\frac{\tilde{d}}{dt}\theta^n, v_h\right) + a\left(\bar{\theta}^n_\delta, v_h\right) = -\left(\omega^n, v_h\right) + \left(f^\delta_h(\bar{\Psi}^n_\delta) - f(\psi(t_{n-\frac{1}{2}})), v_h\right)$$
$$+ \quad b\left(\mathbf{A}_h, v_h, \bar{\Psi}^n_\delta\right) - b\left(\mathbf{A}, v_h, \psi(t_{n-\frac{1}{2}})\right) \forall\, v_h \in V^h. \qquad (7.1.10)$$

To handle the terms which involve the trilinear form $b(\cdot,\cdot,\cdot)$ we add and subtract the terms $\frac{1}{2}b\left(\mathbf{A}_h, v_h, P\psi(t_n)\right)$, $\frac{1}{2}b\left(\mathbf{A}_h, v_h, P\psi(t_{n-1})\right)$ and $\frac{1}{2}b\left(\mathbf{A}_h, v_h, \psi(t_{n-\frac{1}{2}})\right)$ to obtain

$$\begin{aligned}
& b\left(\mathbf{A}_h, v_h, \bar{\Psi}^n_\delta\right) - b\left(\mathbf{A}, v_h, \psi(t_{n-\frac{1}{2}})\right) \\
= \;& b\left(\mathbf{A}_h, v_h, \bar{\theta}^n_\delta\right) + b\left(\mathbf{A}_h, v_h, \frac{P\psi(t_{n-1}) + P\psi(t_n)}{2}\right) \\
- \;& b\left(\mathbf{A} - \mathbf{A}_h, v_h, \psi(t_{n-\frac{1}{2}})\right) - b\left(\mathbf{A}_h, v_h, \psi(t_{n-\frac{1}{2}})\right) \\
= \;& b\left(\mathbf{A}_h, v_h, \bar{\theta}^n_\delta\right) + b\left(\mathbf{A}_h, v_h, P\bar{\psi}^n - \psi(t_{n-\frac{1}{2}}\right) - b\left(\mathbf{A} - \mathbf{A}_h, v_h, \psi(t_{n-\frac{1}{2}})\right).
\end{aligned}$$

Hence equation (7.1.10) transforms into

$$\begin{aligned}
\left(\frac{\tilde{d}}{dt}\theta^n_\delta, v_h\right) \;&+\; a\left(\bar{\theta}^n_\delta, v_h\right) = -\left(\omega^n, v_h\right) + \left(f^\delta_h(\bar{\Psi}^n_\delta) - f(\psi(t_{n-\frac{1}{2}})), v_h\right) \\
&+\; b\left(\mathbf{A}_h, v_h, \bar{\theta}^n_\delta\right) + b\left(\mathbf{A}_h, v_h, P\bar{\psi}^n - \psi(t_{n-\frac{1}{2}}\right) \qquad (7.1.11) \\
&-\; b\left(\mathbf{A} - \mathbf{A}_h, v_h, \psi(t_{n-\frac{1}{2}})\right) \quad \forall\, v_h \in V^h.
\end{aligned}$$

Let us choose the test function in equation (7.1.11) as $v_h = \bar{\theta}^n_\delta \in V^h$. Then we have the following equation for θ^n_δ

$$\begin{aligned}
\left(\frac{\tilde{d}}{dt}\theta^n_\delta, \bar{\theta}^n_\delta\right) \;&+\; a\left(\bar{\theta}^n_\delta, \bar{\theta}^n_\delta\right) = -\left(\omega^n, \bar{\theta}^n_\delta\right) + \left(f^\delta_h(\bar{\Psi}^n_\delta) - f(\psi(t_{n-\frac{1}{2}})), \bar{\theta}^n_\delta\right) \\
&+\; b\left(\mathbf{A}_h, \bar{\theta}^n_\delta, \bar{\theta}^n_\delta\right) + b\left(\mathbf{A}_h, \bar{\theta}^n_\delta, P\bar{\psi}^n - \psi(t_{n-\frac{1}{2}})\right) \\
&-\; b\left(\mathbf{A} - \mathbf{A}_h, \bar{\theta}^n_\delta, \psi(t_{n-\frac{1}{2}})\right). \quad \square
\end{aligned}$$

In order to derive an optimal $\mathcal{L}^2$ error estimate we note that, as before, we need to bound all terms on the right-hand side of the above equation for θ^n_δ. Such bounds are established in Lemmas 7.2-7.6.

Lemma 7.2 *If the weak solution ψ satisfies $\|\psi_{ttt}\| \leq C$ and $\| \triangle \psi_{tt}\|_0$, then we obtain the following estimates*

$$\begin{aligned} \|\omega_1^n\|_0 &\leq Ch^{m+1}, &(7.1.12)\\ \|\omega_j^n\|_0 &\leq Ck^2 \quad \textit{for} \quad j=2,3,4, &(7.1.13)\end{aligned}$$

where C is a generic constant independent of h and k.

Proof

We note that (7.1.12) was already proved in Lemma 6.4. Following [77], we continue with the proof of (7.1.13). We have

$$\begin{aligned} \|\omega_2^n\|_0 &= \|\frac{\tilde{d}}{dt}\psi(t_n) - \psi_t(t_{n-\frac{1}{2}})\|_0 \\ &= \frac{1}{2k}\left\| \int_{t_{n-1}}^{t_{n-1/2}} (s-t_{n-1})^2 \psi_{ttt}(s)\, ds + \int_{t_{n-1/2}}^{t_n} (s-t_n)^2 \psi_{ttt}(s)\, ds \right\|_0 \\ &\leq Ck\int_{t_{n-1}}^{t_n} \|\psi_{ttt}\|_0 ds \leq Ck^2. \end{aligned}$$

On the other hand

$$\begin{aligned} \|\omega_3^n\|_0 &= \left\| - \left(\bar{\psi}^n - \psi(t_{n-\frac{1}{2}})\right)\right\|_0 \\ &\leq Ck\int_{(n-1)k}^{nk} \|\psi_{tt}\|_0\, ds \leq Ck^2. \end{aligned} \tag{7.1.14}$$

Similarly,

$$\begin{aligned} \|\omega_4^n\|_0 &= \left\| \left(\frac{\xi}{l}\right)^2 \triangle \left(\bar{\psi}^n - \psi(t_{n-\frac{1}{2}})\right)\right\|_0 \\ &\leq Ck\int_{t_{n-1}}^{t_n} \| \triangle \psi_{tt}\|_0\, ds \leq Ck^2. \end{aligned}$$

This concludes the proof of Lemma 7.2 $\square$.

Note that Lemma 7.2 implies

$$\|\omega^n\|_0 = \left\| \sum_{j=1}^{4} \omega_j^n \right\|_0 \leq \sum_{j=1}^{4} \|\omega_j^n\|_0 \leq C\left(h^{m+1} + k^2\right). \tag{7.1.15}$$

Let us denote

$$\bar{\rho}^n = P\bar{\psi}^n - \bar{\psi}^n. \tag{7.1.16}$$

Following [77] one may prove the following optimal result.

Lemma 7.3 *If the weak solution ψ of (2.2.20) satisfies $\psi \in \mathcal{V}$ with $\psi(\cdot, \mathbf{x}) \in \mathcal{H}^{m+1}(\Omega)$ and $\|\psi_{tt}\|_0 \leq C$, then the following estimate holds*

$$\|P\bar{\psi}^n - \psi(t_{n-\frac{1}{2}})\|_0 \leq C\left(h^{m+1} + k^2\right). \tag{7.1.17}$$

Proof

Using the triangle inequality we have that

$$\begin{aligned} \|P\bar{\psi}^n - \psi(t_{n-\frac{1}{2}})\|_0 &\leq \|P\bar{\psi}^n - \bar{\psi}^n\|_0 + \|\bar{\psi}^n - \psi(t_{n-\frac{1}{2}})\|_0 \\ &\leq \|\bar{\rho}^n\|_0 + \|\omega_3^n\|_0. \end{aligned}$$

Then by virtue of Lemma 6.1 it follows that

$$\|\bar{\rho}^n\|_0 = \left\| \frac{\rho^n + \rho^{n-1}}{2} \right\|_0 \leq \frac{1}{2}\|\rho^n\|_0 + \frac{1}{2}\|\rho^{n-1}\|_0 \leq Ch^{m+1}. \tag{7.1.18}$$

Finally, combining (7.1.18) with (7.1.14) one arrives at

$$\|P\bar{\psi}^n - \psi(t_{n-\frac{1}{2}})\|_0 \leq C\left(h^{m+1} + k^2\right). \quad \square$$

Similar to the proof of Lemma 6.8 one can show the following result.

Lemma 7.4 *For $\Omega \subset \mathbb{R}^d$ for $d = 2, 3$ and for a positive integer m with $m + 1 > d/2$ we assume that the weak solution of problem (2.2.1) satisfies $\mathbf{A} \in \mathbf{H}_n^1(\Omega) \cap \mathbf{H}^{m+1}(\Omega)$.*

In addition we assume that the dual problem corresponding to (2.2.1) is regular and that $\mathbf{A}_h \in \mathbf{W}^h$ *is the finite element approximation to* $\mathbf{A}$ *which satisfies (3.2.12). We also assume that the weak solution of (2.2.20) satisfy* $\psi \in \mathcal{V}$ *with* $\psi(\cdot,\mathbf{x}) \in \mathcal{H}^{m+1}(\Omega)$*. If* Ψ_δ^n *denote the solution of the auxiliary problem (5.1.3) and if the finite element space* V^h *satisfy (3.2.11) then for any* $\epsilon > 0$ *the following estimate holds*

$$\begin{aligned}
&\left|b\left(\mathbf{A}_h, v_h, \bar{\theta}_\delta^n\right) - b\left(\mathbf{A} - \mathbf{A}_h, v_h, \psi(t_{n-\frac{1}{2}})\right) + b\left(\mathbf{A}_h, v_h, P\bar{\psi}^n - \psi(t_{n-\frac{1}{2}})\right)\right| \\
&\qquad \leq \; C_{b,\epsilon}\left(h^{2m+2} + k^4 + \|\bar{\theta}_\delta^n\|_0^2\right) + \epsilon\|v_h\|_1^2 \quad \forall \; v_h \in V^h. \qquad (7.1.19)
\end{aligned}$$

Proof

Using Lemma 2.4 and Lemma 4.1.3 one can estimate $b\left(\mathbf{A} - \mathbf{A}_h, v_h, \psi(t_{n-\frac{1}{2}})\right)$ as follows

$$\left|b\left(\mathbf{A} - \mathbf{A}_h, v_h, \psi(t_{n-\frac{1}{2}})\right)\right| \leq \|\psi(t_{n-\frac{1}{2}})\|_\infty \|\mathbf{A} - \mathbf{A}_h\|_0 \|v_h\|_1 \leq C_{1,\epsilon_1} h^{2m+2} + \epsilon_1 \|v_h\|_1^2.$$

On the other hand, Lemma 4.5 gives

$$\left|b\left(\mathbf{A}_h, v_h, \bar{\theta}_\delta^n\right)\right| \leq \|\mathbf{A}_h\|_\infty \|v_h\|_1 \|\bar{\theta}_\delta^n\|_0 \leq C_{2,\epsilon_2}\|\bar{\theta}_\delta^n\|_0^2 + \epsilon_2\|v_h\|_1^2.$$

Using Lemma 4.5 and Lemma 7.3 one may bound the last term in (7.1.19) as follows

$$\begin{aligned}
\left|b\left(\mathbf{A}_h, v_h, P\bar{\psi}^n - \psi(t_{n-\frac{1}{2}})\right)\right| &\leq \|\mathbf{A}_h\|_\infty \|v_h\|_1 \|P\bar{\psi}^n - \psi(t_{n-\frac{1}{2}})\|_0 \\
&\leq \; C_{3,\epsilon_3}\left(h^{2m+2} + k^4\right) + \epsilon_3\|v_h\|_1^2.
\end{aligned}$$

By letting $C_{b\epsilon} = \max\{C_{1,\epsilon_1}, C_{2,\epsilon_2}, C_{3,\epsilon_3}\}$ and $\epsilon = \epsilon_1 + \epsilon_2 + \epsilon_3$ the proof of Lemma 7.4 is completed. □

As shown in [77] one can prove the following optimal estimate.

Lemma 7.5 *Let* Ψ_δ^n *and* ψ *be the solutions of (5.1.4) and (2.2.20), respectively. Let* $\psi \in \mathcal{V}$ *with* $\psi(\cdot,\mathbf{x}) \in \mathcal{H}^{m+1}(\Omega)$ *and* $\|\psi_{tt}\|_0 \leq C$*. Then the following estimate holds*

$$\|\bar{\Psi}_\delta^n - \psi(t_{n-\frac{1}{2}})\|_0 \leq \|\bar{\theta}_\delta^n\|_0 + C\left(h^{m+1} + k^2\right). \qquad (7.1.20)$$

Proof

From (7.1.18), (7.1.14) and the triangle inequality it follows that

$$\begin{aligned}
\|\bar{\Psi}_\delta^n - \psi(t_{n-\frac{1}{2}})\|_0 &= \|\bar{\Psi}_\delta^n - P\bar{\psi}^n\|_0 + \|P\bar{\psi}^n - \bar{\psi}^n\|_0 + \|\bar{\psi}^n - \psi(t_{n-\frac{1}{2}})\|_0 \\
&\leq \|\bar{\theta}_\delta^n\|_0 + \|\bar{\rho}^n\|_0 + \|\bar{\psi}^n - \psi(t_{n-\frac{1}{2}})\|_0 \leq \|\bar{\theta}_\delta^n\|_0 + C\left(h^{m+1} + k^2\right)
\end{aligned}$$

and the proof is completed. □

The final preliminary result needed for the derivation of the optimal $\mathcal{L}^2$ error estimate is presented next.

Lemma 7.6 *Let the hypotheses of Lemma 7.4 hold. Then we have the following estimate*

$$\left|\left(f_h^\delta(\bar{\Psi}_\delta^n) - f(\psi(t_{n-\frac{1}{2}})), v_h\right)\right| \leq C_f^\delta\left(h^{2m+2} + k^4 + \|\bar{\theta}_\delta^n\|_0^2 + \|v_h\|_0^2\right) \quad \forall\ v_h \in V^h. \tag{7.1.21}$$

Proof

Let us recall the definitions (5.1.1), (2.2.15) and (3.3.3) of M^δ, $f(\cdot)$ and $f_h^\delta(\cdot)$. We also recall that $f_h^\delta(\cdot)$ is globally Lipschitz continuous. Then one may use the triangle inequality, Lemma 7.5, the definitions for $f(\cdot)$ and $f_h(\cdot)$, Lemma 4.2 and the estimate (7.1.13) to obtain the desired estimate. We have

$$\begin{aligned}
&\left|\left(f_h^\delta(\bar{\Psi}_\delta^n) - f(\psi(t_{n-\frac{1}{2}})), v_h\right)\right| \\
&\leq \left|\left(f_h^\delta(\bar{\Psi}_\delta^n) - f_h^\delta(\psi(t_{n-\frac{1}{2}})), v_h\right)\right| + \left|\left(f_h(\psi(t_{n-\frac{1}{2}})) - f(\psi(t_{n-\frac{1}{2}})), v_h\right)\right| \\
&\leq L^\delta\|\bar{\Psi}_\delta^n - \psi(t_{n-\frac{1}{2}})\|_0\|v_h\|_0 + \left|\left((|\mathbf{A}_h|^2 - |\mathbf{A}|^2)\psi(t_{n-\frac{1}{2}}), v_h\right)\right| \\
&\leq L^\delta\left[\|\bar{\theta}_\delta^n\|_0 + C\left(h^{m+1} + k^2\right)\right]\|v_h\|_0 + C\|\mathbf{A}_h - \mathbf{A}\|_0\|v_h\|_0 \\
&\leq C^\delta\left[\|\bar{\theta}_\delta^n\|_0^2 + \|v_h\|_0^2 + h^{2m+2} + k^4\right] + C\left(h^{2m+2} + \|v_h\|_0^2\right) \\
&\leq C_f^\delta\left(h^{2m+2} + k^4 + \|\bar{\theta}_\delta^n\|_0^2 + \|v_h\|_0^2\right),
\end{aligned}$$

which concludes the proof of Lemma 7.6. □

7.2 Optimal $\mathcal{L}^2$ Error Estimates

As in Chapter 6, in order to obtain an optimal $\mathcal{L}^2$ estimate for θ_δ^n we combine the estimates derived for the terms on the right-hand side of the equation for θ_δ^n. We first present an optimal estimate for $\|\theta_\delta^n\|_0$.

Lemma 7.7 *Under the hypotheses of Theorem 6.1 and the additional assumptions that* $\| \triangle \psi_{tt}\|_0 \leq C$ *and* $\|\psi_{ttt}\|_0 \leq C$*, it follows that for sufficiently small* h *and* k *the following optimal error estimate holds*

$$\|\theta_\delta^n\|_0 \leq C_\delta(h^{m+1} + k^2). \tag{7.2.1}$$

Proof

Let us recall the θ_δ^n-equation (7.1.1)

$$\begin{aligned}\left(\frac{\tilde{d}}{dt}\theta_\delta^n, \bar{\theta}_\delta^n\right) + a\left(\bar{\theta}_\delta^n, \bar{\theta}_\delta^n\right) &= -\left(\omega^n, \bar{\theta}_\delta^n\right) + \left(f_h^\delta(\bar{\Psi}_\delta^n) - f(\psi(t_{n-\frac{1}{2}})), \bar{\theta}_\delta^n\right) \\ &+ \quad b\left(\mathbf{A}_h, \bar{\theta}_\delta^n, \bar{\theta}_\delta^n\right) + b\left(\mathbf{A}_h, \bar{\theta}_\delta^n, P\bar{\psi}^n - \psi(t_{n-\frac{1}{2}})\right) - b\left(\mathbf{A} - \mathbf{A}_h, \bar{\theta}_\delta^n, \psi(t_{n-\frac{1}{2}})\right).\end{aligned}$$

Applying Lemma 7.6 and Lemma 7.4 with $v_h = \bar{\theta}_\delta^n \in V^h$ one has

$$\begin{aligned}\left(\frac{\tilde{d}}{dt}\theta_\delta^n, \bar{\theta}_\delta^n\right) &+ \quad a\left(\bar{\theta}_\delta^n, \bar{\theta}_\delta^n\right) \leq \left|\left(\omega^n, \bar{\theta}_\delta^n\right)\right| + C_f^\delta\left(h^{2m+2} + k^4 + \|\bar{\theta}_\delta^n\|_0^2\right) \\ &+ \quad C_{b,\epsilon}\left(h^{2m+2} + k^4 + \|\bar{\theta}_\delta^n\|_0^2\right) + \epsilon\|\bar{\theta}_\delta^n\|_1^2.\end{aligned} \tag{7.2.2}$$

To shorten our notation let us denote

$$R_4 = h^{2m+2} + k^4. \tag{7.2.3}$$

The coercivity of the bilinear form $a(\cdot,\cdot)$ implies

$$\left(\frac{\tilde{d}}{dt}\theta_\delta^n, \bar{\theta}_\delta^n\right) + C_a\|\bar{\theta}_\delta^n\|_1^2 \leq \left|\left(\omega^n, \bar{\theta}_\delta^n\right)\right| + C_\delta\left(R_4 + \|\bar{\theta}_\delta^n\|_0^2\right) + \epsilon\|\bar{\theta}_\delta^n\|_1^2, \tag{7.2.4}$$

where $C_a = \min\left\{\left(\frac{\xi}{l}\right)^2, 1\right\} > 0$.

Using the definition of $\frac{\tilde{d}}{dt}$, multiplying through the equation (7.2.4) by $k > 0$, and using the Cauchy-Schwarz inequality one has

$$\left(\theta_\delta^n - \theta_\delta^{n-1}, \bar{\theta}_\delta^n\right) + kC_a\|\bar{\theta}_\delta^n\|_1^2 \le k\|\omega^n\|_0\|\bar{\theta}_\delta^n\|_0 + kC_\delta\left(R_4 + \|\bar{\theta}_\delta^n\|_0^2\right) + k\epsilon\|\bar{\theta}_\delta^n\|_1^2.$$

Thus, for any $0 < \epsilon < C_a$ we have the inequality

$$\left(\theta_\delta^n - \theta_\delta^{n-1}, \theta_\delta^n + \theta_\delta^{n-1}\right) \le 2k\|\omega^n\|_0\|\bar{\theta}_\delta^n\|_0 + 2kC_\delta\left(R_4 + \|\bar{\theta}_\delta^n\|_0^2\right),$$

and as a result

$$\|\theta_\delta^n\|_0^2 \le \|\theta_\delta^{n-1}\|_0^2 + k\tilde{C}_\delta\|\bar{\theta}_\delta^n\|_0^2 + k\tilde{C}_\delta\left(\|\omega^n\|_0^2 + R_4\right).$$

Using the definition of $\bar{\theta}_\delta^n$ we find that

$$\|\theta_\delta^n\|_0^2 \le \|\theta_\delta^{n-1}\|_0^2 + k\bar{C}_\delta\|\theta_\delta^n\|_0^2 + k\bar{C}_\delta\|\theta_\delta^{n-1}\|_0^2 + k\tilde{C}_\delta\left(\|\omega^n\|_0^2 + R_4\right).$$

Combining the like terms we obtain

$$\left(1 - \bar{C}_\delta k\right)\|\theta_\delta^n\|_0^2 \le \left(1 + \bar{C}_\delta k\right)\|\theta_\delta^{n-1}\|_0^2 + k\tilde{C}_\delta\left(\|\omega^n\|_0^2 + R_4\right).$$

For sufficiently small $k > 0$, we can divide through by $1 - \bar{C}_\delta k$ in order to get

$$\|\theta_\delta^n\|_0^2 \le \left(\frac{1 + \bar{C}_\delta k}{1 - \bar{C}_\delta k}\right)\|\theta_\delta^{n-1}\|_0^2 + \frac{k\tilde{C}_\delta}{1 - \bar{C}_\delta k}\left(\|\omega^n\|_0^2 + R_4\right). \tag{7.2.5}$$

We recall that (7.1.15) implies $\|\omega^n\|_0 \le CR_0$. On the other hand,

$$\frac{1 + \bar{C}_\delta k}{1 - \bar{C}_\delta k} = 1 + \left(\frac{2\bar{C}_\delta}{1 - \bar{C}_\delta k}\right).$$

Hence for $0 < k \le \frac{1}{2\bar{C}_\delta}$ one has

$$\frac{1 + \bar{C}_\delta k}{1 - \bar{C}_\delta k} \le 1 + 4\bar{C}_\delta k = 1 + \hat{C}_\delta k,$$

where $\hat{C}_\delta = 4\bar{C}_\delta > 0$.

Thus (7.2.5) reduces to

$$\|\theta_\delta^n\|_0^2 \leq \left(1 + \hat{C}_\delta k\right) \|\theta_\delta^{n-1}\|_0^2 + kC_1^\delta R_4, \tag{7.2.6}$$

where $C_1^\delta = \frac{(C+1)\bar{C}_\delta}{1-\bar{C}_\delta}$.

After repeated applications of (7.2.6) it follows that

$$\|\theta_\delta^n\|_0^2 \leq \left(1 + \hat{C}_\delta k\right)^n \|\theta_\delta^0\|_0^2 + knC_2^\delta R_4.$$

Using the initial condition (6.1.12) we obtain

$$\|\theta_\delta^n\|_0 \leq C_\delta(h^{m+1} + k^2),$$

where $C_\delta = \left[\max\{e^{\hat{C}_\delta kn}, knC_1^\delta\}\right]$. This concludes the proof of Lemma 7.7. $\square$

In the next theorem we present the main result of this section.

Theorem 7.1 *Let* $\mathbf{A}$ *and* $\mathbf{A}_h$ *denote the solutions of the weak (2.2.1) and approximate (3.3.1) problems, respectively. For* $1 \leq n \leq N$ *let* $\psi(t_n)$ *and* Ψ_δ^n *denote the solutions of the weak (2.2.20) and the auxiliary problems (5.1.3) at the n-th time level. Let* m *be a positive integer satisfying* $m + 1 > d/2$. *We assume that* $\mathbf{A} \in \mathbf{H}_n^1(\Omega) \cap \mathbf{H}^{m+1}(\Omega)$ *and* $\psi \in \mathcal{V}$ *with* $\psi(\cdot, \mathbf{x}) \in \mathcal{H}^{m+1}(\Omega)$, $\|\psi_{ttt}\|_0 \leq C$ *and* $\| \Delta \psi_{tt}\|_0 \leq C$. *If the initial condition satisfies (6.1.12), then for sufficiently small* h *and* k *the following optimal* $\mathcal{L}^2$ *estimates hold*

$$\|e_\delta^n\|_0 \leq C_\delta(h^{m+1} + k^2), \tag{7.2.7}$$

where C_δ *is a generic constant independent of* h *and* k.

Proof

Let us recall the splitting of the error

$$\|e_\delta^n\|_0 = \|\Psi_\delta^n - \psi(t_n)\|_0 \leq \|\theta_\delta^n\|_0 + \|\rho^n\|_0,$$

where Ψ_δ^n and $\psi(t_n)$ solve (5.1.4) and (2.2.20), respectively. Combining (7.2.1) and (6.1.6) together one arrives at the desired optimal $\mathcal{L}^2$ error estimate

$$\|e_\delta^n\|_0 \leq C_\delta \left(h^{m+1} + k^2\right). \quad \square$$

7.3 Optimal $\mathcal{H}^1$ Error Estimates

In this section we present an optimal $\mathcal{H}^1$ error estimate for the auxiliary problem (5.1.4).

We begin with three preliminary results which will be used in the derivation of the optimal $\mathcal{H}^1$ error estimates for the auxiliary Crank-Nicolson-Galerkin problem (5.1.4).

Lemma 7.8 *Under the hypotheses of Lemma 6.8 hold and the additional condition that* $k = \mathbf{o}\left(h^{d/4}\right)$ *we obtain that for any* $v_h \in V^h$ *and for an arbitrary* $\epsilon > 0$ *the following estimate holds*

$$\begin{aligned}\left|b\left(\mathbf{A}_h, v_h, \bar{\theta}_\delta^n\right) + b\left(\mathbf{A} - \mathbf{A}_h, v_h, \psi(t_{n-\frac{1}{2}})\right) + b\left(\mathbf{A}_h, v_h, P\bar{\psi}^n - \psi(t_{n-\frac{1}{2}})\right)\right| & \\ \leq \; C_{b,\epsilon}\left(R_3 + \|\bar{\theta}_\delta^n\|_1^2\right) + \epsilon\|v_h\|_0^2, & \qquad (7.3.1)\end{aligned}$$

where $R_3 = h^{2m} + k^4$.

Proof

An estimate for the term $\left|b\left(\mathbf{A}_h, v_h, \bar{\theta}_\delta^n\right)\right|$ can be derived similar to the estimate for the term $\left|b\left(\mathbf{A}_h, v_h, \theta_\delta^n\right)\right|$ given in Lemma 6.11. By replacing θ_δ^n with $\bar{\theta}_\delta^n$ it is easily seen that for any $\epsilon_2 > 0$ the following estimate holds

$$\left|b\left(\mathbf{A}_h, v_h, \bar{\theta}_\delta^n\right)\right| \leq \frac{C_2}{\epsilon_2}\left(h^{2m} + \|\bar{\theta}_\delta^n\|_1^2\right) + \epsilon_2\|v_h\|_0^2.$$

Using Lemma 2.4, Lemma 4.1.3 and the inverse inequality (6.3.2) one can estimate the term $b\left(\mathbf{A} - \mathbf{A}_h, v_h, \psi(t_{n-\frac{1}{2}})\right)$ as follows

$$\left|b\left(\mathbf{A} - \mathbf{A}_h, v_h, \psi(t_{n-\frac{1}{2}})\right)\right| \leq \|\psi(t_{n-\frac{1}{2}})\|_\infty\|\mathbf{A} - \mathbf{A}_h\|_0\|v_h\|_1 \leq \frac{C_1}{\epsilon_1}h^{2m} + \epsilon_1\|v_h\|_0^2,$$

for any $\epsilon_1 > 0$.

Finally, for sufficiently smooth ψ, one may use the triangle inequality, the Cauchy-Schwarz inequality and property 2.2.18 to get

$$\begin{aligned}
&\left|b\left(\mathbf{A}_h, v_h, P\bar{\psi}^n - \psi(t_{n-\frac{1}{2}})\right)\right| \\
&\leq \left|b\left(\mathbf{A}_h - \mathbf{A}, v_h, P\bar{\psi}^n - \psi(t_{n-\frac{1}{2}})\right)\right| + \left|b\left(\mathbf{A}, P\bar{\psi}^n - \psi(t_{n-\frac{1}{2}}), v_h\right)\right| \\
&\leq \|\mathbf{A}_h - \mathbf{A}\|_\infty \|v_h\|_1 \|P\bar{\psi}^n - \psi(t_{n-\frac{1}{2}})\|_0 + \left|b\left(\mathbf{A}, P\bar{\psi}^n - \psi(t_{n-\frac{1}{2}}), v_h\right)\right|.
\end{aligned}$$

Let us note that similar to the proof presented in Lemma 7.3 one can show that

$$\|P\bar{\psi}^n - \psi(t_{n-\frac{1}{2}})\|_1 \leq C\left(h^m + k^2\right) \tag{7.3.2}$$

for a sufficiently smooth weak solution ψ.

Further, using Lemma 4.2.9, the inverse inequality (6.3.2), (7.3.2) and (4.2.3) one may estimate $b\left(\mathbf{A}_h, v_h, P\bar{\psi}^n - \psi(t_{n-\frac{1}{2}}\right)$ as follows

$$\begin{aligned}
&\left|b\left(\mathbf{A}_h, v_h, P\bar{\psi}^n - \psi(t_{n-\frac{1}{2}})\right)\right| \\
&\leq \bar{C}_3 h^{m+1-d/2} h^{-1} \|v_h\|_0 \left(h^{m+1} + k^2\right) + \|\mathbf{A}\|_\infty \|P\bar{\psi}^n - \psi(t_{n-\frac{1}{2}})\|_1 \|v_h\|_0 \\
&\leq \bar{C}_3 h^{m-d/2}\left(h^{m+1} + k^2\right)\|v_h\|_0 + \tilde{C}_3\left(h^{m+1} + k^2\right)\|v_h\|_0.
\end{aligned}$$

Since $h^{m-d/2}h^{m+1} \leq h^m$ when $m+1 \geq d/2$ and $h^{m-d/2}k^2 \leq h^m$ when $k \leq h^{d/4}$ it follows that

$$\begin{aligned}
\left|b\left(\mathbf{A}_h, v_h, P\bar{\psi}^n - \psi(t_{n-\frac{1}{2}}\right)\right| &\leq \bar{C}_3 h^m \|v_h\|_0 + \tilde{C}_3\left(h^m + k^2\right)\|v_h\|_0 \\
&\leq \frac{C_3}{\epsilon_3}\left(h^{2m} + k^4\right) + \epsilon_3 \|v_h\|_0^2,
\end{aligned}$$

where $C_3 = \left(\bar{C}_3 + \tilde{C}_3\right)$.

Combining the above estimates together with the notation $C_{b,\epsilon} = \max\{\frac{C_1}{\epsilon_1}, \frac{C_2}{\epsilon_2}, \frac{C_3}{\epsilon_3}\}$, $\epsilon = \sum_{i=1}^{3} \epsilon_i$ and $R_3 = h^{2m} + k^4$ we have that

$$\begin{aligned}
&\left| b\left(\mathbf{A}_h, v_h, \bar{\theta}_\delta^n\right) + b\left(\mathbf{A} - \mathbf{A}_h, v_h, \psi(t_{n-\frac{1}{2}})\right) + b\left(\mathbf{A}_h, v_h, P\bar{\psi}^n - \psi(t_{n-\frac{1}{2}})\right) \right| \\
&\qquad \leq \; C_{b,\epsilon}\left(R_3 + \|\bar{\theta}_\delta^n\|_1^2\right) + \epsilon \|v_h\|_0^2,
\end{aligned}$$

which concludes the proof of Lemma 7.8. □

Similar to Lemma 7.6 we can prove the following result.

Lemma 7.9 *Let the hypotheses of Lemma 7.6 hold. Then for any $v_h \in V^h$ and for any $\epsilon > 0$ we obtain*

$$\left| \left(f_h^\delta(\bar{\Psi}_\delta^n) - f(\psi(t_{n-\frac{1}{2}})), v_h \right) \right| \leq C_{f,\epsilon}^\delta R_3 + \epsilon \|v_h\|_0^2, \tag{7.3.3}$$

where $R_3 = h^{2m} + k^4$.

Proof

Starting with the inequality derived in Lemma 7.6 one can estimate as follows

$$\begin{aligned}
&\left| \left(f_h^\delta(\bar{\Psi}_\delta^n) - f(\psi(t_{n-\frac{1}{2}})), v_h \right) \right| \\
&\leq \; \left(L^\delta \left[\|\bar{\theta}_\delta^n\|_0 + C_1 \left(h^{m+1} + k^2 \right) \right] + C_2 h^{m+1} \right) \|v_h\|_0 \\
&\leq \; \left[L^\delta \|\bar{\theta}_\delta^n\|_0 + L^\delta C_1 h^{m+1} + L^\delta C_1 k^2 + C_2 h^{m+1} \right] \|v_h\|_0 \\
&\leq \; \left[L^\delta \|\bar{\theta}_\delta^n\|_0 + \left(L^\delta C_1 + C_2 \right) h^{m+1} + L^\delta C_1 k^2 \right] \|v_h\|_0 \\
&\leq \; C_f^\delta \left(\|\bar{\theta}_\delta^n\|_0 + h^{m+1} + k^2 \right) \|v_h\|_0,
\end{aligned}$$

where $C_f^\delta = \max\{L^\delta, L^\delta C_1 + C_2\}$.

Using the definition of $\bar{\theta}_\delta^n$ and the optimal estimate (7.2.1) for $\|\theta_\delta^n\|_0$ it follows that

$$\|\bar{\theta}_\delta^n\|_0 = \left\| \frac{\theta_\delta^n + \theta_\delta^{n-1}}{2} \right\|_0 \leq \frac{1}{2}\|\theta_\delta^n\|_0 + \frac{1}{2}\|\theta_\delta^{n-1}\|_0 \leq C_\delta \left(h^{m+1} + k^2 \right).$$

As a result

$$\left|\left(f_h^\delta(\bar{\Psi}_\delta^n) - f(\psi(t_{n-\frac{1}{2}})), v_h\right)\right| \le C_f^\delta (C_\delta + 1)\left(h^{m+1} + k^2\right) \|v_h\|_0.$$

Using the notation for R_3 one has that for any $\epsilon > 0$ the following holds

$$\left|\left(f_h^\delta(\bar{\Psi}_\delta^n) - f(\psi(t_{n-\frac{1}{2}})), v_h\right)\right| \le C_{f,\epsilon}^\delta R_3 + \epsilon \|v_h\|_0^2,$$

where $C_{f,\epsilon}^\delta = \frac{C_f^\delta(C_\delta+1)}{\epsilon}$. This concludes the proof of Lemma 7.9. □

We proceed with one more preliminary result which can be proved similar to Lemma 6.14.

Lemma 7.10 *Let Δ_h be the discrete analog of the Laplacian operator defined in (6.3.14). Then*

$$\begin{aligned}
&\left(\theta_\delta^n - \theta_\delta^{n-1}, -\Delta_h \bar{\theta}_\delta^n\right) + ka\left(\bar{\theta}_\delta^n, -\Delta_h \bar{\theta}_\delta^n\right) \\
&\ge \frac{1}{2}\|\nabla \theta_\delta^n\|_0^2 + kC_a \|\Delta_h \bar{\theta}_\delta^n\|_0^2 - \frac{1}{2}\|\nabla \theta_\delta^{n-1}\|_0^2. \qquad (7.3.4)
\end{aligned}$$

Proof

Using the symmetry of the L^2 inner product, the definition of Δ_h and the definition of $\bar{\theta}_\delta^n$ one has

$$\begin{aligned}
\left(\theta_\delta^n - \theta_\delta^{n-1}, -\Delta_h \bar{\theta}_\delta^n\right) &= \left(-\Delta_h \bar{\theta}_\delta^n, \theta_\delta^n - \theta_\delta^{n-1}\right) = \left(\nabla \bar{\theta}_\delta^n, \nabla\theta_\delta^n - \nabla\theta_\delta^{n-1}\right) \\
&= \left(\frac{\nabla\theta_\delta^n + \nabla\theta_\delta^{n-1}}{2}, \nabla\theta_\delta^n - \nabla\theta_\delta^{n-1}\right) = \frac{1}{2}\|\nabla\theta_\delta^n\|_0^2 - \frac{1}{2}\|\nabla\theta_\delta^{n-1}\|_0^2. \qquad (7.3.5)
\end{aligned}$$

On the other hand the definition of the bilinear form $a(\cdot,\cdot)$, its symmetry and the definition of Δ_h imply that

$$a\left(\bar{\theta}_\delta^n, -\Delta_h \bar{\theta}_\delta^n\right) = C_a\left(\nabla\bar{\theta}_\delta^n, \nabla(-\Delta_h \bar{\theta}_\delta^n)\right) + \left(\bar{\theta}_\delta^n, -\Delta_h \bar{\theta}_\delta^n\right)$$

$$
\begin{aligned}
&= C_a\left(\triangle_h \bar{\theta}_\delta^n, \triangle_h \bar{\theta}_\delta^n\right)+\left(\bar{\theta}_\delta^n,-\triangle_h \bar{\theta}_\delta^n\right) \\
&= C_a\|\triangle_h \bar{\theta}_\delta^n\|_0^2+\left(\nabla \bar{\theta}_\delta^n, \nabla \bar{\theta}_\delta^n\right) \\
&= C_a\|\triangle_h \bar{\theta}_\delta^n\|_0^2+\|\nabla \bar{\theta}_\delta^n\|_0^2 \\
&\geq C_a\|\triangle_h \bar{\theta}_\delta^n\|_0^2 .
\end{aligned}
$$

Hence

$$
a\left(\bar{\theta}_\delta^n,-\triangle_h \bar{\theta}_\delta^n\right) \geq C_a\|\triangle_h \bar{\theta}_\delta^n\|_0^2. \tag{7.3.6}
$$

Combining (7.3.5) and (7.3.6) the desired lower bound easily follows

$$
\begin{aligned}
&\left(\theta_\delta^n-\theta_\delta^{n-1},-\triangle_h \bar{\theta}_\delta^n\right)+k a\left(\bar{\theta}_\delta^n,-\triangle_h \bar{\theta}_\delta^n\right) \\
\geq\; & \frac{1}{2}\|\nabla \theta_\delta^n\|_0^2+k C_a\|\triangle_h \bar{\theta}_\delta^n\|_0^2-\frac{1}{2}\|\nabla \theta_\delta^{n-1}\|_0^2. \quad \square
\end{aligned}
$$

The lower bound established in Lemma 7.10 was the last preliminary result needed for the derivation of the optimal $\mathcal{H}^1$ error estimates for the auxiliary Crank-Nicolson-Galerkin problem (5.1.4).

Theorem 7.2 *Let* $\mathbf{A}$ *and* $\mathbf{A}_h$ *denote the solutions of the weak (2.2.1) and approximate (3.3.1) problems, respectively. For* $1 \leq n \leq N$ *let* $\psi(t_n)$ *and* Ψ_δ^n *denote the solutions of the weak (2.2.20) and the auxiliary problems (5.1.3) at the n-th time level. Let* m *be a positive integer satisfying* $m+1>d/2$. *We assume that* $\mathbf{A} \in \mathbf{H}_n^1(\Omega) \cap \mathbf{H}^{m+1}(\Omega)$ *and* $\psi \in \mathcal{V}$, $\psi(\cdot, \mathbf{x}) \in \mathcal{H}^{m+1}(\Omega)$, $\|\psi_{ttt}\|_0 \leq C$ *and* $\|\triangle \psi_{tt}\|_0 \leq C$. *If the initial condition satisfies*

$$
\|e^0\|_1 \leq C h^m, \tag{7.3.7}
$$

then for sufficiently small h *and* k *with* $k=\mathbf{o}\left(h^{d/4}\right)$ *we have the following optimal* $\mathcal{H}^1$ *error estimate*

$$
\|e_\delta^n\|_1 \leq C_\delta\left(h^m+k^2\right), \tag{7.3.8}
$$

where C is a generic constant independent of h and k.

Proof

Let us recall equation (7.1.11)

$$\begin{aligned}\left(\frac{\tilde{d}}{dt}\theta_\delta^n, v_h\right) &+ a\left(\bar{\theta}_\delta^n, v_h\right) = -\left(\omega^n, v_h\right) + \left(f_h^\delta(\bar{\Psi}_\delta^n) - f(\psi(t_{n-\frac{1}{2}})), v_h\right) \\ &+ b\left(\mathbf{A}_h, v_h, \bar{\theta}_\delta^n\right) + b\left(\mathbf{A}_h, v_h, P\bar{\psi}^n - \psi(t_{n-\frac{1}{2}})\right) \\ &- b\left(\mathbf{A} - \mathbf{A}_h, v_h, \psi(t_{n-\frac{1}{2}})\right) \quad \forall\, v_h \in V^h.\end{aligned} \tag{7.3.9}$$

Using the definition of $\frac{\tilde{d}}{dt}$ and multiplying through the equation (7.3.9) by the time step $k > 0$ it follows that for all $v_h \in V^h$ we have the inequality

$$\begin{aligned}&\left(\theta_\delta^n - \theta_\delta^{n-1}, v_h\right) + ka\left(\bar{\theta}_\delta^n, v_h\right) \le k\left|\left(\omega^n, v_h\right)\right| + k\left|\left(f_h^\delta(\bar{\Psi}_\delta^n) - f(\psi(t_{n-\frac{1}{2}})), v_h\right)\right| \\ &\quad + \left|b\left(\mathbf{A}_h, v_h, \bar{\theta}_\delta^n\right) + b\left(\mathbf{A}_h, v_h, P\bar{\psi}^n - \psi(t_{n-\frac{1}{2}})\right) + b\left(\mathbf{A} - \mathbf{A}_h, v_h, \psi(t_{n-\frac{1}{2}})\right)\right|.\end{aligned} \tag{7.3.10}$$

Recall that $\triangle_h : V^h \longrightarrow V^h$ and that V^h is a linear space. Then we can choose the test function in (7.3.10) as follows: $v_h = -\triangle_h \bar{\theta}_\delta^n$. With this choice of v_h we have the following

$$\begin{aligned}&\left(\theta_\delta^n - \theta_\delta^{n-1}, -\triangle_h \bar{\theta}_\delta^n\right) + ka\left(\bar{\theta}_\delta^n, -\triangle_h \bar{\theta}_\delta^n\right) \le k\left|\left(\omega^n, -\triangle_h \bar{\theta}_\delta^n\right)\right| \\ &+ \quad k\left|\left(f_h^\delta(\bar{\Psi}_\delta^n) - f(\psi(t_{n-\frac{1}{2}})), -\triangle_h \bar{\theta}_\delta^n\right)\right| \\ &+ \quad \left|b\left(\mathbf{A}_h, -\triangle_h \bar{\theta}_\delta^n, \bar{\theta}_\delta^n\right) + b\left(\mathbf{A}_h, -\triangle_h \bar{\theta}_\delta^n, P\bar{\psi}^n - \psi(t_{n-\frac{1}{2}})\right)\right. \\ &+ \quad \left. b\left(\mathbf{A} - \mathbf{A}_h, -\triangle_h \bar{\theta}_\delta^n, \psi(t_{n-\frac{1}{2}})\right)\right|.\end{aligned}$$

Using the lower bound (7.3.4) derived in Lemma 7.10, the Cauchy-Schwarz inequality, Lemma 7.9 and Lemma 7.8 we obtain

$$\begin{aligned}&\frac{1}{2}\|\nabla\theta_\delta^n\|_0^2 + kC_a\|\triangle_h \bar{\theta}_\delta^n\|_0^2 - \frac{1}{2}\|\nabla\theta_\delta^{n-1}\|_0^2 \le k\|\omega^n\|_0\|\triangle_h \bar{\theta}_\delta^n\|_0 \\ &+ \quad k\left(C_{f,\epsilon}^\delta R_3 + \epsilon\|\triangle_h \bar{\theta}_\delta^n\|_0^2\right) + k\left(C_{b,\epsilon}\left(R_3 + \|\bar{\theta}_\delta^n\|_1^2\right) + \epsilon\|\triangle_h \bar{\theta}_\delta^n\|_0^2\right).\end{aligned}$$

Note that (7.1.15) implies

$$\begin{aligned} k\|\omega^n\|_0\| \triangle_h \bar{\theta}^n_\delta\|_0 &\le \frac{k}{\epsilon}\|\omega^n\|_0^2 + k\epsilon\| \triangle_h \bar{\theta}^n_\delta\|_0^2 \\ &\le \frac{k}{\epsilon}CR_3 + k\epsilon\| \triangle_h \bar{\theta}^n_\delta\|_0^2. \end{aligned}$$

Using the definitions of $\|\cdot\|_1$, $\bar{\theta}^n_\delta$, the notation (7.2.3) for R_4, and the optimal estimate $\|\theta^n_\delta\|_0 \le C_\delta R_4$ we have that

$$\begin{aligned} \|\bar{\theta}^n_\delta\|_1^2 &= \|\nabla\bar{\theta}^n_\delta\|_0^2 + \|\bar{\theta}^n_\delta\|_0^2 \\ &\le \frac{1}{2}\|\nabla\theta^n_\delta\|_0^2 + \frac{1}{2}\|\nabla\theta^{n-1}_\delta\|_0^2 + \frac{C_\delta}{2}R_4, \end{aligned}$$

and

$$\begin{aligned} &\frac{1}{2}\|\nabla\theta^n_\delta\|_0^2 + kC_a\| \triangle_h \bar{\theta}^n_\delta\|_0^2 \le \frac{1}{2}\|\nabla\theta^{n-1}_\delta\|_0^2 \\ &+ \ \frac{k}{\epsilon}CR_3 + k\epsilon\| \triangle_h \bar{\theta}^n_\delta\|_0^2 + k\left(C^\delta_{f,\epsilon}R_3 + \epsilon\| \triangle_h \bar{\theta}^n_\delta\|_0^2\right) \\ &+ \ kC_{b,\epsilon}\left(R_3 + \frac{1}{2}\|\nabla\theta^n_\delta\|_0^2 + \frac{1}{2}\|\nabla\theta^{n-1}_\delta\|_0^2 + \frac{C_\delta}{2}R_4\right) + k\epsilon\| \triangle_h \bar{\theta}^n_\delta\|_0^2. \end{aligned}$$

Collecting the like terms above we obtain

$$\left(\frac{1}{2} - \frac{k}{2}C_{b,\epsilon}\right)\|\nabla\theta^n_\delta\|_0^2 + k\left(C_a - \epsilon\right)\| \triangle_h \bar{\theta}^n_\delta\|_0^2 \le \left(\frac{1}{2} + \frac{k}{2}C_{b,\epsilon}\right)\|\nabla\theta^{n-1}_\delta\|_0^2 + kC_{b,\epsilon}R_3.$$

Let us choose $\epsilon = \frac{C_a}{2} > 0$. Dropping the nonnegative term $k\frac{C_2}{2}\| \triangle_h \bar{\theta}^n_\delta\|_0^2$ and multiplying by two one has

$$\left(1 - k\bar{C}\right)\|\nabla\theta^n_\delta\|_0^2 \le \left(1 + k\bar{C}\right)\|\nabla\theta^{n-1}_\delta\|_0^2 + kC^\delta_2 R_3,$$

where $\bar{C} = \frac{C_{b,\epsilon}}{2}$ and $C^\delta_2 = 2\tilde{C}^\delta_\epsilon$.

Proceeding similar to the proof of Lemma 7.7 and using the initial condition (7.3.7) it follows that for sufficiently small k we have the optimal estimate

$$\|\nabla\theta^n_\delta\|_0 \le \tilde{C}_\delta\left(h^m + k^2\right). \tag{7.3.11}$$

The optimal estimate for the $\mathcal{H}^1$ seminorm of θ_δ^n together with the optimal $\mathcal{L}^2$ estimate implies that

$$\|\theta_\delta^n\|_1 \leq C_\delta \left(h^m + k^2\right). \tag{7.3.12}$$

Finally, combining the estimate for $\|\theta_\delta^n\|_1$ with the estimate for $\|\rho^n\|_1$ we obtain

$$\|e_\delta^n\|_1 \leq C_\delta(h^m + k^2),$$

which concludes the proof of Theorem 7.2. $\square$

Chapter 8

Existence, Uniqueness and Optimal Error Estimates for the Fully Discrete Problems

The goal of this chapter is to establish existence and uniqueness results and to derive optimal error estimates for the fully-discrete problems (3.3.5) and (3.3.6). To accomplish this we shall use the approach outlined in [5]. Recall that in Chapter 5 as a preliminary step in the derivation of the estimates for the fully discrete problems we introduced the two auxiliary problems given by (5.1.3) and (5.1.4). These auxiliary problems differ from the original fully-discrete problems only by the fact that the nonlinear function $f_h(\cdot)$ is replaced by a suitably defined globally Lipschitz continuous function $f_h^\delta(\cdot)$ which agrees with $f_h(\cdot)$ on M^δ. Also in Chapter 5 we have obtained existence and uniqueness for the solutions Ψ_δ^n of the auxiliary problems (5.1.3) and (5.1.4) and in Chapters 6-7 we have derived optimal estimates for the errors $e_\delta^n = \psi(t_n) - \Psi_\delta^n$ in both $\mathcal{L}^2$ and $\mathcal{H}^1$ norms. In this chapter we shall combine all these results in order to prove the optimal error estimates for Ψ^n; that is, we shall use results established for Ψ_δ^n in order to prove the corresponding results for Ψ^n. As usual, throughout this chapter C will denote a generic constant independent of the discretization parameters h and k. We also recall that $\Omega \subset \mathbb{R}^d$ where $d = 2,\ 3$.

8.1 Existence, Uniqueness and Optimal $\mathcal{L}^2$ and $\mathcal{H}^1$ Error Estimates for the Backward-Euler-Galerkin Problem

In this section we prove a global existence and uniqueness result and derive optimal $\mathcal{L}^2$ and $\mathcal{H}^1$ error estimates for the Backward-Euler-Galerkin problem (3.3.5). They are based on the corresponding results for the auxiliary problem (5.1.3) established in Chapter 5 and Chapter 7.

We begin by recalling the weak problem for the order parameter ψ given in (2.2.20) and the Backward-Euler-Galerkin problem for Ψ^n given in (3.3.5). These problems are as follows.

Seek $\psi \in V$ such that

$$\begin{aligned} (\psi_t, v) + a(\psi, v) - b(\mathbf{A}, v, \psi) &= (f(\psi), v) \quad \text{for all} \quad v \in V, t \geq 0 \, , \\ \psi(0) &= \psi^0. \end{aligned}$$

Seek $\Psi^n \in V^h$ such that

$$\begin{aligned} (\frac{\tilde{d}\Psi^n}{dt}, v_h) + a(\Psi^n, v_h) - b(\mathbf{A}_h, v_h, \Psi^n) &= (f_h(\Psi^n), v_h) \;\; \forall \, v_h \in V^h \;\; 1 \leq n \leq N \, , \\ \Psi^0 &= \tilde{\psi}^0. \end{aligned}$$

Definition 8.1 *In analogy with the definition of e_δ^n we define the* **error** *in the fully discrete problem (3.3.5) at the n-th time level by*

$$e_{be}^n = \Psi^n - \psi(t_n), \tag{8.1.1}$$

where Ψ^n solves (3.3.5).

In the next theorem we prove existence and uniqueness results and derive optimal $\mathcal{L}^2$ and $\mathcal{H}^1$ error estimates for the Backward-Euler-Galerkin problem (3.3.5) using the existence and uniqueness results for Ψ_δ^n presented in Theorems 5.1-5.2, and the optimal error estimates (6.2.8)-(6.3.19) established in Theorems 6.1-6.2. We note that the properties of the finite element space V^h given in (3.2.10) and (3.2.11) are used in our proof.

Theorem 8.1 *Let ψ denote the solution of the weak problem (2.2.20) and for $1 \leq n \leq N$ let Ψ^n denote the solution of the fully-discrete problem (3.3.5). For a positive integer m with $m \geq d/2$ we assume that $\psi \in \mathcal{V}$ and that $\psi(\cdot, \mathbf{x}) \in \mathcal{H}^{m+1}(\Omega)$. In addition, we assume that $\|\psi_{tt}\|_0 \leq C$ and $\mathbf{A}$ denotes the solution of the weak problem (2.2.1). If $\mathbf{A} \in \mathbf{H}_n^1(\Omega) \cap \mathbf{H}^{m+1}(\Omega)$, and if the initial condition e_{be}^0 satisfies*

$$\|e_{be}^0\|_j \leq Ch^{m+1-j} \quad , j = 0, 1, \tag{8.1.2}$$

then for sufficiently small h and k with $k = \mathbf{o}\left(h^{\frac{d}{2}}\right)$, there exists a unique solution Ψ^n of (3.3.5). Moreover, we have the optimal error estimate

$$\|e_{be}^n\|_j \leq C(h^{m+1-j} + k) \quad , j = 0, 1 \; , \tag{8.1.3}$$

where C is a generic constant independent of h and k.

Proof

Let us recall that for a fixed parameter $\delta > 0$ we have defined M^δ, see (5.1.1), as an appropriate δ-neighborhood of the weak solution ψ. Theorem 5.1 and Theorem 5.2 guarantee existence of the unique solution Ψ_δ^n to the auxiliary, fully discrete problem (5.1.3). In Theorem 6.1 we have established the following optimal error estimate, see (6.2.1)

$$\|\theta_\delta^n\|_0 = \|\Psi_\delta^n - P\psi(t_n)\|_0 \leq C_\delta \left(h^{m+1} + k\right).$$

The idea here is to use this optimal $\mathcal{L}^2$ estimate for $\theta_\delta^n \in V^h$ and the property (3.2.10) of V^h in order to show that the auxiliary function Ψ_δ^n is "close" to the weak solution $\psi(t_n)$ with respect to the metric used in the definition of M^δ; i.e. $\Psi_\delta^n \in M^\delta$ for $n \in [0, N]$. Indeed, we have

$$\|e_\delta^n\|_\infty = \|\theta_\delta^n + \rho^n\|_\infty \leq \|\theta_\delta^n\|_\infty + \|\rho^n\|_\infty. \tag{8.1.4}$$

Let us recall that in the proof of Lemma 6.6 we have used the approximation property of V^h given in (3.2.11) to show that

$$\|\rho^n\|_\infty \leq Ch^{m+1-d/2} + \left(Ch^{-d/2}\|\psi(t_n) - v_h\|_0 + \|\psi(t_n) - v_h\|_\infty\right) \leq \frac{\delta}{4}. \tag{8.1.5}$$

Combining (8.1.4) with (8.1.5) we obtain

$$\|e_\delta^n\|_\infty \leq \|\theta_\delta^n\|_\infty + \frac{\delta}{4}.$$

Using the inverse inequality (3.2.10) it follows that

$$\|e_\delta^n\|_\infty \leq Ch^{-d/2}\|\theta_\delta^n\|_0 + \frac{\delta}{4}.$$

The optimal estimate for $\|\theta_\delta^n\|_0$ given in (6.2.1) implies

$$\|e_\delta^n\|_\infty \leq C_\delta Ch^{-d/2}\left(h^{m+1} + k\right) + \frac{\delta}{4}.$$

Thus, given $n \in [0, N]$ it follows that for sufficiently small h and k with $k = \mathbf{o}\left(h^{\frac{d}{2}}\right)$ we have

$$\|e_\delta^n\|_\infty \leq \frac{\delta}{2}.$$

To summarize, we have established that under the assumptions of Theorem 8.1 it follows that

$$\Psi_\delta^n \in M^\delta \text{ for } 0 \leq n \leq N. \tag{8.1.6}$$

Next, using the local Lipschitz property of $f_h(\cdot)$ and the inclusion (8.1.6) we will show that

$$\Psi_\delta^n = \Psi^n \quad \text{for} \quad 0 \leq n \leq N. \tag{8.1.7}$$

Consider the two fully discrete problems (3.3.5) and (5.1.3) and let n=1. Then by the bound on the initial conditions (8.1.2) we have

$$\Psi_\delta^0 = \Psi^0. \tag{8.1.8}$$

Using (8.1.6) it follows that

$$f_h^\delta(\Psi_\delta^1) = f_h(\Psi_\delta^1). \tag{8.1.9}$$

As a result, the function Ψ_δ^1 also satisfies equation (3.3.5). By the local uniqueness of this problem and (8.1.6) we must have that $\Psi_\delta^1 = \Psi^1$ and $\Psi^1 \in M^\delta$.

Next we proceed to establish (8.1.7) for $n = 2, 3, ..., N$ by induction. Assume that (8.1.7) holds for $n = 2, 3, ..., k$, where $k \leq N - 1$. We will show that

$$\Psi_\delta^{k+1} = \Psi^{k+1}. \tag{8.1.10}$$

Indeed, since $\Psi_\delta^{k+1} \in M^\delta$ it follows that $f_h^\delta(\Psi_\delta^{k+1}) = f_h(\Psi_\delta^{k+1})$. Moreover, since by assumption $\Psi_\delta^k = \Psi^k$ and the fact that the problem (3.3.5) has a locally unique solution Ψ^{k+1} we must have that (8.1.10) holds. This concludes the proof of (8.1.7).

Now, Theorem 5.1 and Theorem 5.2 guarantee that there exists a unique solution Ψ^n of the fully discrete problem (3.3.5). On the other hand, Theorem 6.1 gives

$$\|e_{be}^n\|_0 \leq C\left(h^{m+1} + k\right) , \tag{8.1.11}$$

and Theorem 6.2 gives

$$\|e_{be}^n\|_1 \leq C\left(h^m + k\right). \tag{8.1.12}$$

Combining (8.1.11) and (8.1.12) the proof of Theorem 8.1 is completed $\Box$.

8.2 Existence, Uniqueness and Optimal $\mathcal{L}^2$ and $\mathcal{H}^1$ Error Estimates for the Crank-Nicolson-Galerkin Problem

In this section we prove a global existence and uniqueness result and derive optimal $\mathcal{L}^2$ and $\mathcal{H}^1$ error estimates for the Crank-Nicolson-Galerkin problem (3.3.6). The derivation is analogous to the one presented in Theorem 8.1. We note that due to the optimal error estimate for θ_δ^n, see (7.2.7), established in Theorem 7.1 the condition between the time step k and the spatial discretization parameter h can be relaxed to $k = \mathbf{o}\left(h^{d/4}\right)$. For completeness we shall present the proof.

Let us recall that the Crank-Nicolson-Galerkin problem is defined by

Seek $\Psi^n \in V^h$ such that

$$(\frac{\tilde{d}\Psi^n}{dt}, v_h) + a(\bar{\Psi}^n, v_h) + b(\mathbf{A}_h, \bar{\Psi}^n, v_h) = (f_h(\bar{\Psi}^n), v_h) \, \forall \, v_h \in V^h \ , \ 1 \leq n \leq N \ ,$$

$$\Psi^0 = \tilde{\psi}^0.$$

Definition 8.2 *We define the* **error** *in the fully discrete problem (3.3.6) at the n-th time level by*

$$e_{cn}^n = \Psi^n - \psi(t_n), \tag{8.2.1}$$

where Ψ^n solves (3.3.6).

In analogy with the proof of Theorem 8.1 we use the existence and uniqueness results proved in Theorem 5.3 and Theorem 5.4, and the optimal error estimates (7.2.7), (7.3.8) given in Theorem 7.1 and Theorem 7.2 in order to establish the desired results for the fully-discrete solution Ψ^n.

Theorem 8.2 *Let ψ denote the solution of the weak problem (2.2.20) and for $1 \leq n \leq N$ let Ψ^n denote the solution of the fully-discrete problem (3.3.5). For a positive integer m*

with $m \geq d/2$ we assume that $\psi \in \mathcal{V}$ with $\psi(\cdot, \mathbf{x}) \in \mathcal{H}^{m+1}(\Omega)$. In addition, we assume that $\|\psi_{ttt}\|_0 \leq C$ and $\| \triangle \psi_{tt}\|_0 \leq C$. If $\mathbf{A}$ denotes the solution of the weak problem (2.2.1) and if $\mathbf{A} \in \mathbf{H}_n^1(\Omega) \cap \mathbf{H}^{m+1}(\Omega)$, then for sufficiently small h and k satisfying $k = \mathbf{o}\left(h^{d/4}\right)$, there exists unique solution Ψ^n of the fully discrete problem (3.3.6). Moreover, we have the optimal error estimates

$$\|e_{cn}^n\|_j \leq C(h^{m+1-j} + k^2) \ , \ j = 0, 1. \tag{8.2.2}$$

Proof

We fix the parameter $\delta > 0$ in M^δ and then proceed as in Theorem 8.1 to find that

$$\begin{aligned} \|e_\delta^n\|_\infty &\leq \|\theta_\delta^n\|_\infty + \|\rho^n\|_\infty \leq Ch^{-d/2}\|\theta_\delta^n\|_0 + \frac{\delta}{4} \\ &\leq CC_\delta\left(h^{m+1} + k^2\right) + \frac{\delta}{4}. \end{aligned}$$

Hence for $n \in [0, N]$ and for h and k sufficiently small one has

$$\|e_\delta^n\|_\infty \leq \frac{\delta}{2} \ ,$$

provided that $\psi \in \mathcal{H}^{m+1}$, $m + 1 > d/2$ and $k = \mathbf{o}\left(h^{\frac{d}{4}}\right)$.

Following [5], we note that for sufficiently small k the following bound is valid

$$\left\|\psi(t_{n-1/2}) - \bar{\psi}^n\right\|_\infty < \frac{\delta}{2}, \quad \text{for} \quad 0 \leq n \leq N - 1. \tag{8.2.3}$$

Thus (8.2.3) implies that

$$\bar{\Psi}_\delta^n(x) \in M^\delta, \quad \text{for} \quad x \in \Omega, \quad 0 \leq n \leq N - 1. \tag{8.2.4}$$

In order to show that the solution Ψ_δ^n of the auxiliary problem (5.1.4) satisfies

$$\Psi_\delta^n = \Psi^n, \quad \text{for} \quad 0 \leq n \leq N, \tag{8.2.5}$$

where Ψ^n is the solution of the fully discrete Crank-Nicolson-Galerkin problem (3.3.6) we can use the same argument as in the proof of (8.1). Once (8.2.5) is established, one can apply Theorem 5.3 and Theorem 5.4 to prove that the fully discrete problem (3.3.6) has a unique solution Ψ^n. On the other hand, (8.2.5) and Theorem 7.1 imply that

$$\|e_{cn}^n\|_0 \leq C\left(h^{m+1}+k^2\right) , \tag{8.2.6}$$

and from Theorem 7.2 it follows that

$$\|e_{cn}^n\|_1 \leq C\left(h^{m}+k^2\right) . \tag{8.2.7}$$

Combining (8.2.6) and (8.2.7) the proof of Theorem 8.2 is completed $\square$.

Chapter 9

Numerical Results

In this chapter we discuss several numerical schemes used for the approximation of the High kappa model. We present computational results which are in a good agreement with the theoretical predictions and some well-known experimental observations. In particular, we show that for sufficiently large values of the Ginzburg-Landau parameter κ, the steady states of the model system, computed using the High kappa model, are virtually identical with the results computed using the full TDG-L equations. Such numerical results confirm the theoretical predictions made in [37]. We also illustrate numerically the optimal rates of convergence in both h and k for the $\mathcal{L}^2$ and $\mathcal{H}^1$ norms of the error in the approximate solution generated using the High kappa model.

Finally, our numerical approximations illustrate some well known experimentally observed properties of high T_c superconductors, such as the appearance of vortices in type II materials, the effect of increasing the applied magnetic field, the effect of applying a constant current and the effect of increasing the applied current.

The material is organized in four sections. The first section begins with a list of numerical methods used for approximations of the TDG-L equations. Then we discuss some implementation details which are common for both the full TDG-L equations and the High kappa model, such as the spatial and time discretizations, initial conditions, methods for linearizing the system for the order parameter, and some typical samples and meshes.

The second section contains numerical results obtained from the High kappa model with no applied current. In this case, time evolution of the system leads to a steady-state of the superconducting sample. Several issues, which are important for the numerical simulations, such as:

1 the accuracy of the numerical approximations using the High kappa model compared with the results from the full TDG-L model,

2 the need for sufficient grid resolution, depending on the size of the superconducting sample and the applied field $\mathbf{H}$,

3 problems concerning local minimizers of the Gibbs free energy,

4 the effect of increasing the applied magnetic field,

and

5 the effect of increasing the sample size

are addressed in this section.

In the third section we present and discuss results concerning numerical estimates for the $\mathcal{L}^2$ and $\mathcal{H}^1$ rates of convergence in both space and time.

In the fourth section we present numerical approximations based on the High kappa model in the case of an applied constant current and show that computer simulations obtained with a finite element code based on the High kappa model agree with theoretical and experimental results. In particular, we demonstrate that depending on the magnitude of the applied constant current, vortices move at right angles to the current flow or superconductivity is lost if a strong current is applied.

9.1 Introduction

Let us recall from Chapter 1 that superconductors are divided in two classes which we call type I and type II, respectively. As we have already discussed, type II materials are of practical interest mainly due to the presence of mixed states which allow the material to maintain superconductivity under larger applied magnetic fields and currents than type I materials. In addition, all known high-T_c superconductors, including the recently discovered cuprate oxides, are of type II.

There have been many attempts to formulate G-L type models which adequately describe type II superconducting phenomena. The inability to perform simulations for typical material samples of type II superconductors have led to extensive studies of the periodic G-L type models. Such models have been addressed in [2], [13], [38],[53], [56], [58], [63] and [79]. In the past few years several initial boundary-value models have been proposed. Based on different modifications of the G-L model, they were used to approximate the solutions of the steady-state and the time-dependent G-L equations, see, e.g., [17], [18], [19], [32], [33], [34], [35] and [37]. In this work we present a two-dimensional boundary value model valid in the high κ, high field regime.

Numerical solution of the full G-L equations, especially for the simulation of vortices, has been successful only in the recent years. Among the different numerical methods used for approximations of the G-L model are Monte Carlo methods, relaxation, optimization and finite elements. For more details one may reference, e.g., [4], [17], [18], [19], [31], [32], [34], [36], [37] and [42].

An attractive feature of Monte Carlo type methods is that they carry good assurance for finding the global minimizer of the energy functional. Other approaches often yield local critical points which may not be the physically meaningful global minimizer. The relaxation method is simple in theory, but time consuming due to the small time steps that are required to avoid instability of the numerical scheme. Among the advantages of the finite element method are its applicability to various geometries and the possibility for high-order refinements.

The objective of our computational experiments is to study the vortex dynamics in type II superconductors under constant applied field and current. This is accomplished using a two dimensional finite element code based on the High kappa model presented in Chapter 2. We recall that in this model the leading order time independent linear system for the magnetic potential $\mathbf{A}$, see (2.1.33)-(2.1.35), decouples from the leading order time dependent nonlinear system for the order parameter ψ, see (2.1.39)-(2.1.41). As a result, one may first solve the system for $\mathbf{A}$ and then substitute the solution into the system for ψ. This is a valuable computational property of the High kappa model since it simplifies significantly the numerical experiments both in terms of speed and storage requirements.

All results presented in this work were obtained on an Alpha 2100 4/275 workstation. These results include simulations of square superconducting samples with sides equal to 10ξ, 20ξ and 30ξ, where ξ is the coherence length. Spatial discretization is by piecewise biquadratic elements on a uniform grid. In addition, we use piecewise linear finite elements in one of our experiments to approximate the spatial rates of convergence. All numerical results in this chapter are obtained using a fixed value $\xi = 0.1l$ for the coherence length, where l is the length scale used in the nondimensionalization of the equations. We often refer to a square sample size with sides equal to 10ξ, 20ξ and 30ξ, as a 1x1, 2x2, 3x3 sample. To discretize the spatial variable we use uniform meshes having a given number of grid lines in x and y directions. For example, a 13x13 mesh means that there are 13 grid lines in each coordinate direction. For the time discretization of the system for the order parameter ψ, we have developed two different codes which implement the Backward-Euler-Galerkin and the Crank-Nicolson-Galerkin schemes given in (3.3.5) and (3.3.6).

We recall that the approximation problem for $\mathbf{A}_h$, see (3.3.1), represents a linear system of algebraic equations with a symmetric and positive definite banded coefficient matrix. This system may be solved using banded Cholesky factorization. The full discretization of the nonlinear IBVP for the order parameter ψ results in a nonlinear algebraic system for Ψ^n, see (3.3.5) and (3.3.6). This nonlinear system is solved using Newton's method. As a result, at each iteration one has to solve a linear system of algebraic equations which is symmetric and positive definite, if there is no applied current. However, in the applied constant current case the linearized system has a positive definite, but nonsymmetric coefficient matrix. To solve this system we use banded LU decomposition. In order to detect that a steady-state configuration has been reached we use the following criteria. The number of Newton iterations has to be less than or equal to a prescribed upper bound ITOP for N consecutive iterations. In particular we have used the combination ITOP=1 and N=4.

In all experiments the initial conditions correspond to a perfect superconducting sample. Numerical results are visualized using the contour plots of the level curves of the magnitude of the order parameter at a fixed moment in time. The figures representing the time evolution of the order parameter should be read from left to right and top to bottom. All graphics were created on a Macintosh 8100/100 using Mathematica. For 1x1 and 2x2 samples we typically plot level curves of the magnitude of the order parameter with values up to 0.5.

9.2 Steady-State Numerical Results

We start with a brief discussion of some properties of type II superconductors, introduced earlier, which will be illustrated by the numerical results presented in this section.

In the present work we are concerned with modeling type II superconductors which exhibit several experimentally observed properties. One such property with important practical consequences is that when the applied field surrounding the superconductor is increased but remains below the critical value, vortices begin to form. As mentioned earlier, the order parameter ψ vanishes at the center of each vortex. When the applied field varies the distance between vortices changes and results in a change in the vortex density. In particular, as $\mathbf{H}$ increases vortices become more and more densely packed.

We recall that the main postulate in the G-L theory is that the Gibbs free energy of the sample is minimized at the superconducting state. Based on the G-L theory, Abrikosov [2] predicted that in order to minimize the energy of the system, vortices will form a regular triangular lattice pattern Today it is known that the most favorable arrangement of the vortices corresponds to a hexagonal lattice pattern.

In our steady-state numerical simulations, we start with a pure superconducting state and apply a constant (in space and time) magnetic field $\mathbf{H}$ directed perpendicular to the cross-section of the superconducting sample. As a result, vortices appear and time evolution leads to a steady-state in which the vortex configuration corresponds to the global minimum of the Gibbs free energy.

In Figures 9.1-9.6 we compare numerical results obtained using the full TDG-L code for a fixed large value of κ with results from the High kappa model code; no current is applied. In both cases we use the Backward-Euler-Galerkin formulation given in (3.3.5) so

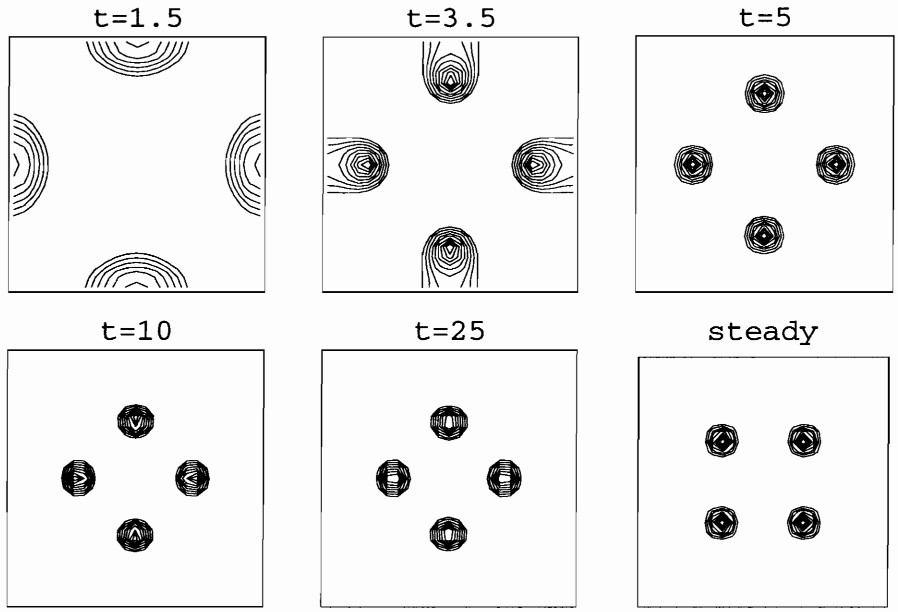

Figure 9.1: Time evolution for a 1x1 model system using the full TDG-L model with κ=30 and $H = 0.5\kappa$; Backward-Euler-Galerkin scheme.

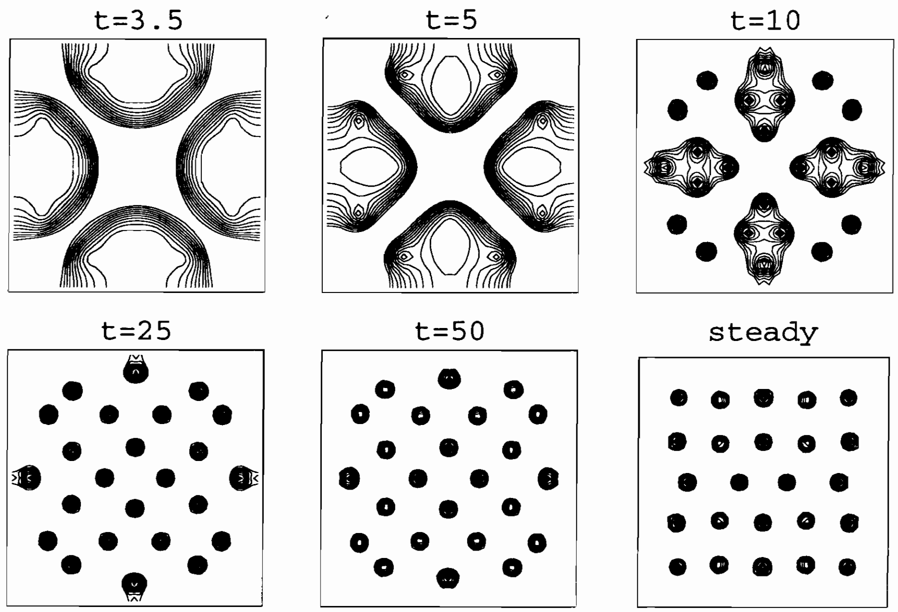

Figure 9.2: Time evolution for a 2x2 model system using the full TDG-L model with κ=30 and $H = 0.5\kappa$; Backward-Euler-Galerkin scheme.

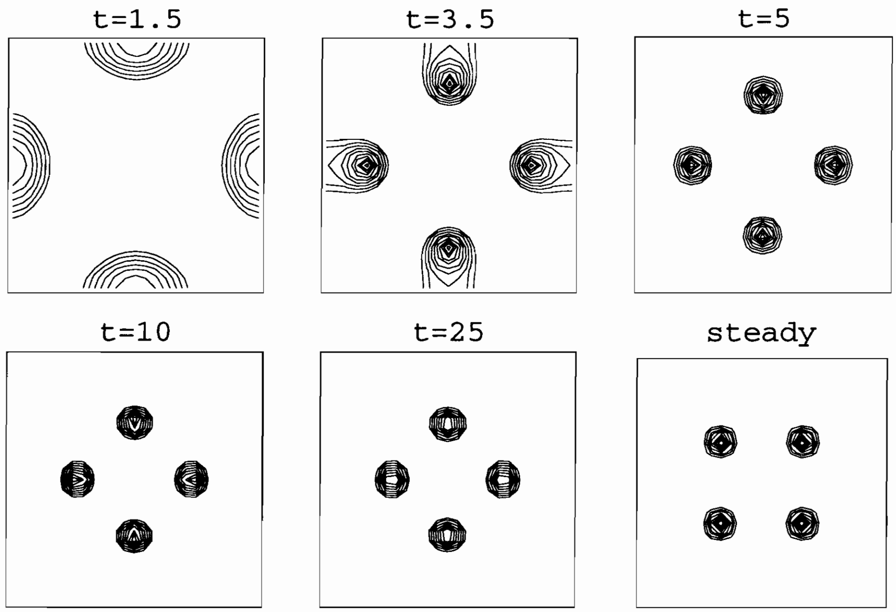

Figure 9.3: Time evolution for a 1x1 model system using the High kappa model with $H_0 = 0.5$; Backward-Euler-Galerkin scheme.

that results can be compared at the same moments in time. In Figures 9.1-9.2 we present the time evolution for the magnitude of the order parameter $|\psi(t, \mathbf{x})|$ obtained using the full TDG-L equations for a fixed magnetic field $\mathbf{H}$ and a fixed value of the G-L parameter κ. In particular, we use $H = 0.5\kappa$ and $\kappa = 30$. Figures 9.1-9.2 correspond to 1x1 and 2x2 samples, respectively. To obtain these results the systems for $\mathbf{A}$ and ψ have to be solved simultaneously because in the full TDG-L model they are coupled.

In Figures 9.3-9.4 we present the time evolution of $|\psi(t, \mathbf{x})|$ obtained using the High kappa model code with $H_0 = 0.5$ and the Backward-Euler scheme. Figures 9.3-9.4 correspond to 1x1 and 2x2 samples, respectively. Biquadratic finite elements are used in all calculations presented in Figures 9.1-9.4.

The results presented in Figures 9.1-9.4 demonstrate the appearance of vortices in type

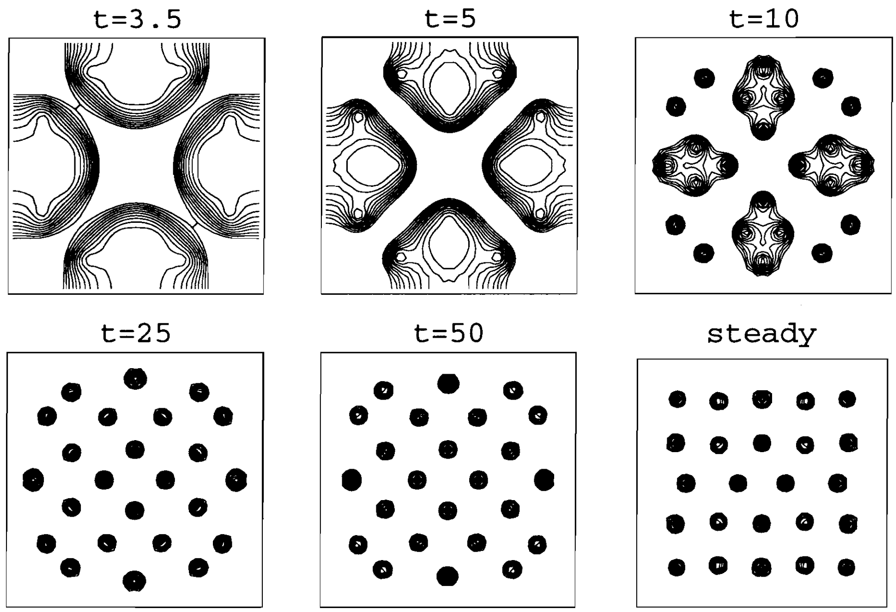

Figure 9.4: Time evolution for a 2x2 model system using the High kappa model with $H_0 = 0.5$; Backward-Euler-Galerkin scheme.

II materials. The arrangement of the vortices in a hexagonal lattice pattern may be observed in Figures 9.2 and 9.4, where we present results for a superconducting sample with sides equal to 20 coherence lengths.

Comparing Figure 9.1 with Figure 9.3 and Figure 9.2 with Figure 9.4, one may conclude that numerical results obtained with the finite element code based on the High kappa model are in good agreement with the corresponding results from the full G-L code for this specific values of κ.

Recall that out model is valid in the high κ, high field regime. We first demonstrate numerically that our model is valid for high values of κ. For a fixed value of the applied field we generate steady-state solutions for increasing values of κ in the full G-L equations and compare these with the steady-states solutions from the High kappa model. In Figures

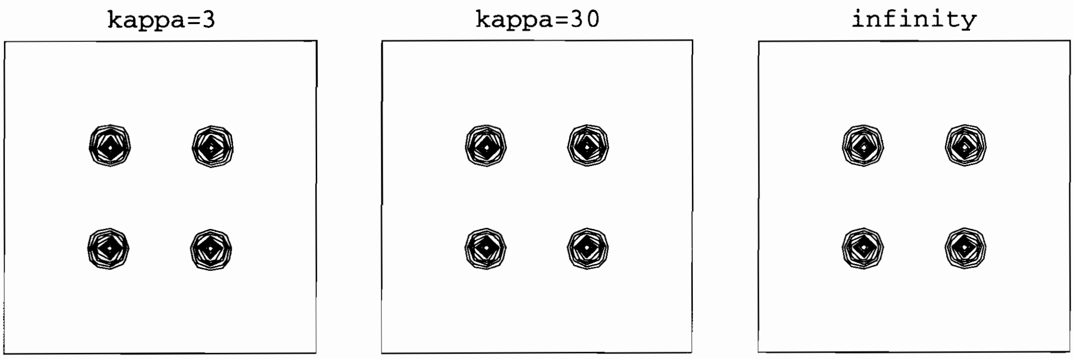

Figure 9.5: Steady-state vortex configurations for a 1x1 sample using the full G-L model with increasing values of κ and the High kappa model; H=0.5.

Table 9.1: Maximum and minimum values of the magnetic field for different values of κ and the applied field H_e.

κ	H_e/κ	H_{max}/κ	H_{min}/κ
3	0.3	0.2961	0.2868
5	0.3	0.3002	0.2943
20	0.5	0.5005	0.4906
30	0.3(3)	0.3337	0.3271

9.5-9.6 we present results for $H = 0.5$ and model samples having sides equal to 10ξ and 20ξ, respectively. The first two plots in Figure 9.5 correspond to approximations of the full G-L equations using values of $\kappa = 5$ and 30; the last plot represents the High kappa model approximation valid for $\kappa = \infty$. In Figure 9.6 we present results for a 2x2 sample for $\kappa = 5$ and 100 using the full G-L model, and the steady-state solutions for our model. It is evident that for values of κ exceeding 5 the contour plots appear virtually identical.

In Table 9.1 we examine the magnetic field in the superconductor for different values of κ and the applied field H_e. We present the maximum and minimum values of the magnetic field computed from the full TDG-L equations at various values of κ. Similar to the numerical results in [19] we demonstrate that for large values of κ the magnetic field in

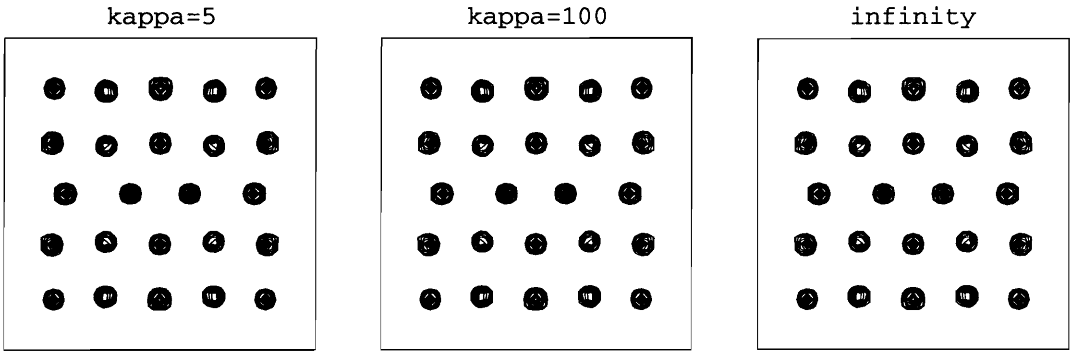

Figure 9.6: Steady-state vortex configurations for a 2x2 sample using the full G-L model with increasing values of κ and the High kappa model; H=0.5.

the superconductor is nearly a constant and it is equal to the applied field.

In the rest of this chapter we present numerical results computed using the High kappa model only.

Our first goal is to illustrate the need of adequate spatial resolution in order to resolve the vortices for a sample with a fixed size. We expect that the mesh resolution will depend on the size of the sample as well as on the magnitude of the applied field. Indeed, we know that increasing either the sample size or the applied field's magnitude results in the appearance of more vortices. Hence, finer grids are needed in order to resolve the solution for larger sample sizes or higher values of the applied field.

Figure 9.7 represents the steady-state configurations for a 1x1 sample with $H_0 = 0.7$ computed using grid sizes of 7x7, 9x9, 11x11 and 13x13, respectively. These results demonstrate that for a 1x1 sample with magnitudes of the applied field up to 0.7, it suffices to consider 9x9 grids. In Figure 9.8 we present the steady-states for a 2x2 sample with $H_0 = 0.5$ computed using mesh sizes 13x13, 19x19, 25x25 and 31x31, respectively. Our results indicate that for 2x2 samples with $H_0 \leq 0.5$ it suffices to use 25 grid lines in each coordinate direction.

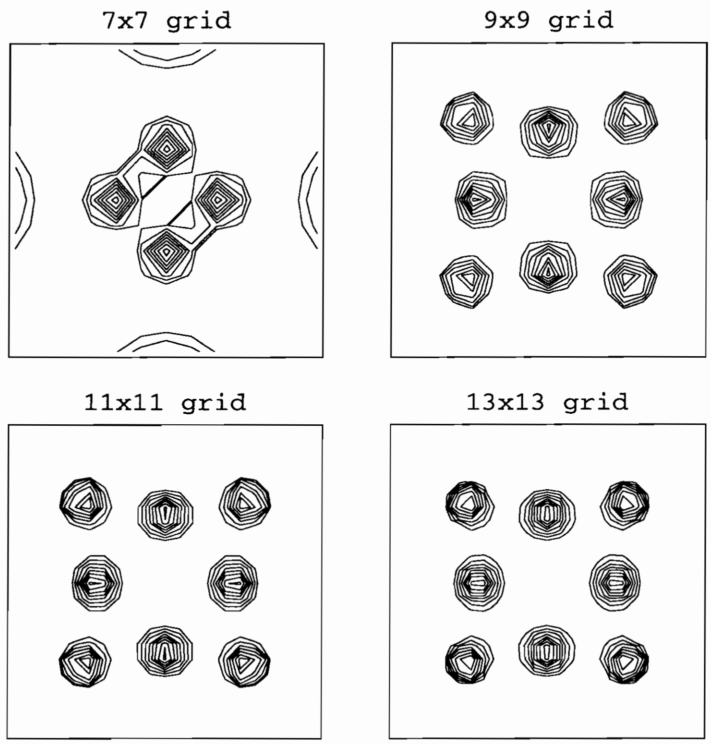

Figure 9.7: Steady state configurations for a 1x1 model system using increasing mesh resolution in the High kappa model with $H_0 = 0.7$.

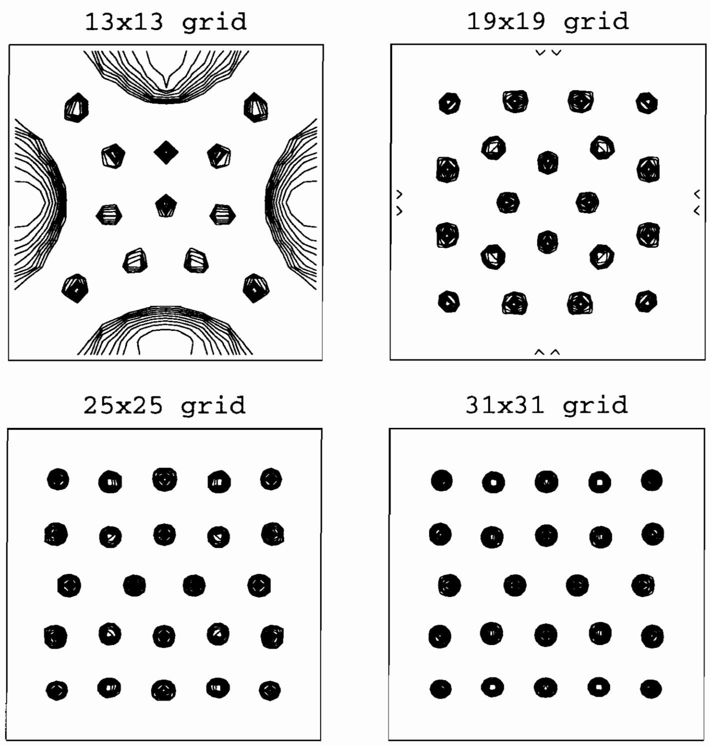

Figure 9.8: Steady state configurations for a 2x2 model system using increasing mesh resolution in the High kappa model with $H_0 = 0.5$.

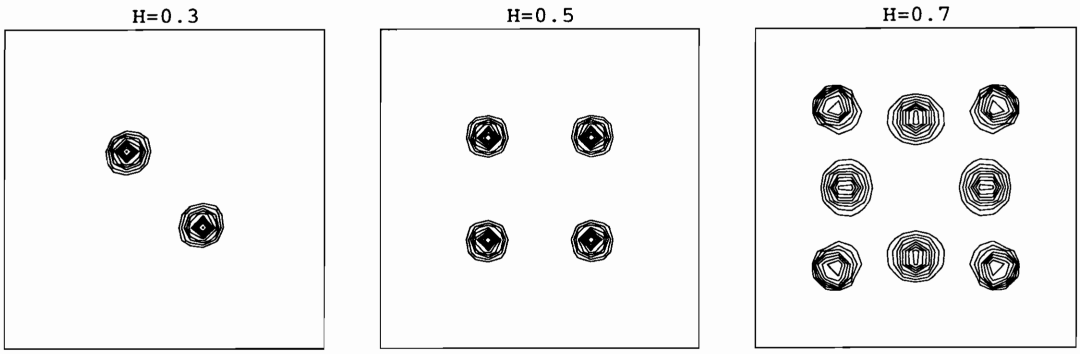

Figure 9.9: Steady state configurations for a 1x1 model sample using the High kappa model with increasing values of the applied field H_0.

Next, we turn our attention to computations with increasing applied fields which are known experimentally to cause the appearance of more vortices. We demonstrate this phenomena numerically in Figures 9.9-9.10. Figure 9.9 presents the steady-states for a 1x1 sample using $H_0 = 0.3, 0.5, 0.7$, respectively. The same stopping criteria is used in all cases. Figure 9.10 gives the steady-states for 2x2 sample for $H_0 = 0.3$ and 0.5, respectively.

The appearance of more vortices when the size of the superconducting sample is increased is demonstrated numerically in Figure 9.11. In this figure we present the steady-state configurations for 1x1, 2x2 and 3x3 samples for fixed $H_0 = 0.3$. Evidently, increasing the size of the sample leads to a significant increase in the number of vortices.

We continue with addressing the critical question of successfully avoiding local minimizers of the Gibbs free energy. Our results are presented in Figure 9.12 for a 1x1 sample. We consider only a 1x1 sample size since our experiments indicate that similar results hold for other sample sizes. In each column of Figure 9.12 we plot the steady states obtained using a fixed Newton tolerance Tol; each row represents a different value for the magnitude of the applied magnetic field, specifically $H_0 = 0.3, 0.5$ and 0.7.

Figure 9.12 demonstrates that significantly different values for the tolerance in the New-

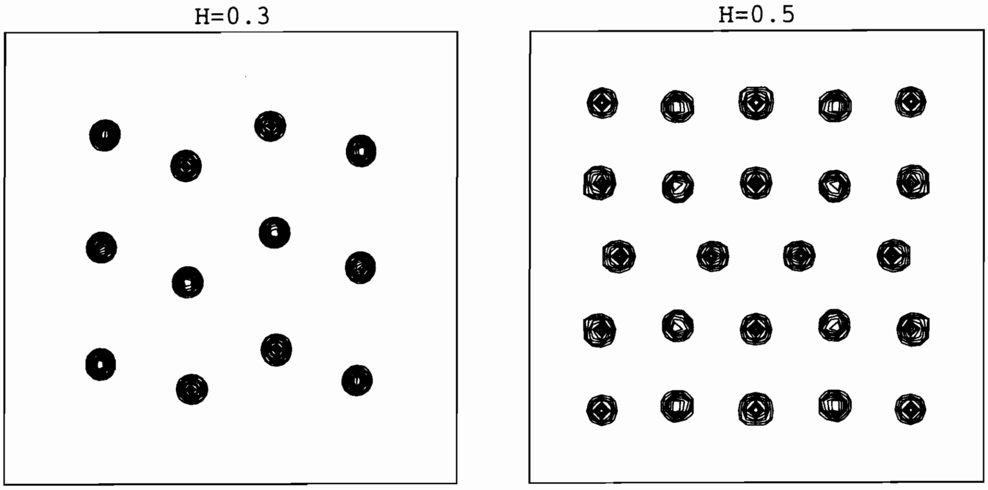

Figure 9.10: Steady state configurations for a 2x2 model sample using the High kappa model with increasing value of the applied field H_0.

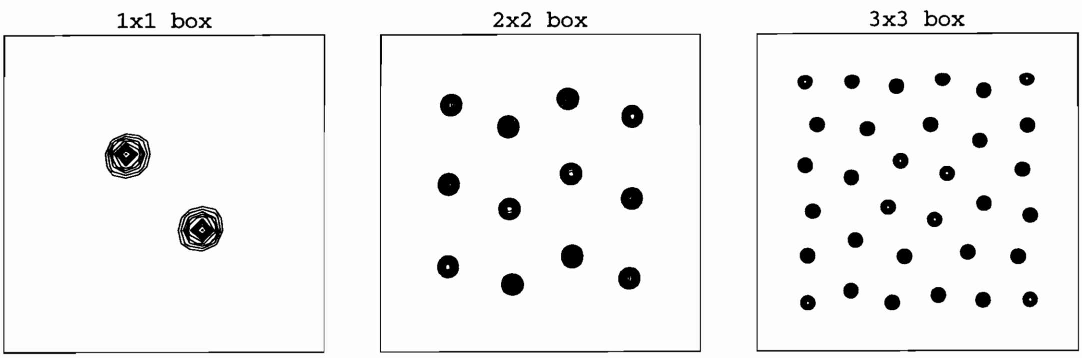

Figure 9.11: Steady state configurations for increasing size of the model system using the High kappa model with $H_0 = 0.3$.

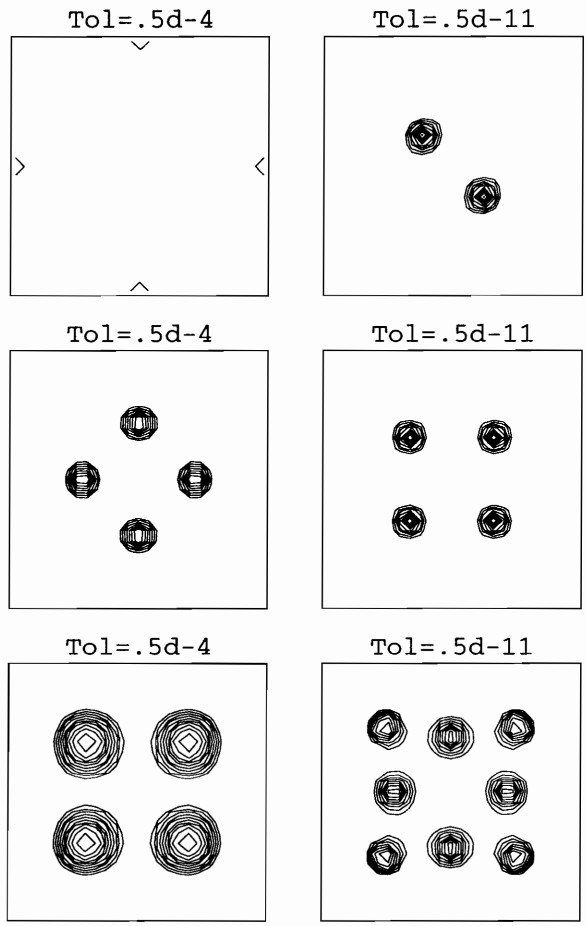

Figure 9.12: Steady state configurations for a 1x1 model system using the High kappa model with different values for the Newton's tolerance *Tol* and H=0.3, 0.5, 0.7

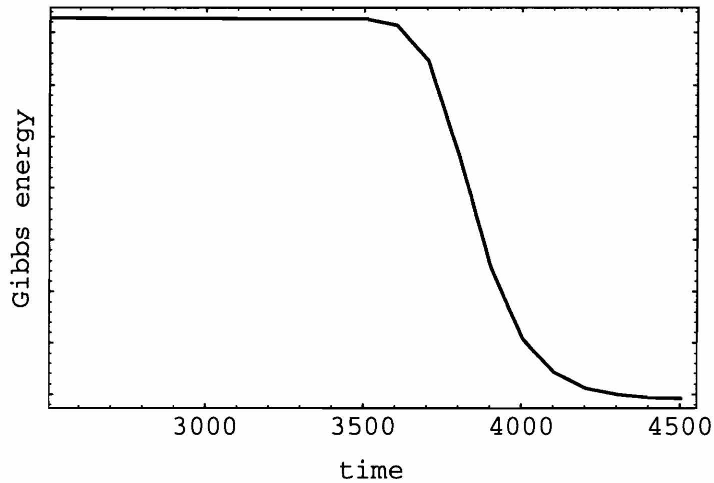

Figure 9.13: Gibbs free energy evolution for $H_0 = 0.3$.

ton's method may lead to different steady-state configurations. In Figure 9.13 we present the time evolution of the Gibbs free energy for $H_0 = 0.3$. Figures 9.12-9.13 demonstrate that, indeed, allowing for larger tolerances in the Newton iteration, the steady-state criteria may be satisfied at a local minimum of the system's energy. However, choosing the Newton's tolerance more conservatively, we have better assurance that the true global minimizer is found.

Next, we compare results in which two different time discretization schemes are used. In particular, we demonstrate that, as expected, using a higher order scheme with a variable time-stepping algorithm allows us to reach the steady state in fewer steps. Computational experiments have been performed for a 1x1 and 2x2 samples using both the Backward-Euler-Galerkin method and the Crank-Nicolson-Galerkin method with a variable time step and identical execution parameters, such as steady state criteria and Newton tolerances. The time evolutions by both methods are very similar, however the number of time steps required to reach the steady-state is reduced if we use the higher order Crank-Nicolson-

Galerkin scheme. In particular, in our numerical experiments with a variable time step k starting with the initial value $k = 0.5$ and using the Backward-Euler-Galerkin method steady state is reached in 61 (for 1x1 sample) and 92 (for 2x2 sample) time steps. Same computations with the Crank-Nicolson-Galerkin scheme result in reaching the steady state in 38 (for 1x1 sample) and 51 (for 2x2 sample) time steps. An additional advantage of the higher order scheme is that it yields a better approximation of the initial transient time period.

9.3 Numerical Approximations of the Convergence Rates

In this section we present numerical results concerning approximation of the $\mathcal{L}^2$ and $\mathcal{H}^1$ rates of convergence in both space and time. The theoretical rates established in this work are valid for a wide range of finite element spaces. In this section we shall present computational experiments for the spatial rates using bilinear and biquadratic finite elements. These elements are convenient for computations in rectangular regions, have good approximation properties, and are easy to implement. Bilinear finite elements lead to algebraic problems with relatively moderate storage requirements. This feature of the bilinear finite elements will be exploited in one of our numerical experiments, where the use of biquadratic elements would lead to prohibitively large (with respect to the available computational equipment) storage requirements. At the same time, they do not provide a particularly high convergence rate. Therefore, for sufficiently regular exact solutions it is more beneficial to use the more accurate biquadratic elements. Thus in order to approximate the rates in time we shall use biquadratic finite elements. All numerical results demonstrate a very good agreement with the optimal theoretical values derived in Chapter 8.

Let us recall the optimal error estimates derived under appropriate smoothness requirements. For $j = 0, 1$ one has

$$\|e_{be}^n\|_j \le C\left(h^{m+1-j} + k\right)$$

and

$$\|e_{cn}^n\|_j \le C\left(h^{m+1-j} + k^2\right),$$

where e_{be}^n and e_{cn}^n denote the error in the Backward-Euler-Galerkin and Crank-Nicolson-Galerkin scheme, respectively. We plan to demonstrate that these rates are also valid numerically.

This task is complicated by the absence of a closed form exact solution for our model which can be used in order to estimate the actual rates of convergence. To overcome this difficulty we compute a finite element solution using a very fine grid and an appropriate time step and call this solution the "exact" solution. In addition, this "exact" solution should be calculated at some physically interesting time.

In Table 9.2 we present numerical results for the approximations of the h-rates obtained using biquadratic finite elements. To calculate the rates in space we generate an initial state for the model system which corresponds to a nontrivial (nonconstant) behavior of the order parameter, and then use it as a starting point for a single, very small time step. In particular, the initial state is generated using a 69x69 grid at $t = 3.5$ and $t = 10.5$. We then make one time step with $k = 10^{-7}$ on this fine grid to generate our "exact" solution at $t = 3.5 + k$ and $t = 10.5 + k$. The initial guesses at $t = 3.5$ and $t = 10.5$ are used as starting points on a sequence of coarser meshes. In Table 9.2 we present results for the approximate rates obtained by comparing solutions generated on 7x7, 13x13, 25x25 and 39x39 grids with the "exact" solution. After computing the errors corresponding to the above approximate solutions we calculate the rates of convergence in the usual manner using a sequence of grids.

Table 9.2: Numerical rates of convergence in h for the High kappa model using biquadratic finite elements and refining the mesh in the approximate solution.

	L^2 error rates		
Time	$R_{7,13}$	$R_{13,25}$	$R_{25,39}$
$3.5+10^{-7}$	3.22	3.16	3.03
$10.5+10^{-7}$	3.26	3.15	3.02
	H^1 error rates		
Time	$R_{7,13}$	$R_{13,25}$	$R_{25,39}$
$3.5+10^{-7}$	2.12	2.08	1.98
$10.5+10^{-7}$	2.15	2.08	1.98

Here $R_{j,k}$ represents the rate computed using a sequence of $j \times j$ and $k \times k$ meshes. Our numerical approximations for the rates of convergence illustrate the theoretical results of $O(h^2)$ in $\mathcal{H}^1$ and $O(h^3)$ in $\mathcal{L}^2$ using biquadratics. Finally, we note that the use of different schemes for time discretizations does not influence the spatial rates of convergence.

Next we address the following question: what happens to the numerical rates of convergence when the mesh used in the "exact" solution is refined? It seems reasonable to expect that in such a case the approximations for the rates will improve. This observation is confirmed by the results in Table 9.3, where we present numerical approximations for the h-rates obtained using bilinear finite elements. The choice of bilinear finite elements for this experiment is motivated by the substantially smaller storage requirements of the bilinear elements. This allows us to achieve greater separation between the "exact" and the approximate solution than with biquadratic finite elements. Let us recall that the theoretical rate of convergence for bilinear finite elements is 2 for the $\mathcal{L}^2$-rate and 1 for the $\mathcal{H}^1$-rate. Results presented in Table 9.3 were obtained using the Backward-Euler-Galerkin scheme. Experiments performed with the Crank-Nicolson-Galerkin scheme produced virtually identical results. In contrast to the results in Table 9.2 here we fix two approximate solutions computed using uniform meshes having 7 and 13 grid lines, respectively, and then

Table 9.3: Numerical rates of convergence in h for the High kappa model using bilinear finite elements and refining the mesh in the "exact" solution; time=$3.5 + 10^{-7}$.

	L^2 error rates						
Grid	39x39	69x69	81x81	121x121	151x151	181x181	201x201
$R_{7,13}$	0.6	1.4	1.7	1.8	2.0	1.9	1.9
	H^1 error rates						
Grid	39x39	69x69	81x81	121x121	151x151	181x181	201x201
$R_{7,13}$	0.9	1.1	1.1	1.1	1.1	1.0	1.1

generate a sequence of "exact" solutions using uniform meshes with 39, 69, 81, 121, 151, 181 and 201 grid lines. The corresponding sequences of $\mathcal{L}^2$ and $\mathcal{H}^1$ rates are presented in Table 9.3. We expect that as the mesh used in the "exact" solution is refined this will lead to an improvement in the estimates for the rates. Our results presented in Table 9.3 confirm this observation and demonstrate a very good agreement of the numerically computed rates with the theoretically predicted optimal values. We note that the experimental rates become particularly close to the theoretical ones for mesh sizes above 121x121. In terms of biquadratic elements the same accuracy can be achieved using 61x61 grids. Recall that results in Table 9.1 were obtained using biquadratic elements and 69x69 grids, which corresponds to 137x137 grids and bilinear elements. From results presented in Tables 9.2 and 9.3 it appears that these are the coarsest possible grid sizes which can be used for the "exact" solution in order to obtain reasonable estimates of the convergence rates.

Next we turn to numerical results concerning approximations of the $\mathcal{L}^2$ and $\mathcal{H}^1$ rates in time. Let us recall that these rates should have the order of the scheme used in the time discretization, that is we expect to observe $O(k)$ for the Backward-Euler and $O(k^2)$ for Crank-Nicolson scheme. In Table 9.4 we present results obtained at three different moments in time. More precisely, we approximate the $\mathcal{L}^2$ and $\mathcal{H}^1$ rates in k at t= 1.6, 4.1 and 11.1. The corresponding initial states for times $1.0, 3.5$ and 10.5 are generated using a

Table 9.4: Numerical rates of convergence in k for the High kappa model

	L^2 error rates		
Time discretization	time=1.6	time=4.1	time=11.1
B-E	0.97	1.04	1.03
C-N	2.12	2.03	2.21

	H^1 error rates		
Time discretization	time=1.6	time=4.1	time=11.1
B-E	0.95	1.01	1.07
C-N	2.16	1.98	1.93

uniform mesh with 39 grid lines, a fixed step $k = 0.5$ and performing a prescribed number of $nt = 2, 7$ and 21 steps, respectively. An "exact" solution is obtained using a uniform grid with 39 grid lines, starting with the initial states, and using a fixed time step $k = 0.01$ and $nt = 60$. Two approximate solutions are computed starting from each of the initial states using $k = 0.1, 0.3$, and $nt = 6,\ 2$, respectively; a 39x39 grid is used. The results presented in Table 9.4 illustrate that our numerical rates approximate the theoretical values for the $\mathcal{L}^2$ and $\mathcal{H}^1$ rates in time with good accuracy.

9.4 Vortex Dynamics Under Applied Constant Current

Numerical results presented in the previous section deal with the case when the superconducting sample is subjected only to an applied magnetic field of magnitude H_0. Below, we present numerical results obtained in the presence of an applied constant current of magnitude J_0. Let us recall that when current is passed through a type II superconductor in the presence of applied magnetic field, then vortices begin to move in a direction transverse to the transport current, see Figure 2.3. This motion was first observed in [28]. As a result of the viscous flow of the vortices, energy is dissipated. This induces voltage and thus produces resistance in the sample.

We use two different approaches to model the applied current. In the first one, both the current and the magnetic field are applied from the initial moment. In the second approach at the initial moment we apply only the magnetic field, while the current is applied after the steady-state vortex configuration has been formed. Before presenting our numerical results let us recall that throughout this chapter we use a fixed value $\xi = 0.1l$ for the coherence length. We also remind the reader that all figures presenting the time evolution of the vortex configurations should be read from the top to the bottom and from the left to the right.

We first present numerical results in the case when both the current, and the magnetic field are applied from the initial moment. In this case vortices start to move across the sample (from left to right) instead of reaching a steady-state configuration. We recall that in the High kappa model the current $\mathbf{J}_0$ is directed in the y-direction, see (2.1.17). For such a current theory predicts that as a result of the Magnus force, vortices will move in a transverse direction to the current flow. This phenomena is clearly observed in Figures 9.14-9.15, where we give results for current of magnitude $J_0 = 0.01$. The results in Figure 9.14 are for a 1x1 sample with applied magnetic field of magnitude $H_0 = 0.5$. In Figure 9.15 we collect results for a 2x2 sample with $H = 0.5$. A steady state configuration is not reached and the vortices continue to move at right angles to the current flow.

In the remaining part of this section we present results for the case when current is applied after the steady-state has been reached. In this case at the initial moment there is only an applied magnetic field so that vortices start forming and eventually reach a steady-state vortex configuration. Figure 9.16 gives the results for a 1x1 sample with $H = 0.5$ and $J_0 = 0.01$. The six plots given in the first two rows visualize time evolution until a steady-state is reached. This enables us to carry on the numerical simulations starting with

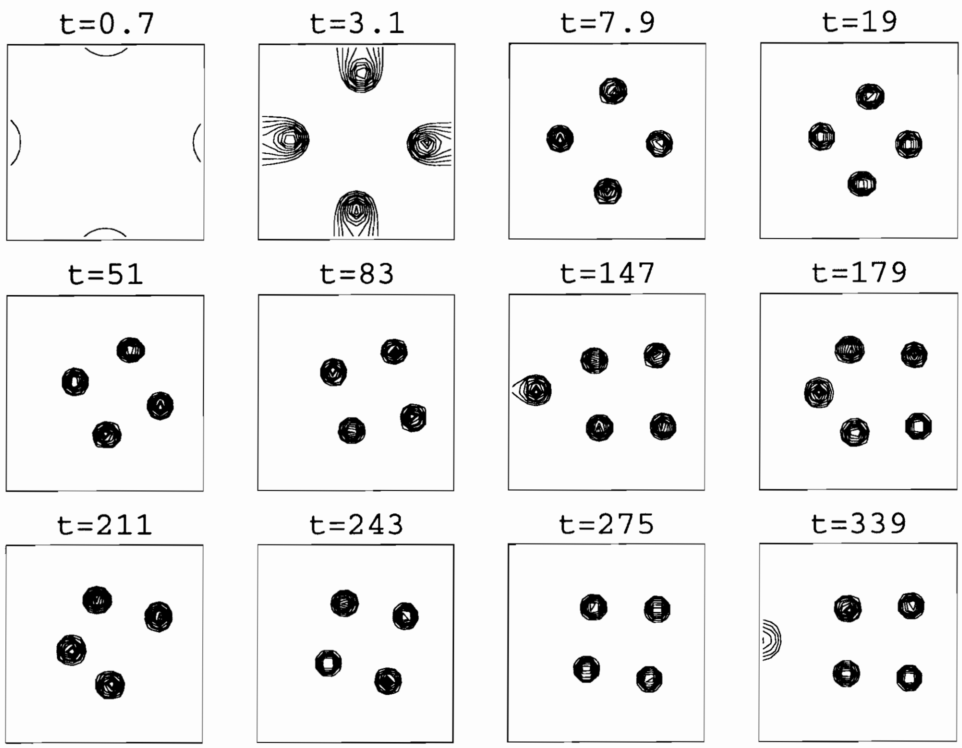

Figure 9.14: Vortex dynamics with $H_0 = 0.5$ and $J_0 = 0.01$; current applied from the initial moment; 1x1 box.

the steady-state configuration, instead of starting with the pure superconducting state.

The last question we want to address here is what happens when the magnitude of the applied current increases. From the theory and experiment we know that at some point, when the current reaches the critical magnitude, superconductivity will be lost. All results in Figures 9.14-9.16 were based on computations with a fixed $J_0 = 0.01$. Now fixing both the sample size to 1x1 and the magnitude of the applied magnetic field to $H = 0.5$ we increase the applied current in order to demonstrate numerically that if the current is strong enough then the model system is not able to retain superconductivity and the sample transforms into the normal (nonsuperconducting) state. For example, Figure 9.17 shows

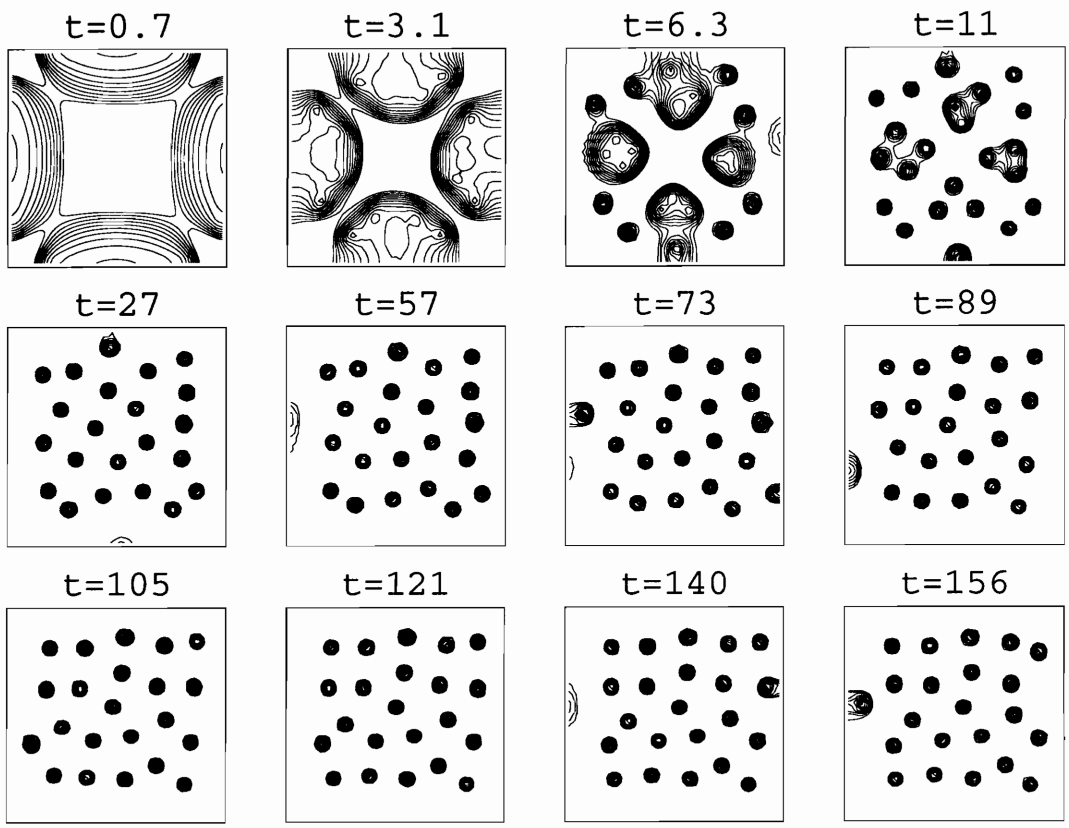

Figure 9.15: Vortex dynamics with $H_0 = 0.5$ and $J_0 = 0.01$; current applied from the initial moment; 2x2 box.

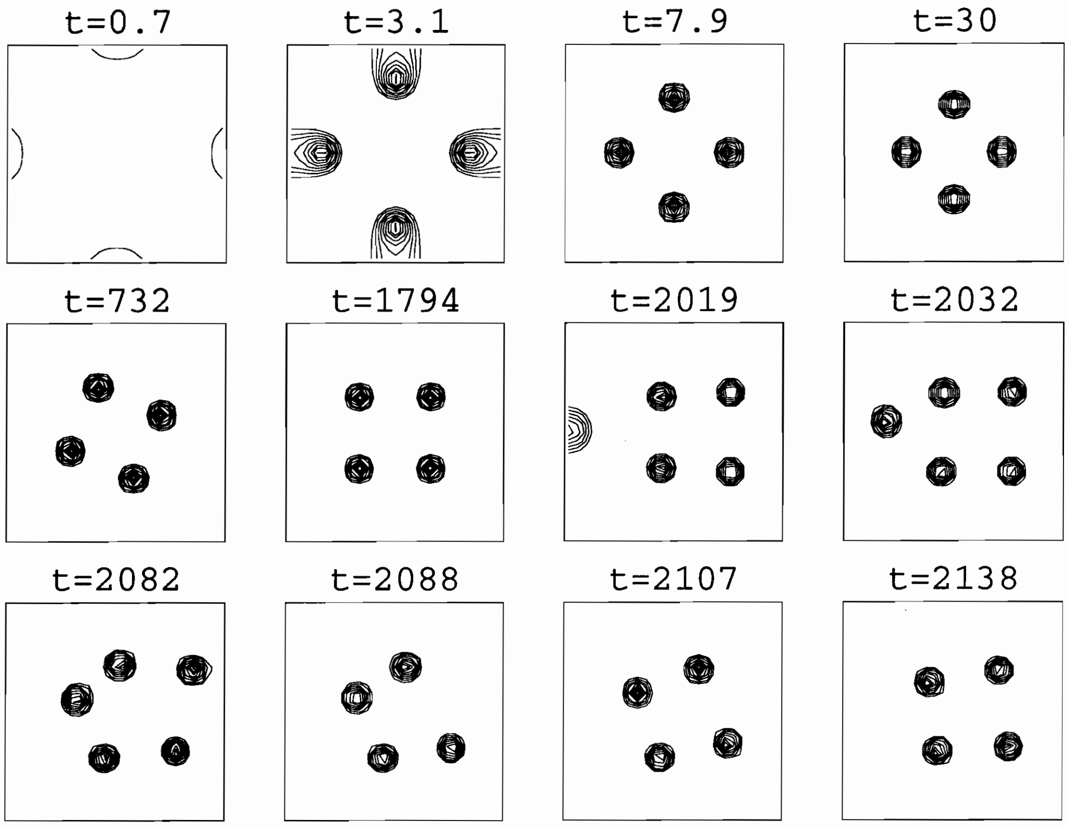

Figure 9.16: Vortex dynamics with $H_0 = 0.5$ and $J_0 = 0.01$; current applied after steady state is reached; 1x1 box.

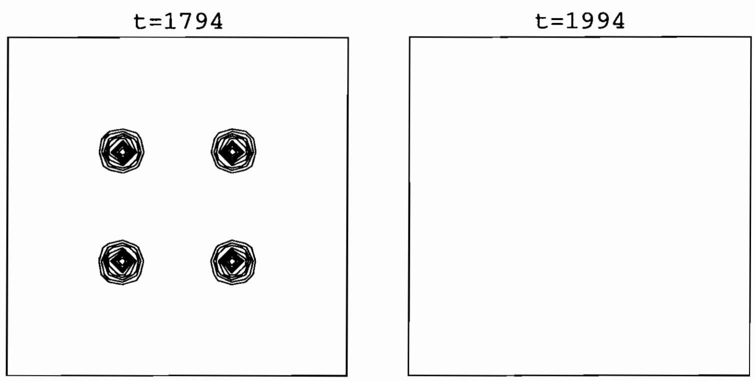

Figure 9.17: Vortex dynamics for a 1x1 sample with $H_0 = 0.5$ and $J_0 = 0.5$; strong current destroys superconductivity.

that if $J = 0.5$ then superconductivity is lost very quickly. Note that the last "clear" plot in Figure 9.17 corresponds to the normal state which is characterized by the zero value of the order parameter. Experiments were performed indicating that application of larger currents J leads to an even faster loss of superconductivity.

REFERENCES

[1] A. Abrikosov, **Fundamentals of Theory of Metals**, North-Holland, 1988.

[2] A. Abrikosov, *On the Magnetic properties of Superconductors of the Second Type*, **Zh. Eksperim. i Teor. Fis.**, 32, pp. 1442-1452, 1957. [English translation: Soviet Phys. -JETP, 5, pp. 1174-1182, 1957.]

[3] R. Adams, **Sobolev Spaces**, Academic Press, New York, 1975.

[4] S. Adler and T. Piran, *Relaxation Methods for Gauge Field Equilibrium Equations*, **Reviews of Modern Phys.**, 56, pp. 1-40, 1984.

[5] G. Akrivis, V. Dougalis, and O. Karakashian, *On Fully Discrete Galerkin Methods of Second-order Temporal Accuracy for the Nonlinear Schrodinger Equation*, **Numerishe Mathematik**, 1991.

[6] K. E. Atkinson, **An Introduction to Numerical Analysis**, Second Edition, John Wiley and Sons, New York, 1988.

[7] J. Bardeen, **Theory of Superconductivity**, In Encyclopedia of Physics XV, edited by S. Flugge, pp.17-369, Springer, Berlin, 1956.

[8] J. Bardeen, L. Cooper, and J. Schrieffer, *Theory of Superconductivity*, **Phys. Rev.**, 108, pp. 1175-1204, 1957.

[9] C. Baker and C. Phillips, editors, **The Numerical Solution of Nonlinear Problems**, Clarendon Press, Oxford, 1981.

[10] M. Berger and Y. Chen, *Symmetric Vortices for the Ginzburg-Landau Equations for Superconductivity and the Nonlinear desingularization phenomena*, **J. Funct. Anal.**, 82, pp. 259-295, 1989.

[11] D. Bishop, P. Gammel, and David Huse, *Resistance in High-Temperature Superconductor*, **Scientific American**, February 1993.

[12] A. Bourdillon and N. X. Tan Bourdillon, **High Temperature Superconductors: Processing and Science**, Academic Press, Inc., Boston, 1994.

[13] E. Brandt, *Ginzburg-Landau theory of the Vortex Lattice in Type II Superconductors for all Values of κ and B*, **Phys. Stat. Sol.(b)**, 51, pp. 345-358, 1972.

[14] F. Brezzi and M. Fortin, **Mixed and Hybrid Finite Element Methods**, Springer-Verlag, New York, 1991.

[15] R. Carroll and A. Glick, *On the Ginzburg-Landau Equations*, **Arch. Rat. Mech. Anal.**, 16, pp. 373-384, 1964.

[16] S. Chapman, **Macroscopic models of superconductivity**, Ph.D thesis, Oxford University, 1992.

[17] S. Chapman, Q. Du, and M. Gunzburger, *On the Laurence-Doniach and Anisotropic Ginzburg-Landau Models for Layered Superconductivity*, Preprint.

[18] S. J. Chapman, Q. Du, M. D. Gunzburger, and J. S. Peterson, *A Ginzburg-Landau Type Model of Superconducting/Normal Junctions Including Josephson Junctions*, to appear in **SIAM Journal of Applied Math.**

[19] S. J. Chapman, Q. Du, M. D. Gunzburger, and J. S. Peterson, *Simplified Ginzburg-Landau Models for Superconductivity Valid for High Kappa and High Fields*, to appear in **SIAM Journal of Applied Math.**

[20] S. Chapman, S. Howison and J. Ockendon, *Macroscopic models of superconductivity*, **SIAM Review**, 34, pp. 529-560, 1992.

[21] Y. Chen, *Nonsymmetric Vortices for the Ginzburg-Landau Equations in the Bounded Domain*, **J. Math. Phys.**, 30, pp. 1942-1950, 1989.

[22] P. G. Ciarlet, **The Finite Element Method for Elliptic Problems**, North-Holland Publishing Company, New York, 1980.

[23] C. Cuvelier, A. Segal, and A.A. van Steenhoven, **Finite Element Methods and Navier-Stokes Equations**, D. Reidel Publishing Company, Boston, 1986.

[24] M. Cyrot and D. Pavume, **Introduction to Superconductivity and High-T_c Materials**, World Scientific, 1992.

[25] P. F. Dahl, **Superconductivity. Its Historical Roots and Development from Mercury to the Ceramic Oxides**, American Institute of Physics, New York, 1992.

[26] R. Dautray and J.-L. Lions, **Mathematical Analysis and Numerical Methods for Science and Technology**, Springer-Verlag, New York, Volume 5, Evolutional Problems I, 1992.

[27] P. DeGennes, **Superconductivity in Metals and Alloys**, Benjamin, New York, 1966.

[28] P. DeGennes and J. Matricon, *Rev. Mod. Phys.*, 36, pp. 45, 1964.

[29] J.E. Dendy, Jr., *Galerkin's Method for Some Highly Nonlinear Problems*, **SIAM J. Numer. Anal.**, 14, No. 2, pp. 327-347, April 1977.

[30] J. Douglas, Jr. and T. Dupont, *Galerkin Method for Parabolic Equations*, **SIAM J. Numer. Anal.**, 7, No. 4, December 1970.

[31] M. Doria, J. Gubernatis, D. Rainer, *Solving the Ginzburg-Landau Equations by Simulated Annealing*, **Phys. Rev. B**, 41, pp. 6335-6340, 1990.

[32] Q. Du and M. Gunzburger, *A Model for Superconducting Thin Films Having Variable Thickness*, **Physica D**, 69, pp. 215-231, 1993.

[33] Q. Du, *Global Existence and Uniqueness of Solutions of the Time-Dependent Ginzburg-Landau Model for Superconductivity*, to appear in **Applicable Analysis**.

[34] Q. Du, *Finite Element Methods for the Time-Dependent Ginzburg-Landau Model of Superconductivity*, **Computers Math. Applic.**, 27, No 12, pp. 119-133, June 1994.

[35] Q. Du, M. Gunzburger, and J. Peterson, *Analysis and Approximation of the Ginzburg-Landau Model of Superconductivity*, **SIAM Review**, 34, No. 1, pp. 54-81, March 1992.

[36] Q. Du, M. Gunzburger, and J. Peterson, *Solving the Ginzburg-Landau Equations by Finite-Element Methods*, **Physical Review B**, 46, No 14, pp. 9027-9034, 1992.

[37] Q. Du and P. Gray, *High-Kappa Limits of the Time-Dependent Ginzburg-Landau Model*, Preprint, 1995.

[38] G. Eilenberger, *Zu Abrikosovs Theorie der Periodischen Lösungen der GL-Gleichüngen fur Suparaleiter 2*, **Art. Z. für Phys.**, 180, pp. 32-42, 1964.

[39] G. Fairweather, **Finite Element Galerkin Methods for Differential Equations,** Marcel Dekker, Inc. New York .

[40] A. Fetter and P. Hoemberg, **Theory of Type II Superconductivity**, (edited by R. Parks), Marcel Dekker, New York, pp. 817-923, 1969.

[41] H. Frahm, S. Ullah, and A. Dorsey, *Flux Dynamics and the Growth of the Superconducting Phase*, **Phys. Rev. Letters**, 66, pp. 3067-3072, 1991.

[42] G. Garner, M. Spanbauer, R. Benedek, K. Stranburg, S. Wright. P. Plassmann, *Critical Fields of Josephson-Coupled Superconducting Multilayers*, **Physical Review B**, 45, pp. 7973-7983, 1992.

[43] V. L. Ginzburg and D. A. Kirzhnitz, **High-Temperature Superconductivity**, translated from russian by A. Agyei, edited by J. Birman, Consultants Bureau, New York, 1982.

[44] V. Ginzburg and L. Landau, *On the Theory of Superconductivity*, **Zh. Eksperim. i Teor. Fiz.**, 20, pp. 1064-1082, 1950. [English translation: Men of Physics: L.D. Landau, I, edited by D. ter Haar, Pergament, Oxford, pp. 138-167, 1965.]

[45] V. Girault and P.-A. Raviart, **Finite Element Methods for Navier-Stokes Equations, Theory and Algorithms**, Springer-Verlag, New York, 1986.

[46] L. Gor'kov and G. Eliashberg, *Generalization of the Ginzburg-Landau Equations for the Non-Stationary Problems in the Case of Alloys with Paramagnetic Impurities*, **Soviet Phys.,-JETP**, 27, pp. 328-334, 1968.

[47] L. Gor'kov and N. Kopnin, *Vortex Motion and Resistivity of Type II Superconductors in a Magnetic Field*, **Sov. Phys. Usp.**, 18, No 7, pp. 496-513, 1975.

[48] M. Gunzburger, **Superconductivity Seminar**, VA TECH, 1994.

[49] J. Woods Halley, Editor, **Theories of High Temperature Superconductivity**, Addison-Wesley Publishing Company, Inc., Redwood City, California, 1988.

[50] R. M. Hazen, **The Breakthrough. The Race for the Superconductor**, Summit Books, New York, 1988.

[51] J. Heywood and R. Rannacher, *Finite-Element Approximation of the Nonstationary Navier-Stokes Problem; Part IV: Error Analysis for Second-Order Time Discretization*, **SIAM J. Numer. Anal.**, 27, No. 2, pp. 353-384, April 1990.

[52] C. Hu and R. Thompson, *Dynamic structure of Vortices in Superconductors*, **Phys. Rev. B**, 6, pp. 110-120, 1972.

[53] L. Jacobs and C. Rebbi, *Interaction Energy of Superconducting Vortices*, **Phys. Rev. B**, 9, pp. 4486-4494, 1979.

[54] D. St. James, G. Sarma, and E. Thomas, **Type II Superconductivity**, Pergamon, Oxford, 1969.

[55] C. Johnson, **Numerical Solutions of Partial Differential Equations by the Finite Element Method**, Cambridge University Press, 1987.

[56] W. Kleiner, L. Roth, and L. Autler, *Bulk Solutions of Ginzburg-Landau Equations for Type II Superconductors: Upper Critical Field Region*, **Phys, Rev.**, 133, A1226-A1227, 1964.

[57] V. Klimov, *Nontrivial Solutions of the Ginzburg-Landau Equations*, **Teoret. Math. Fiz.**, 50, pp. 383-389, 1982. [English translation: **Theor. Math. Phys.**, 50 pp. 252-256, 1982.]

[58] H. Koppe and J. Wilebrand, *Approximate Calculation of the Reversible Magnetization Curves for Type II Superconductors*, **Low Temp. Phys.**, 2, pp. 499-506, 1970.

[59] H.-O. Kreiss and J. Lorenz, **Initial-Boundary Value Problems and the Navier-Stokes Equations**, Academic Press, Inc., Boston, 1989.

[60] V. Kresin and S. A. Wolf, **Fundamentals of Superconductivity**, Plenum Press, New York, London, 1990.

[61] C. Kuper, **An Introduction of the Theory of Superconductivity**, Clarendon, Oxford, 1968.

[62] M. Kwong, *Sweeping Algorithms for Inventing the Discrete Ginsburg-Landau Operator*, Preprint MCS-P307-0492, Argonne National Lab, 1991.

[63] G. Lasher, *Series Solution of the Ginzburg-Landau Equations for the Abrikosov Mixed State*, **Phys. Rev. A**, 140, pp. 523-528, 1965.

[64] F. Liu, M. Mondello, N. Goldenfeld, *Kinetics of the Superconducting Transition*, **Phys. Rev. Lett.**, 66. pp. 3071-3074, 1991.

[65] F. London and H. London, *The Electromagnetic Equations of the Supraconductor*, **Proc. Roy. Soc. London**, A149, pp. 71-88, 1935.

[66] G.I. Marchuk, **Methods of Numerical Mathematics**, Second Edition, Springer-Verlag, New York, 1981.

[67] R. K. Miller and A. Michel, **Ordinary Differential Equations**, Academic Press, 1982.

[68] A.R. Mitchel and R. Wait, **The Finite Element Method in Partial Differential Equations**, John Wiley and Sons, New York, 1977.

[69] F. Odeh, *Existence and Bifurcation Theorems for the Ginzburg-Landau Equations*, **J. Math. Phys.**, 8, pp. 2351-2356, 1967.

[70] T. P. Orlando and Kevin A. Delin, **Foundations of Applied Superconductivity**, Addison-Wesley Publishing Company, 1991.

[71] L. Pismen and J. Rodrigues, *Mobility of Singularities in the Dissipative Ginzburg-Landau equations*, **Phys. Rev. A**, 42, pp. 2471-2474, 1990.

[72] M. Renardy and R. Rogers, **Introduction to Partial Differential Equations**, Springer, Berlin, 1993.

[73] G. Taubes, *Holding the Lines in High-Temperature Superconductors*, **Science**, 261, September 1993.

[74] C. Taubes, *Arbitrary N-vortex Solutions of the First Order Ginzburg-Landau Equations*, **Commun. Math. Phys.**, 72, pp. 277-292, 1980.

[75] C. Taubes, *On the Equivalence of the First and Second Order Equations for Gauge Theories*, **Commun. Math. Phys.**, 75, pp. 207-227, 1980.

[76] R. Temam, **Navier-Stokes Equations**, Edited by Lions, Papanicolaou and Rockafellar, Studies in Mathematics and its Applications, Volume 2, North-Holland Publishing Company, New York, 1979.

[77] V. Thomée, **Galerkin Finite Element Methods for Parabolic Problems,** Springer Verlag, New York, 1984.

[78] M. Tinkam, **Introduction to Superconductivity**, McGraw-Hill, 1975.

[79] E. Weinberger, *Multivortex Solution of the Ginzburg-Landau Equations*, **Physical Review D**, 19, pp. 3008-3011, 1979.

[80] M. Wheeler, *A Priory L_2 Estimates for Galerkin Approximations to Parabolic Partial Differential Equations*, **SIAM J. Numer. Anal.**, 10, No. 4, September 1973.

[81] Y. Yang, *Existence, Regularity and Assymptotic Behavior of the Solutions to the Ginzburg-Landau Equations on R^3*, IMA Preprint Series, 464, University of Minnesota, Minneapolis, 1988.

[82] Y. Yang, *Boundary Value Problems of the Ginzburg-Landau Equations*, **Proc. Royal Soc. Edingburg**, 11A, pp. 355-365, 1990.

[83] O.C. Zienkiewicz and K. Morgan, **Finite Elements and Approximation**, John Wiley and Sons, New York, 1982.

VITA

Rossitza Karamikhova

Address

Department of Mathematics

University of Texas at Arlington

Arlington, Tx 76019-0408

Phone: (817) 277 4975 (Home)

E-mail: rossi@utamat.uta.edu (Internet)

Education

1995-present	Lecturer, UT Arlington
1991-1995	Ph.D. Mathematics, Virginia Polytechnic Institute and State University.
1980-1985	Magistrate in Mathematics, University of Sofia, Bulgaria

Positions

1991 - 1994	Graduate Teaching Assistant, VPI&SU
1986 - 1990	Research Associate, Research Laboratory of Statistical Mechanics and Thermodynamics at the Bulgarian Academy of Sciences

Fellowships and Grants

1986 - 1990	Committee of Science, Bulgaria

Awards and Honors

1992-1994 Tuition scholarships, VA Tech.

Professional affiliation

1992 - present AMS

1992 - present SIAM

1993 - present Pi Mu Epsilon

Presentations and research visits

1993 - Seattle:	Mathematics of Superconductivity, AMS-IMS-SIAM Summer research Conference
1990 - Bulgaria:	National Conf. on Mechanics, Varna 90
1988 - USSR:	Institute of Applied Mechanics, Novosibirsk, research visit
1988 - Bulgaria:	Int. Conf. , Mathematical Models in Biology, Varna
1987 - Bulgaria:	Euromech Colloquium 224, Kinetic Theory Aspects of Evaporation-Condensation Phenomena, Kardjali
1986 - USSR:	Institute of Applied Mechanics, Novosibirsk, research visit

Research Experience

- Numerical methods for partial differential equations: finite element methods for elliptic and parabolic equations

- Mathematical models of superconductivity: Ginzburg-Landau type models of low-temperature and high-temperature superconductivity

- Two-dimensional lattice models: interacting dimers

- Numerical methods in Statistical mechanics: Monte Carlo metods; Metropolis Monte Carlo method

- Mathematical models in biology: simple models of lipid membranes
- Numerical methods with result verification: computer arithmetic and algorithms; linear systems of equations; two-sided, interval methods

Languages

English, Russian, Bulgarian

Family Status

Married, one child.